INCORPORATION OF BIO-INSPIRED MICROPARTICLES WITHIN EMBRYONIC STEM CELL AGGREGATES FOR DIRECTED DIFFERENTIATION

A Thesis
Presented to
The Academic Faculty

By

Denise Sullivan

In Partial Fulfillment
Of the Requirements for the Degree
Master of Science in Biomedical Engineering

Georgia Institute of Technology
Emory University

December, 2015

INCORPORATION OF BIO-INSPIRED MICROPARTICLES WITHIN EMBRYONIC STEM CELL AGGREGATES FOR DIRECTED DIFFERENTIATION

Approved by:

Dr. Todd McDevitt, Advisor

School of Biomedical Engineering

Georgia Institute of Technology

Dr. Johnna Temenoff

School of Biomedical Engineering

Georgia Institute of Technology

Dr. Jane Lebkowski

President of R&D

Asterias Biotherapeutics

Date Approved: July 20th, 2015

To my family- Beate, Robert, Nick, and Nina

ACKNOWLEDGEMENTS

I would like to first acknowledge the guidance and advice of my committee members, Dr. Johnna Temenoff, Dr. Jane Lebkowski, and my thesis advisor, Dr. Todd McDevitt. I have been very fortunate to have Dr. Temenoff as both a professor when I took her Advanced Seminar on Biomaterials and Regenerative Medicine, and as an unofficial collaborator as her lab and ours have worked closely together on development of glycosminoglycan-based materials for stem cell differentiation. Dr. Temenoff has always been very responsive and willing to provide advice on any questions during my graduate career and have truly appreciated the help and advice I've received from all her past and present graduate students, Song Seto, Jen Lei, Liane Tellier, and Torri Rinker. I am thankful to have Dr. Lebkowski on my committee and her unique perspective that she brings based on her impressive career in industry. I would also like to thank my advisor, Todd, for always encouraging me to keep pushing, even when I was ready to give up. I know that Todd's attention to detail and high standards for scientific work produced in the lab has prepared me for a successful in all of my future endeavors. I also truly appreciate that Todd is protective of his student's time and is always willing to fight for them.

I am extremely grateful for the support and advice from all present and past McDevitt graduate students. I joined the lab the same day as Josh Zimmermann during the Summer of 2011 and we quickly bonded while we worked on experiments together. I will miss our good-natured banter and jokes (such as Josh's love for chicken) that always served as amusement for other students in the lab. Josh always provides good critical scientific advice and I know he will become a very successful scientist. Marian Hettiaratchi and Melissa Goude also joined the lab the same year as me. Marian has

been incredibly kind and helpful, by always providing an ear to listen to my concerns and questions. Melissa was always very supportive and easy to talk to and she was my go to shopping buddy anytime needed to partake in some retail therapy. I would also like to thank Jenna Wilson, Dr. Anh Nguyen, and Dr. Doug White who joined the lab the year before me. Jenna was my mentor when I joined the lab and was very patient in showing me the ropes of working in the lab. I will dearly miss our weekly discussion about college football in the fall. Doug has been extremely supportive and always full of encouragement, and his extensive knowledge on stem cell biology always amazed me. I've truly enjoyed getting to know Anh over the past couple of years and she has always provided a shoulder to lean on in tough times. I always enjoyed hearing her describe her various culinary adventures and loved trying new foods with her. Olivia Burnsed, Emily Jackson, and Alex McKinlay joined the lab the year after I joined and each has brought a new dynamic to the lab group.I miss seeing Alex after he decided to leave with a Masters degree and our discussions about SEC football. Emily is very sweet and always willing to help other students in the lab. Olivia and I became close friends over the past and has been my main confidant in the lab. She always manages to brighten my day, and I've enjoyed all the fun we've had together from taking dance lessons to listening to hip hop music together. The most recent graduate students to join the lab, Katy Hammersmith, Jessie Butts, Liane Tellier, and Chad Glenn, are wonderful students and I look forward to seeing their careers develop. In particular, I've enjoyed getting to work alongside Katy and seeing her transition from an undergrad in the lab to a graduate student. Dr. Mellisa Kinney I would like to also thank past graduate students, Dr. Melissa Kinney, Dr. Andrés Bratt-Leal, Dr. Barbara Nsiah, Dr. Alyssa Nganga, and Dr. Ken Sutha. Melissa has been a tremendous source of advice and support and I can't wait to see what else she accomplishes in the future. While brief, I enjoyed learning from the

other past students and seeing them move on to have very successful careers. Additionally, I would like to thank Marissa Cooke, Alex Ortiz, Christian Mandrycky, and Elizabeth Peijnenburg for all their support and advice.

I would also like to acknowledge all the guidance and encouragement I received from present and past post-docs in our lab. I am grateful for all the mentoring and advice I received from Dr. Pirya Baraniak and Dr. Krista Fridley during my first year as a graduate student. Dr. Tobias Miller has been incredibly helpful in answering any questions I ever had regarding about the chemistry of microparticle synthesis. While she was only here for 1 year, Dr. Lindsay Fitzpatrick was very helpful and took the time to teach me how to make wounds on the backs of mice. Dr. Yun Wang is an intelligent, caring person who was always willing to provide input on experimental designs I had and I always enjoyed running into her at Target. I will be forever indebted to Dr. Tracy Hookway who acted as a surrogate mentor during the lab move to Gladstone. She is an incredibly caring individual who always found the time to listen to my concerns, read over abstracts, and give me the encouragement to pursue my goals. I have also been fortunate to participate with professors outside my department and want to thank my collaborators, Dr. Andrew Lyon and Dr. Ronghu Wu. I am also very appreciative that Dr. Lyon shared his expertise in materials synthesis and characterization and always providing helpful feedback during our many meetings. I was also very fortunate to work alongside his previous graduate student, Dr. Shalini Saxena, who always provided encouragement and was full of excitement for our joint project. Dr. Wu has been incredibly helpful in providing help during our mass spectrometry studies and I've enjoyed working in collaboration with his student Johanna Smeekens, who has always been incredibly helpful.

I am also thankful for the friendships I have formed outside of the lab. I truly appreciate all the laughs and fun I've had with Torri Rinker, Reggie Tran, and Ariel Kniss over the years from taking early morning biology classes at Emory to white water rafting trips. I would especially like to thank Torri Rinker and Tom Bongiorno, my BBUGS Education and Outreach co-chairs, for all her help when we had to set up the many school trips and Buzz on Biotechnology. I've been fortunate to receive many fellowships during my graduate career, which has introduced me to many people. I would like to than all the friends I've made through the GT UCEM program, Stefany Holguín, Jada Selma, Michelle Collins, Daniel Largo, Sergio Garcia, and Yancy Mercado. In particular, I have grown incredibly close with Stefany and Jada,, who have helped me to keep my sanity during the rough patches. Each of them have been incredibly supportive and are always willing to provide a shoulder to lean on and an ear to listen. They are both such fun to talk to and I've truly enjoyed all of our political and social discussions we've had over the years. Additionally, I would like to thank all of my friends, especially Jillian Terry, and trainers at my gym, X3 sports, where I would go to let off steam when I was frustrated by lab work. I am also thankful for the IBB staff, Andrew Shaw and Aqua Asberry, Colly Mitchell, and Meg McDevitt and the BME dept, Shannon Sullivan, Shannon Barker, Tracey Dinkins, and Sandra Powell and for all their support and advice during my graduate career.

Last, but definitely not least, I would like to thank my mom, dad, sister, brother, and grandparents. I want to thank my parents, Beate and Robert Sullivan, for not only providing emotional support, but also providing financial support so that I could concentrate on my graduate studies. I've also appreciated the many trips we took as a family to Germany, the Netherlands, and to Charleston, providing me with min-vacations from grad school to re-charge my batteries. I would also like to thank my sister, Nina, for

always willing to go on shopping sprees with me, and my brother, Nick, for always making sure I stayed humble. I would also like to thank the Brake family (Andreas, Andrea, Inga, and Annika) for all their support throughout the years and treating me like a surrogate daughter. I also want to thank my dog, Lily, and my two cats, Leela and Leo.

TABLE OF CONTENTS

LIST OF TABLES

LIST OF FIGURES

LIST OF ABBREVIATIONS

AFP	α-Fetoprotein
FGF2	Basic Fibroblast Growth Factor
BMP4	Bone Morphogenetic Protein-4
CM	Conditioned Media
EB	Embryoid Body
ESC	Embryonic Stem Cell
ECM	Extracellular matrix
GAG	Glycosaminoglycan
GF	Growth Factor
HBGF	Heparin-Binding Growth Factor
HMAm	Heparin-methacrylamide
IGF2	Insulin-Like Growth Factor Binding Protein
MS	Mass Spectrometry
NPC	Neural Precursor Cell
PAGE	Polyacrylamide Gel Electrophoresis
Pax6	Paired Box Protein-6
PCR	Polymerase Chain Reaction
pNIPMAm	Poly(N-isopropyl Methacrylamdie)
SDS	Sodium Dodecyl Sulfate
VEGF	Vascular Endothelial Growth Factor

SUMMARY

Embryonic stem cells (ESCs) represent a unique cell population that can differentiate into all three embryonic germ layers-endoderm, mesoderm, and ectoderm, rendering them an invaluable cell source for studying the molecular mechanisms of embryonic morphogenesis. Signaling molecules that direct tissue patterning during embryonic development are secreted by ESC aggregates, known as embryoid bodies (EBs), which emulate aspects of embryonic morphogenesis. ESCs within EBs spontaneously differentiate during *in* vitro culture synthesizing a complex array of various factors and soluble cues that direct cell fate. Furthermore, EB models provide an attractive *in vitro* platform from which cells of specific developmental stages, including vasculogenesis, can be enriched and analyzed for morphogen expression. Strategies to direct differentiation of EBs often employ an "outside-in" approach by addition of soluble factors to culture medium. However, diffusion of soluble factors into EBs is limited due to formation of dense outer cell layer, resulting in nonhomogenous differentiation. One method to direct differentiation and potentially overcome diffusion limitations is via incorporation of engineered microparticles (MPs), within 3D multicellular aggregates.

Extracellular matrix (ECM) components, such as glycosaminoglycans (GAGs), play crucial roles in cell signaling and regulation of morphogen gradients during early embryonic development through binding and concentration of secreted growth factors, thus directing patterns of tissue morphogenesis. ECM-mimetic materials or engineered MPs amenable to conjugation of highly sulfated GAGs, such as heparin, provide ideal matrices for manipulation of ESC morphogens via reversible electrostatic and affinity interactions. The long term goal of this work was to develop a novel biomaterial based approach to direct ESC differentiation and identify important molecules in stem cell signaling. The overall hypothesis of this proposal was that microparticles that mimic the

extracellular matrix can modulate ESC differentiation through sequestration of endogenous morphogens present within the EB microenvironment.

Synthetic *N*-isopropylmethacrylamide (NIPMAm) MP constructs were investigated as a biomaterial-based strategy to control the temporal release of BMP4 within ESC aggregates to induce mesoderm differentiation. pNIPMAm microgels were coupled to core polystyrene particles to combine the hydrophilic and morphogen-releasing properties of hydrogels with a dense core material that enhanced incorporation within EBs. MP synthesis produced well-coated population of MPs in terms of microgel coverage and low polydispersity. However, MPs incorporated with low efficiency within ESC aggregates. MP delivery of BMP4 within ESC aggregates demonstrated similar expression of mesoderm (Flk1) as compared to soluble BMP4 delivery, while ectoderm expression (Pax6) was significantly decreased as compared to soluble delivery. In addition, sentinel cells were used to monitor the spatiotemporal activation of BMP signaling in ESC aggregates, where maximum reported (CFP) expression was observed at day 2 of culture, coinciding with the burst release of BMP4 from MPs. Interestingly, ESC aggregates treated with unloaded MPs and soluble BMP4 demonstrated greater CFP expression over soluble BM4 treated aggregates, suggesting that unloaded MPs may bind and concentrate exogenously added BMP4 within aggregates to induce BMP signaling. Notably, the total amount of BMP4 delivered by MP was 10-fold less total growth factor as compared to soluble delivery to achieve comparable ESC differentiation, indicating that MP approaches can improve efficiency of differentiation, by reducing over delivery of soluble growth factor.

Given that native GAGs modulate important ESC signaling pathways, supplementation (or incorporation) of heparin may enable strategies to manipulate endogenous cell signaling. Heparin-derived MPs can thus serve as a biomimetic material that dynamically regulates growth factor presentation. Engineered materials

that mimic the ECM in its ability to actively sequester proteins present in cell culture or *in vivo*, as opposed to delivery of bound proteins via biomaterials, introduces a new paradigm to harness native sequestering interactions between cells and ECM. Incorporation of HMAm MPs within EBs demonstrated the native ability of natural GAG-based materials to modulate ESC differentiation. Incorporation of HMAm MPs within ESC aggregates demonstrated changes in gene and protein expression of neuorectodermal marker, Pax6. Histological analysis of aggregates with incorporated HMAm MPs exhibited more internal organized structures as observed via histolgical staining and more abundant protein expression for Nestin, a marker of neural precursor cells, as compared to untreated aggregates. It was also demonstrated that HMAm MPs can be used as a tool to sequester and concentrate biomolecules present in ESC conditioned media, while simultaneously reducing the amount of abundant species, such as bovine serum albumin (BSA), for gel electrophoresis and mass spectrometry analysis. Notably, MPs demonstrated approximately 20x less BSA binding, Furthermore, comparison of HMAm MPs with other GAG-based MPs exhibited different binding capacities for complex mixtures of proteins present in conditioned media, suggesting that MPs composed of different ECM components could be formulated to direct ESCs toward specific lineages. Ultimately, biomaterials capable of capturing morphogens in a reversible and concentrated manner similar to native GAG species will enable novel strategies for directed differentiation of ESCs toward defined cell types.

CHAPTER I

INTRODUCTION

Embryonic stem cells (ESCs) are a unique cell population that can differentiate into all three embryonic germ layers (endoderm, mesoderm, and ectoderm), rendering them an invaluable cell source for studying the molecular mechanisms of embryonic morphogenesis. Signaling molecules that direct tissue patterning during embryonic development are secreted by ESC aggregates, known as embryoid bodies (EBs), which emulate aspects of morphogenesis observed during embryonic development. As many of these signaling proteins interact with the extracellular matrix (ECM), manipulation of the ESC extracellular environment provides a means to direct stem cell differentiation. Extracellular matrix (ECM) components, such as glycosaminoglycans (GAGs), play crucial roles in cell signaling and regulation of morphogen gradients during early development through binding and concentration of secreted growth factors. Engineered biomaterials fabricated from highly sulfated GAGs, such as heparin, provide ideal matrices for manipulation and efficient capture of ESC morphogens via reversible electrostatic and affinity interactions. In particular, heparin can simultaneously bind and influence the activity of multiple factors (FGF, BMP, VEGF etc). **Thus, biomaterials designed to efficiently capture and retain bioactive ESC-derived morphogens offer an attractive platform to enhance the differentiation of ESCs toward defined cell types.** The *long term goal* of this work was to develop a novel biomaterial based approach to direct ESC differentiation and identify important molecules in stem cell signaling. The overall ***objective*** of this work was to examine the ability of microparticles synthesized from both synthetic and naturally-derived materials to enhance the local

presentation of morphogens to direct ESC differentiation. The overall ***hypothesis*** of this work was that microparticles that mimic the ECM can modulate ESC differentiation through sequestration of morphogens present within the EB microenvironment. The *rationale* for this work is that ECM-mimetic biomaterials can capture morphogens in a reversible and concentrated manner similar to native ECM species *in vivo*, thereby enabling strategies to define and examine ESC morphogens produced during differentiation. The central hypothesis of this proposal will be tested by the following specific aims:

Specific Aim 1: Evaluate the use of synthetic ECM-mimetic MPs for directed differentiation of ESCs within EBs. The *working hypothesis* was that engineered synthetic MPs that mimic the ability of the native ECM to sequester and release BMP4 within EBs will enhance the efficiency of ESC differentiation as compared to soluble delivery. BMP4 loading and release from MPs will be assessed as well as the efficiency of MP incorporation within EBs. Mesoderm differentiation of ESCs will be assessed by gene expression of markers of pluripotency (Oct4 and Nanog) and mesoderm (BrachyuryT and Flk1). Analysis of BMP signaling in ESCs in response to BMP will examined.

Specific Aim 2A: Evaluate the incorporation of heparin-based microparticles on ESC lineage differentiation. The *working hypothesis* was that incorporation of heparin MPs would enhance neuroectodermal differentiation of EBs. MP incorporation in EBs was performed by forced aggregation of ESCs and MPs at various cell to MP ratios. The impact of MP incorporation on cell morphology was assessed by histological staining (H&E, Safrinin-O, and Alcian Blue) and EB plating for presence of neurite outgrowth and Nestin expression. Gene and protein expression for neuroectodermal markers (Pax6

and Nestin) as well as markers of mesoderm (Flk1 and BrachyuryT) and endoderm (AFP) were assessed by PCR and immunostaining.

Specific Aim 2B: Characterize the profile of ESC morphogens captured by heparin MPs using gel electrophoresis and mass spectrometry analysis. The *working hypothesis* was that heparin MPs could be used to enrich for specific groups of morphogens secreted by differentiating ESCs. MPs were separated from dissociated embryoid bodies by density gradient centrifugation using a Percoll gradient. MP captured morphogens were analyzed by SDS-PAGE and mass spectrometry in order to characterize the classes of molecules presented by heparin MPs to ESCs during differentiation.

This proposal is ***innovative*** because it harnesses the native ability of ECM-based materials to sequester endogenous growth factors present within the EB microenvironment to drive ESC differentiation. Additionally, heparin-based materials can be used as an analytical tool to identify molecular factors involved in stem cell signaling. Ultimately, this proposal aims to develop a new class of biomaterials capable of capturing stem cell derived morphogens in a biomimetic manner to yield more efficient approaches for directed stem cell differentiation. It is anticipated that the results of this work will demonstrate the utility of an ECM mimetic biomaterial approach to harness the endogenous growth factors produced during ESC differentiation and ultimately encourage the use of biomaterials for directed stem cell differentiation approaches.

CHAPTER II

BACKGROUND

2.1 Embryonic stem cells

Embryonic stem cells (ESCs) have a unique regenerative capacity due to their ability to both self-renew and differentiate into a multitude of cells from various lineages, thus providing a promising avenue for tissue engineering and regenerative medicine therapies for treatment of cancer, diabetes, degenerative disorders and traumatic injuries. For instance, differentiation of ESCs toward cardiomyocytes [1–5], neurons [6–9], endothelial cells [10–12], and pancreatic β-cells [13–16] has already been achieved. ESCs were derived from the inner cell mass of mouse blastocysts and are capable of differentiating into all three embryonic germ layers - endoderm, mesoderm, and ectoderm, as well as germ cells [17,18]. Unlike adult stem cell populations, which are multipotent and limited in their ability to differentiate towards specific cell types, ESCs retain pluripotency through the process of self-renewal, rendering them an invaluable source for studying the molecular mechanisms of embryonic morphogenesis and cell fate decisions. Typical differentiation strategies require specific media formulations, requiring addition of cocktails of small molecules or supraphysiological doses of biomolecules. However, the plasticity of ESCs also makes the generation of defined cell types difficult, thus motivating the need for differentiation strategies that enhance the efficiency and yield of homogenous ESC populations for therapeutic applications.

2.2 ESC differentiation

During embryonic development, gastrulation is characterized by the formation of the three germ layers. More specifically, epiblast cells mobilize to the primitive streak (PS) where they subsequently undergo epithelial-to-mesenchymal (EMT) transition to generate mesoderm and definitive endoderm [19,20]. Although the regulation of cell fates observed during gastrulation are not fully understood, the spatiotemporal separation of various cell types in the PS suggest the presence of different signaling cues that direct stem cell differentiation. Previous studies have established that morphogenic factors from the transforming growth factor (TGFβ) [21], Nodal [22], and Wnt [23] family are essential for germ layer development.

Hematopoietic, cardiac, skeletal muscle and vascular lineages are derived from mesoderm supopulations during embryonic development. Following the formation of a PS-like population, early mesoderm is defined by the expression of brachyuryT, following upregulation of cell surface receptors, Flk1 and PDGFR [24,25]. In the absence of serum in cell culture, mesoderm formation is induced with supplementation of soluble BMP4 [26–28]. Furthermore, addition of Wnt to cell cultures with serum supplementation accelerates mesoderm development, while inhibition of Wnt blocks generation of brachyuryT expressing cells [29–31]. Nodal signaling is activated by addition of Activin A, inducing formation of mesoderm or endoderm populations [32]. In contrast, derivation of neural and skin lineages from ectoderm is induced by inhibition of BMP, Wnt, and Activin/Nodal signaling [32,33]. Characterized as the “default” pathway, neuroectoderm readily develops in the absence of serum or other PS inducers, and instead relies on endogenous FGF signaling [33]. Overall, these observations clearly indicate an important role for these signaling pathways in ESC differentiation and that manipulation of these pathways can be utilized to control differentiation *in vitro*.

2.3 Embryoid body differentiation

Differentiation of ESCs is commonly performed in monolayer, providing a defined substrate for cell attachment and uniform exposure to exogenously added soluble molecules, such as growth factors or small molecules; however, 3D approaches allow for a biological model of embryonic morphogenesis by facilitating multicellular interactions [34]. The 3D organization and proliferation, migration, and differentiation of an embryo can be modeled by the formation of pluripotent stem cell aggregates, known as embryoid bodies (EBs) [35]. EB formation has traditionally been used to induce spontaneous differentiation of ESCs towards the three germ lineages. Differentiation of EBs is characterized by the initial formation of two epithelial layers, with the specification of exterior cells toward primitive endoderm (PE), mediated by fibroblast growth factor (FGF) signaling via the PI 3-kinase pathway [36,37]. The PE layer eventually differentiates to form visceral and parietal endoderm, while cells at the exterior deposit a basement membrane composed of ECM components including type IV collagen and laminin [37,38]. The basement membrane serves to separate the PE layer from the internal undifferentiated cell population, where cells not in direct contact with the basement membrane may undergo apoptosis to form cystic cavities [39,40].

Culture platforms for EB formation include static suspension, hanging drop and forced aggregation [41]. Spontaneous formation of EBs is initiated by suspension of ESCs in a non-adhesive culture dish in the absence mouse embryonic fibroblasts (MEFs) feeder layers and/or Leukemia inhibitory factor (LIF). Dissociated ESCs are transferred to suspension cultures and allowed to aggregate to form 3-dimensional structures through the homophilic binding of the cell-cell adhesion molecule E-cadherin, which is highly expressed on the cell surface of undifferentiated ESCs [41,42]. However, static suspension of EBs often results in a heterogeneous population due to variable aggregate sizes and agglomeration, ultimately reducing the efficiency of differentiation.

More controlled EB formation can be accomplished by the hanging drop method, which involves the suspension of a relatively small number of cells within a single drop (10-20 μL) from the lid of a Petri dish [2]. While allowing for greater control of EB size, the hanging drop technique is labor-intensive and not amenable to scale up for bioprocessing applications. Alternatively, formation of EBs by rotary suspension culture has demonstrated improved aggregate formation, cell yield and homogeneity within the population [43]. Furthermore, high throughput culture formats have also been developed to improve uniform EB formation, such as AggreWell™ technology[44], dielectrophoresis [45], and bioprinting [46,47]. Ultimately, 3-dimensional culture of ESCs reduces the surface area required for cell culture, allowing for the scale up of culture systems for bioprocessing platforms, and ultimately generating larger quantities of specialized cell types for therapeutic applications.

EBs emulate aspects of morphogenesis observed during embryonic development rendering them an invaluable cell source for studying the molecular mechanisms of embryonic morphogenesis. [48] For instance, EBs cultured under angiogenic conditions exhibit formation of primitive vascular structures and expression of pro-angiogenic growth factors [11,49,50]. The appearance of early tissue structures such as neurite extensions, indicative of neuronal differentiation, and contractile activity, indicative of cardiomyocyte differentiation, have also been observed during EB differentiation [51]. Recent studies have demonstrated the formation of more complex structures, including tissues resembling the optic-cup [52], brain [53], and thyroid follicle from pluripotent stem cell aggregates [54]. The process of cell specification during EB differentiation is governed by the deposition of extracellular matrix (ECM) and subsequent cell integrin-ECM interactions. Additionally, various morphogens present in the embryonic environment collaborate with the ECM to coordinate the spatial and temporal differentiation of ESCs, suggesting that the regenerative potential of ESCs can be

harnessed by understanding the complex system of signaling molecules that function to control cell fate decisions. As many of these signaling proteins are derived from the extracellular matrix (ECM), manipulation of the ESC extracellular environment provides a means to alter stem cell behavior in order to induce specific cell behavior for therapeutic applications.

2.4 Extracellular matrix-cell interactions

2.4.1 Extracellular matrix in embryonic development

In addition to the intrinsic properties of ESCs that direct cell fate, embryonic development is also governed by ECM-growth factor interactions. At the earliest stages of embryogenesis, cellsbegin to produce endogenous ECM components such as collagen, laminin, fibronectin, and glycosaminoglycans (GAGs) that serve an important role in the regulation of cellular proliferation and differentiation during [55–58]. For instance, laminin appears as early as the 2-cell stage [59] and fibronectin and type IV collagen appear in the inner cell mass of day 3/4 blastocysts [60]. The ECM functions to control the spatiotemporal release of growth factors, facilitate growth factor-receptor interactions, and mediate morphogen gradients by providing a reservoir of proteins [61]. During cell specification, the ECM also serves to define boundaries between different cell types and provide scaffolding for developing organs. Furthermore, ECM facilitates cellular migration by providing an adhesive substrate for cell attachment during embryogenesis.

GAGs function to form morphogen gradients during early embryonic development by sequestration of secreted growth factors, thus directing the pattern of tissue morphogenesis. GAGs are ubiquitous in the pericellular space and are found bound to core proteins present on the cell surface and within the extracellular matrix.

GAGs are composed of linear polysaccharide chains consisting of repeating disaccharide units of an amino sugar (*N*-acetylglucosamine or *N*-acetylgalactosamine*)* and an uronic sugar (glucuronic acid or iduronic acid) or galactose and are classified into four types known as heparin/heparin sulfate (HS), chondroitin sulfate (CS)/dermatan sulfate (DS), keratan sulfate (KS), and hyaluronic acid (HA). In particular, HS has been extensively studied for its role in embryonic development, specifically in the regulation of FGF signaling where HS facilitates the formation of the FGF-FGFR complex [62–64].

Heparan sulfate (HS) is a negatively charged GAG that binds via electrostatic interactions to growth factors including VEGF, FGF2, and PDGF [65,66]. The sugar structure of HS chains consist of repeating units of glucuronic acid (GlcUA) and *N*-acetylglucosamine (GlcNAc), which are polymerized by the enzymatic complex Exostosin1/2 (EXT1/EXT2) during chain eleongation [67]. The backbone of HS is subjected to further modification such as de-N-acetylation, N-sulfation, 6-O-sulfation, 3-O-sulfation of glucosamine residues by enzymes N-deacetylase and N-sulfotransferases (NDST) as well as epimerization of GlcUA residues to iduronic acid (IdoUA) and 2-O-sulfation of IdoUA residues [68,69]. The resulting HS structure is characterized by regions of variably sulfated groups separated by nonsulfated regions along the backbone [70,71]. In contrast, heparin, a closed related GAG, is highly sulfated along the entire backbone length. Sulfation patterns are critical for the regulation recognition of soluble and matrix proteins such as members of the FGF family, ultimately governing their ability to influence cellular signaling activity.

2.4.2 HS/heparin in stem cell differentiation

The presence of GAGs is not only critical for embryonic development, but crucial for differentiation of ESCs in culture. Interestingly, approximately 80% of GAGs synthesized by ESCs are HS chains [72,73]. HS is known to bind to various signaling molecules, such as BMP, Wnt, and FGFs that regulate ESC self-renewal and differentiation. For example, HS acts as a co-receptor in the formation of the FGF-FGFR complex to initiate intracellular FGF signaling and ultimately drive ESC differentiation toward other cell lineages. Undifferentiated ESCs express a low sulfated form of heparan sulfate (HS), but begin synthesis of more complex and sulfated variants of HS in a spatiotemporal manner as stem cells differentiate toward specific lineages [70–72,74–76]. Furthermore, increases in overall sulfation are observed in ESCs undergoing differentiation [70,72,77]. It is hypothesized that remodeling of HS structure alters the affinity in of HS for specific biomolecules, ultimately affecting downstream signaling and cell fate decisions. For instance, neural differentiation is characterized by increased N- and 6-O- sulfation of HS chains, resulting in decreased binding of FGF2 as compared to HS of undifferentiated ESCs [70]. Microarray technology has also been utilized to probe GAG-protein interactions to demonstrate that HS binding with proteins is dependent on specific sulfation patterns [78].

Targeted deletion of chain elongation enzymes EXT1 or EXT1 prevents successful gastrulation in mice embryos and results in failure to form mesoderm and extrembryonic tissues [67][79]. In parallel, EXT1/EXT2$^{-/-}$ stem cells retain their pluripotency *in vitro* and fail to undergo yield successful ectodermal or mesodermal differentiation, [70,73,80,81]**.** Genetic removal of NDST1 reduces the sulfation of heparin resulting in death of mice shortly after birth due to respiratory difficulties [82,83], while NDST2-deficient mice remain viable but are unable to produce sulfated heparin [84]. ESCs derived from NDST1/2$^{-/-}$ mice produce HS chains without N-sulfation groups [83]**,**

and ultimately remain in a pluripotent state even under differentiation conditions *in vitro* [81,85]. EXT1$^{-/-}$ mouse ESCs (mESCs) fail to differentiate into Pax6^{+} neural precursor cells and BrachyuryT^{+} mesoderm due to limited FGF and BMP signaling [86]. Furthermore, NDST1/2$^{-/-}$ ESCs demonstrated reduced ERK1/2 phosphorylation, due to diminished FGF signaling even in the presence of exogenous FGF4 addition [81]. However, differentiation of heparin deficient ESCs can be recovered by the addition of soluble heparin to the culture medium [70,80,86]. Interestingly, the addition of soluble heparin to HS-competent ESCs has also been show to modulate differentiation. Supplementation of heparin to wild-type cells supported hematopoiesis at low concentrations, yet inhibited differentiation at high concentrations, demonstrating that GAGs can act as both positive and negative regulators of differentiation [80]. Furthermore, HS/heparin of specific concentrations, saccharide length, and sulfation pattern were observed to support the formation of Sox1^{+} neural progenitor cells from ESCs [87]

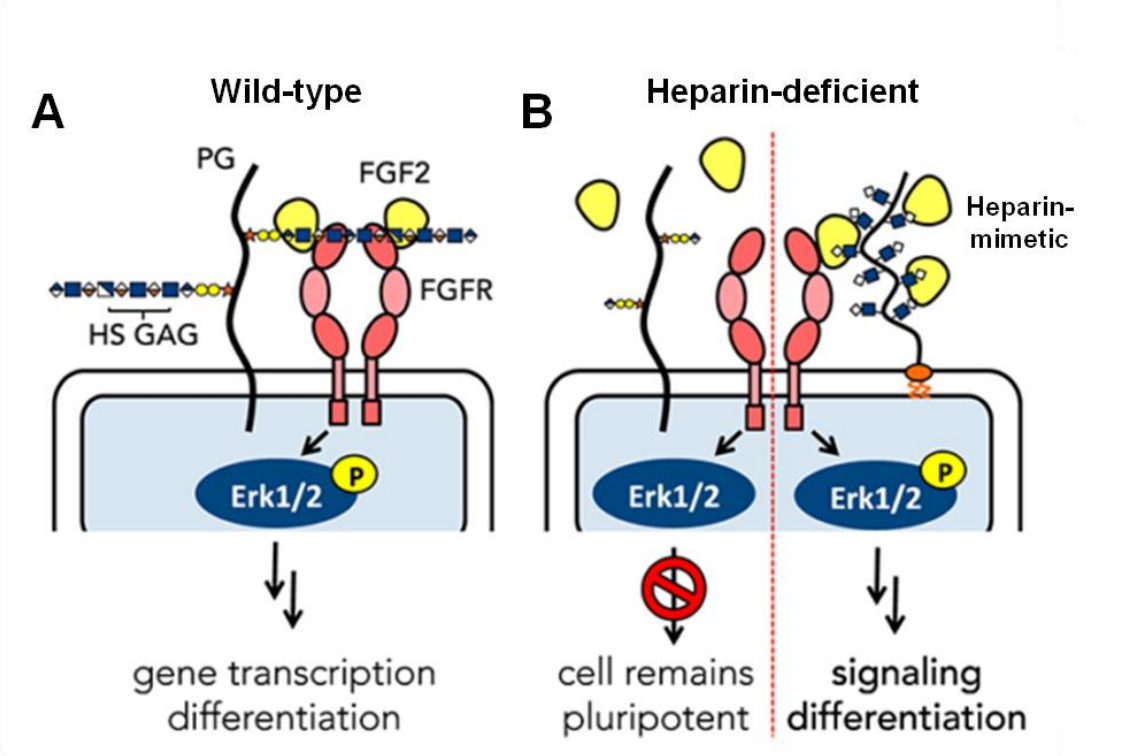

Figure 2.1. HS/heparin-based strategies for ESC differentiation. A) HS mediates intracellular signaling through the sequestration and binding of growth factors. For example, heparin facilitates the formation of the ternary HS-FGF-FGF complex to induce Erk1/2 phosphorylation and subsequent gene transcription. B) Heparin-dependent signaling pathways are reduced in heparin-deficient ESCs, but addition of exogenous heparin or heparin mimetic materials can be used to rescue or enhance ESC differentiation. Adapted from Huang et al. *JACS*, 2014.

2.5 Biomaterial strategies for directed stem cell differentiation

2.5.1 ECM-mimetic materials that regulate growth factor activity

The niche encompasses the stem cell microenvironment, including growth factors, cell-cell interactions, and cell-matrix contacts that work together to regulate cell fate. In embryonic development, growth factors are tightly regulated in a spatiotemporal manner to regulate cell fate. For *in vitro* cell culture, growth factors can be endogenously produced by cells or added exogenously to direct cell fate. One method to

impart control over niche interactions *in vitro* is use of synthetic or naturally derived ECM biomaterials. Fabrication of ECM materials that preserve the unique signaling capabilities of native ECM enhances the potential of biomaterials to be used for regenerative therapies. Fabrication of biomaterials that incorporate heparin, chondroitin, laminin, and other ECM components have been used to localize and concentrate growth factor activity [88,89]. Therefore, engineering materials that mimic the ECM in its ability to actively sequester proteins have gained significant interest to regulate stem cell behavior. Ultimately, manipulation of ECM-cell interactions can be used to regulate growth factor signaling and improve the generation of defined cell populations as well as enable advancement of stem cell-based therapies.

2.5.1a Synthetic strategies to localize growth factor activity

A number of synthetic biomaterial strategies have been employed to mimic the ability of the ECM in order to regulate growth factor activity through the binding and release of molecules present in the cellular microenvironment. Synthetic peptides that mimic native GAG growth factor binding abilities have been investigated. PEG hydrogel microspheres with incorporated synthetic VEGF binding peptides were synthesized to reversibly bind VEGF, enabling targeted control over upregulation or downregulation of signaling activity by either release or sequestration [90,91]. Hubbell et al. identified synthetic heparin mimetics by screening a library of peptides with specific sulfate groups that bound VEGF with high affinity [92]. Synthetic peptides with variable sulfation patterns were synthesized that bound with high affinity and specificity to multiple heparin-binding peptides, such as human platelet factor 4 and antithrombin III, and growth factor VEGF [93]. Ultimately, synthesis of peptides can be used locally to control

growth factor activity, but with improved levels of specificity for growth factors of interest as compared to native ECM which interacts with a multitude of biomolecules.

Cell surface engineering strategies to mimic the function of native HS-mediated growth factor signaling have been investigated. Remodeling of the glycocalyx, a glycoprotein-polysaccharide complex surrounding the cell membrane, has emerged as a promising method to introduce specific glycan epitopes to the cell surface to influence various biological processes, such as GAG-growth factor interactions. Synthetic neoproteoglycans (neoPGs) with affinity for FGF2 were incorporated into plasma membranes of heparin deficient ESCs in order to rescue FGF-mediated kinase signaling and support neural differentiation [94]. Membranes of neurons were remodeled with CS functionalized-liposomes, inducing increased activation of key neurotrophin signaling pathways and enhanced axon outgrowth from cells [95]. Accelerated neural differentiation was observed in mESCs with membrane-bound HaloTag proteins (HTPs) functionalized with specific HS derivatives [96]. While remodeling of the glycocalyx presents a unique opportunity to regulate cell signaling, strategies to control presentation of specific glycan epitopes, such as manipulation of metabolic pathways for glycan biosynthesis [97,98], covalent grafting of glycans to surface proteins [99], or passive incorporation of synthetic glycans into the cell membrane [100,101], rely on altering the native cell structure.

2.5.1b ECM-derived biomaterials for localized growth factor activity

Cell-derived ECM has been previously used to in culture to support cell expansion and differentiation *in vitro*, in addition to *in vivo* tissue regeneration [102,103]. Decellularization of ESC aggregates has been performed to isolate and characterize morphogens and ECM components retained by acellular EB matrices [104–106].

Decellularized ECM (dECM) obtained from undifferentiated ESC monolayers, undifferentiated aggregates, and differentiated EBs at various stages of lineage specifications influenced ESC proliferation and differentiation, suggesting that dECM maintains its signaling capability [79,107]. ECM derived from ESCs and fibroblasts were used to direct cell specification of naïve mESCs, where differentiation of cells toward definitive endoderm was enhanced with laminin addition [108]. Ultimately, bioactive ECM could potentially be utilized as a scaffold to regulate ESC differentiation; however, more thorough characterization, such as mass spectrometry analysis, of morphogenic factors retained by dECM is necessary to completely identify the complex milieu of factors that work together to govern cell fate.

Due to their strong binding interactions with a variety of growth factors present in the ESC microenvironment, GAGs present an attractive source for the fabrication of biomaterial delivery vehicles. Past approaches to immobilize GAGs on biomaterials have focused on incorporation of sulfated GAGs within polymer gels or covalent attachment of GAGs onto synthetic scaffolds. In particular, heparin and HS have been covalently and non-covalently incorporated into biomaterials for the delivery of well-known heparin binding growth factors. Heparin has been conjugated to fibrin [109,110], PLGA [88] and polyethylene (PEG) [111] gels for sustained release of factors such as FGF2 and VEGF. Other studies have examined the effect of heparin and other GAGs, without addition of exogenous factors. Notably, stem cells cultured on heparin-PEG gels demonstrated decreased activation of mitogen-activated protein kinase (MAPK), a critical protein in the FGF signaling pathway [111]. These results suggest that heparin is capable of binding FGF2 and modulating downstream signaling. Encapsulation and coculture of MSCs with osteoblasts in heparin-functionalized PEG gels exhibited improved osteogenic differentiation, suggesting that heparin limited the diffusion of osteoblastic factors away from MSC [112]. Previous studies have also incorporated heparin within plasma

polymerized alluylamine (ppAm) electropsun scaffolds to provide signaling cues to seeded ESCs during culture [113]. The fabrication of electrospun meshes with non-covalent immobilization of heparin was used to mimic the fibrous architecture of the native ECM and ultimately support the expansion and neural differentiation of ESCs. Non-covalent interactions of heparin and biomaterials have also been explored. Self-assembling monolayers (SAMs) fabricated with heparin-binding peptides were used to sequester heparin present in serum, resulting in enhanced MSC proliferation and osteogenic differentiation through local amplification of FGF and BMP signaling activity [114,115]. Improved signaling was achieved without supraphysiological doses of soluble growth factor supplementation, providing further evidence that GAG-based materials can be used to study the influence of endogenous factors on cell behavior.

In contrast to previously described materials that incorporated ECM or GAG components within polymer networks, the fabrication of microparticles (MPs) composed solely of GAG or ECM has been established as a novel means to improve growth factor binding and retention as well as delivery to specific cell populations. MPs composed of heparin-methacrylamide (HMAm) demonstrated improved binding of several heparin-binding proteins such as BMP2, VEGF, and bFGF over other growth factor delivery vehicles, as well as maintaining growth factor bioactivity when used to stimulate ALP activity in skeletal myoblasts [116]. Similarly, chondroitin sulfate methacrylamide (CSMA) micro- and nanoparticles were synthesized to characterize the electrostatic interaction and release between positively charged TGF-β1 and negatively charged TNF-α from CSMA particles [117]. Furthermore, fabrication of MPs from gelatin, obtained from denatured collagen, provides a biomaterial that not only binds and releases growth factors such as BMP4 and bFGF, but can be degraded by collagenase to modulate growth factor release kinetics [118].

2.5.2 Microparticles for ESC differentiation

Strategies to direct differentiation of embryonic stem cell EBs often employ an "outside-in" approach by addition of soluble factors to culture medium. For example, soluble BMP4 is often added to induce mesoderm differentiation in ESCs. However, diffusion into EBs is limited by the formation of a dense outer layer composed of ECM and cells [119]. One method to direct differentiation and potentially overcome diffusion limitations is incorporation of engineered MPs, which have been widely used to control delivery of entrapped molecules, within 3D aggregates. Multiple parameters such as MP size, material, and delivery of small molecules or growth factors have been examined to determine their influence on stem cell differentiation. For example, incorporation of poly(lactic-*co*-glycolic acid) (PLGA) MPs of varied diameters demonstrated that MP size can modulate stem cell differentiation [120].

Several studies have examined the delivery of growth factors or small molecules from MPs incorporated within EBs. Delivery of retinoic acid via PLGA MPs incorporated within aggregates induced formation of cysts, with an outer epiblast layer resembling the structure of an early stage mouse embryo [121]. Furthermore, delivery of PIGF, VEGF, and bFGF from PLGA MPs demonstrated enhanced differentiation of hESCs down the vascular lineage, and limited differentiation toward ectoderm and endoderm [122]. PLGA MPs loaded with simvastatin or BMP2 were incorporated within EBs to promote osteogenic differentiation, while MPs loaded with VEGF demonstrated improved endothelial differentiation [123]. Local delivery of BMP4 and thrombopoietin by incorporated type A gelatin microparticles functionalized with heparin enhanced the generation of hematopoietic progenitors as compared to soluble bulk delivery [124]. Both gelatin and heparin-functionalized gelatin MPs have been utilized to deliver BMP4 to support mesoderm differentiation, requiring almost 12-fold less total protein as compared to traditional bulk delivery methods [125]. Delivery of growth factors via microparticles

has also been used to direct differentiation of multipotent stem cells. Chondroitin sulfate fabricated microparticles were used to deliver TGFβ to examine chondrogenesis within mesencyhmal stem cell (MSC) aggregates [126]. These results demonstrate that localized release of drugs or morphogenic factors directly within stem cell aggregates can direct differentiation. While MP mediated delivery of growth factors to stem cell aggregates has been successfully used to direct differentiation, previous studies have also observed that different materials used to fabricate MPs can also be modulate cell fate. For instance, agarose, PLGA, and gelatin microparticles affected the emergence of specific ell phenotypes [127]. Ultimately, the development of a new class of biomaterials capable of capturing and modulating the activity of stem cell derived morphogens in a biomimetic manner will provide new insights into stem cell differentiation.

CHAPTER III

pNIPMAm MICROPARTICLES FOR DELIVERY OF BMP4 TO PLURIPOTENT STEM CELL AGGREGATES

Introduction

Embryonic stem cells (ESCs) were first derived from the inner cell mass of mouse blastocysts and represent a unique cell population that can differentiate into all three embryonic germ layers (endoderm, mesoderm, and ectoderm), rendering them an invaluable cell source for studying the molecular mechanisms of embryonic morphogenesis [17,18]. While previous studies have modeled differentiation of ESCs in monolayer, formation of ESC aggregates, known as embryoid bodies (EBs) can be used to model the organization, migration, and differentiation of cells during embryonic development [48,51,128,129]. The spatial and temporal differentiation of ESCs within EBs is regulated by numerous coordinated interactions between soluble factors, cell-cell interactions, and extracellular matrix, which help to define the biochemical and mechanical properties of the EB microenvironment to regulate cell fate [128,130]. Strategies to direct differentiation of ESC aggregates often employ an "outside-in" approach by addition of soluble factors to culture medium. For example, soluble BMP4 is often supplemented to direct mesoderm differentiation by inducing expression of transcription factor BrachyuryT [28,131]. However, the formation of a dense outer layer composed of ECM and cells during EB differentiation limits the diffusion of exogenously added soluble factors, which may in part, be responsible for heterogenous cell differentiation [132,133]. One method to direct differentiation more effectively and

potentially overcome diffusion limitations is incorporation of engineered microparticles (MPs), which have been widely used to control molecular delivery locally, within 3D multicellular aggregates [121,122,124,125]. Delivery of retinoic acid via PLGA MPs induced formation of cystic cavities within aggregates [121], whereas gelatin and heparin-functionalized MPs have been used to delivery BMP4 to support mesoderm differentiation, requiring almost 12-fold less total protein as compared to traditional bulk delivery methods [125]. However, MP synthesis is limited with respect to control over uniformity in MP size, growth factor payload, and release rates.

The use of synthetic materials offers customized control over biomolecule release as the physical and chemical properties, such as degree of crosslinking, overall charge, and type of polymer,can be altered for specific stem cell differentiation strategies [128]. Commonly used in drug delivery and tissue engineering applications, hydrogels are three-dimensional networks of physically or chemically cross-linked, hydrophilic polymers that can be designed to mirror the flexibility of native tissuedue to their high water content (~90%) [134–137]. Hydrogel properties such as overall charge, which can enhance loading or retention of biomolecules, and network mesh size, which determines the mobility and diffusion rate of embedded biomolecules and is characterized by the cross-linking density and polymer-solvent interactions, can also be tailored for specific applications [138]. Furthermore, hydrogels maintain growth factor bioactivity for delivery. Biomolecule loading is performed by the “breathing in” method, in which a concentrated volume of protein is added to lyophilized hydrogels, where upon exposure to water, hydrogels swell and imbibe growth factors [139].

Poly(N-isopropylacrylamide) (pNIPAM), a commonly used thermosensitive polymer can be chemically modified by the addition of a methyl group to form p(N-isopropylmethacrylamide) (pNIPMAm). Increasing the transition temperature from 31 to 43℃ allows the polymer to maintain a swollen hydrated state at physiological

temperatures and permit passive diffusion of entrapped soluble factors. Hydrogel MPs, termed microgels ranging in size from 100 nm to 1μm, have been previously fabricated from pNIPMAm for use in drug delivery studies [140–143]. “Raspberry-like” particles composed of core polystyrene MPS surrounded by a shell of microgels have been fabricated using colloidal-phase mediated heteroaggregation [144]. Ultimately, coupling of pNIPMAm microgels to core particles combines the hydrophilic and morphogen-releasing properties of hydrogels with a dense material that enhances incorporation within EBs. The overall objective of this study was to characterize pNIPMAm MPs for controlled delivery of bioactive BMP4 and incorporation in ESC aggregates.

Methods

Synthesis and characterization of pNIPMAm MPs

The MP construct is a core-shell structure. The shell consists of microgels composed of 68% *N*-isopropylmethacrylamide (NIPMAm), 2% *N,N’*-methylenebis(acrylamide) (BIS), 30% acrylic acid (AAc) and was synthesized by precipitation polymerization[1]. Microgels were synthesized by dissolving 140 mM of NIPMAm and BIS in dI H_2O to a final total monomer concentration of 140 mM and purged with nitrogen for 1 hour. AAc and ammonium persulfate (APS) were added and the solution was held at ~70 °C overnight. The microgel solution was filtered through glass wool, purified via centrifugation, and lyophilized for storage. Microgel hydrodynamic radius (R_H) values were determined using a DynaPro Dynamic Light Scattering (DLS) system (Wyatt, Technology, Santa Barbara, CA). Carboxylated-PS core particles (Spherotech, Inc, Lake Forest, IL) were functionalized with 4-aminobenzophenone (AB) (25 mM) using EDC (2 mM)/NHS (5 mM) coupling in DMSO.

Microgel heteroaggregates were prepared by solvating microgels in dI H_2O and mixing with AB-functionalized core particles resuspended in 0.75% w/w ethanol. The samples were exposed to UV for 30 minutes and purified via sequential centrifugation. Microparticles were imaged using a NOVA FIB FEI Scanning Electron Microscope (FEI, Hillsboro, OR) and a Zeiss confocal microscope. All reagents were purchased from Sigma-Aldrich (St. Louis, MO).

BMP4 loading and release from MPs

MP concentration in PBS was counted using a hemacytometer. MPs were dehydrated prior to growth factor loading by resuspending MPs in 70% ethanol in microcentrifuge tubes and allowing for evaporation of ethanol overnight at room temperature. Lyophilized BMP4 (R&D) was resuspended in 0.1% BSA in PBS prior to addition to dehydrated MPs. The BMP4 binding capacity of MPs was examined by addition of 1 ml of a low (10ng/mg MP) and high (100 ng/mg MP) dose of BMP4 in 0.1%BSA over 18 hours at either 4 °-C to promote rehydration of MPs and subsequent uptake of BMP4. Depletion of BMP4 from solution by MPs from the growth factor solution was quantified by analyzing the supernatant BMP4 concentration via an enzyme-linked immunosorbent assay (ELISA). After addition of BMP4 solution, MPs were centrifuged at 5,000 RPM for 5 minutes for removal of supernatant (or unbound BMP4). One ml of 0.1% BSA in PBS solution was added to pelleted MPs. Passive release of BMP4 at 37 ° C was determined by removal of 300 µl of supernatant after centrifugation of BMP4-loaded MPs every day for the first week of release and at two weeks.

Alkaline phosphatase (ALP) activity assay

Skeletal myoblasts (C2C12) were seeded at 20,000 cells per well in a 96-well plate in growth media (DMEM with 16% FBS) for 6 hours to promote cell attachment.

Cells were then switched to low serum media (DMEM with 1% FBS) immediately prior to treatment with soluble BMP4, unloaded MPs, unloaded MPs and soluble BMP4, or BMP4 loaded MPs. ALP activity of C2C12 cells was quantified by addition of 50 µL of cell lysate with 50 µL of CellLytic M and 100 µL of substrate solution consisting of 3.33 mM $MgCl_2$ (VWR, West Chester, PA), 400 mM 2-amino-2-methyl-1-propanol (Sigma Aldrich), and 6.67 mM p-nitrophenyl phosphate (pNPP, Sigma Aldrich). After termination of the reaction with 0.2 M NaOH, the absorbance was measured at 405 nm on a microplate reader (Biotek, Winooski, VT) and total ALP activity was determined using a standard curve generated from 4-nitrophenol.

Cell culture

Undifferentiated D3 ESCs were maintained in monolayer culture on 0.1% gelatin coated tissue culture dishes in Dulbecco's modified Eagle's medium (DMEM) media with high glucose supplemented with 15% fetal bovine serum (FBS) (Hyclone), 2 mM L-glutamine (Gibco), non-essential amino acids (NEAA) (Gibco), penicillin and streptomycin (Gibco), 0.1mM β-mercaptoethanol (Gibco), and 10^3 U/ml leukemia inhibitory factor (LIF). D3 ESCs were cultured at 37 °C in a humidified 5% CO_2 atmosphere. Approximately 10 mL of media was exchanged during ESC culture occurred every 2 days and cells were passaged every 3 days before reaching approximately 75% confluency. Monolayer cultures of undifferentiated BMP sentinel cells were maintained in the KO-N2B27 media composed of Knock-out DMEM (Gibco) supplemented with N2 (Gibco) , B27 (Gibco), 100 U/ml penicillin, 100 U/ml streptomyocin, 0.25 mg/ml amphotericin, 2 mM L-glutamine, 10 ng/ml bone morphogenetic protein 4 (BMP4) and 10^3 U/ml LIF. Serum-free KO-N2B27 media without BMP4 and LIF was used for all suspension ESC aggregate cultures.

Embryoid body formation and culture

Prior to EB formation, ESCs were trypsinized into single-cell suspension culture. EBs were formed by forced aggregation of single cell ESCs in micro-well inserts composed of 3% agarose. Briefly, 1000-cell EBs were formed by addition of 1.2 million cells resuspended in 0.5 ml of media and added to each insert, containing approximately 1200 wells. Inserts containing cells were centrifuged at 200 x g for 5 minutes to aggregate cells within individual wells. After 18 hours of culture, aggregated cells were removed from wells by gently pipetting with a wide bore pipette tip. Next, EBs were transferred in petri dishes at a concentration of 1200 EBs/ml and maintained in KO N2B27 media. EBs were maintained in suspension culture on rotary orbital shaker at 45 RPM to prevent agglomeration. EBs were re-fed every 3 days and 90% of spent media was exchanged with fresh media. In studies using BMP4 supplementation, 10 ng/ml of soluble BMP4 was added to culture media during initial centrifugation of ESCs in inserts, after transfer of EBs to suspension culture, and at all subsequent media exchanges. Prior to centrifugation, MPs were resuspended with ESCs in media and added to inserts. After 24 hours of formation, aggregates were collected and volumes chose to contain approximately 40-50 aggregates from each MP to cell incorporation ratio was chosen to count the precise number of aggregates per volume. After enzymatic dissociation of aggregates, the number of MPs was counted using a hemacytometer and normalized to the number of lysed aggregates to determine the number of MPs incorporated per EB.

Gene expression analysis

Differentiation of EBs treated with BMP4-loaded MPs was assessed via quantitative PCR. RNA was extracted from undifferentiated ESCs and EBs at Day 2, 4, and 6 of differentiation using the RNeasy Mini Kit (Qiagen). Reverse transcription of RNA to complementary DNA was performed using the iScript cDNA synthesis kit

(BioRad) and was analyzed using SyberGreen technology on the MyIQ cycler (BioRad). Forward and reverse primer sequences for *Oct4, Nanog, BrachyuryT, Flk1, Pax6, AFP,* and *18S* were designed with Beacon Design software and are described in Table 1. Gene expression was quantified with respect to levels of gene expression of undifferentiated ESCs and EBs without MPs or BMP4 supplementation.

Table 3.1. PCR sequence and conditions for qPCR

Gene	Forward Sequence	Reverse Sequence	Melt Temp
18S	CTCTAGTGATCCCTGAGAAGTTCC	ACTCGCTCCACCTCATCCTC	58.0
Oct-4	CCG GTGAGGTGGAGTCTGGAG	GCGATGTGAGTGATCTGCTGTAGG	58.0
Nanog	GAA ATCCCTTCCCTCGCCATC	CTCAGTAGCAGACCCTTGTAAGC	58.0
Brachyury-T	CACACCACTGACGCACAC	GAGGCTATGAGGAGGCTT TG	58.0
Flk-1	GGCGGTGGTGACAGTATC	TGACAGAGGCGATGAATGG	64.3
Pax-6	ACGGCATGTATGATAAACTAAG	GCTGAAGTCGCATCTGAG	58.0
AFP	CACACCCGCTTCCCTCATCC	TTCTTCTCCGTCACGCACTGG	58.0

Histology

EBs were collected, fixed in 10% formalin, and embedded in Histogel (Thermo Scientific), processed and paraffin embedded. Paraffin embedded samples were cut into 5 µm thick sections (Microm HM 355S). Deparaffinized sections were stained with hematoxylin and eosin (H&E) and imaged with a Nikon 80i upright microscope using the SPOT flex camera (15.2 64 MP Shifting Pixel, Diagnostic Instruments, Sterling Heights, MI).

Flow Cytometry

EBs were washed with PBS and dissociated to single cell suspension with 0.25% trypsin-EDTA and trituration for 10 minutes. The single cell suspension was washed 3 times in PBS and fixed in 10% formalin with centrifugation at 200 x g for 5 minutes between each wash. Flow cytometry was performed with a BD LSRII flow cytometer (Becton Dickinson, East Rutherford, NJ) with a minimum of 10,000 events per sample collected within the FSC/SSC gate for cell populations. Microparticles and undifferentiated BMP sentinel cells were used to establish appropriate gates and controls. Polygonal gating was used on the FSC/AmCyan (405 nm excitation; 491± emission) plots to limit 1% of untreated embryoid body population ("No MP" group) via FlowJo software (Tree Star, Inc., Ashland, OR).

Confocal microscopy

The presence of rhodamine-labeled microgels and CFP expressing sentinel cells within EBs was analyzed using a LSM 700-405 confocal microscope (Zeiss, Thornwwod, NY). EBs were washed in PBS 3 times, fixed in 10% formalin for 30 minutes, and stained with either Hoescht (1:100) or ethidium homodimer (1:500) before imaging.

Statistical Analysis

ll data are reported as mean ± standard error for a minimum of triplicate experimental samples. A Box-Cox power transformation was used to normalize data to a Gaussian distribution before statistical analysis. Statistical significance was assessed using a one-way ANOVA with Tukey's post hoc analysis. A *p*-value of less than 0.05 was considered statistically significant.

Results

pNIPMAm MP characterization

pNIPMAm MPs were fabricated using a modified version of colloidal-phase mediated heteroaggregation in order to produce large batches of microparticles to enable investigation of *in vitro* applications (Figure 3.1). Phase images of pNIPMAm MPs indicated that MPs exhibit round shapes and a low polydisperse population (Figure 3.2A). SEM imaging revealed that polystyrene core particle are fully covered by a shell of microgels, presenting a soft, biocompatible surface to surrounding cells (Figure 3.2B). Confocal imaging of rhodmaine functionalized microgels indicated that microgels were fully swollen and cover the majority of the core particle in solution (Figure 3.2C). Fabrication of MPs produced approximately 18 million MPs per mg of polymer with an average diameter of 4.6 $\pm$ 1.0 μm (Figure 3.2D).

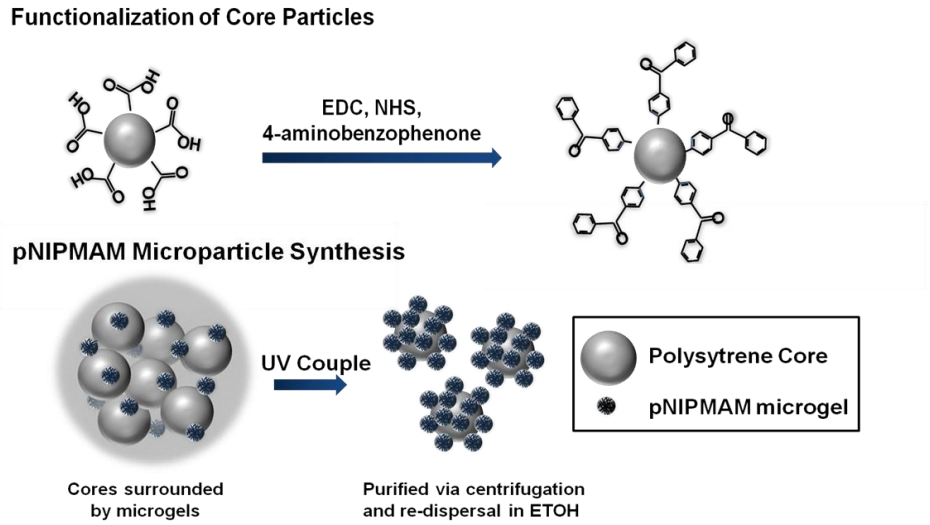

Figure 3.1. Schematic of pNIPMAm MP synthesis. The MP construct is a core-shell structure synthesized by preciptitation polymerization. The the shell consists of microgels composed of 68% NIPMAm, 2% BIS, 30% AAc Carboxylated-PS core particles were functionalized with 4-aminobenzophenone using EDC/NHS chemistry Microgel hetteroaggregates were prepared by mixing microgels functionalized core particles and exposing samples to UV.

BMP4 loading and release from pNIPMAm MPs

The hydrophilic nature of the microgels promotes immediate swelling upon exposure to water, subsequently imbibing growth factors present in the surrounding solution. Additionally, microgels are negatively charged due to their acrylic acid content, allowing for electrostatic interactions with positively charged BMP4 (pI = 8.97). The binding capacity of MPs for BMP4 was examined by measuring the depletion of BMP4 from solution, ranging in concentration from 2-2,000 ng protein per milligram of MP (Figure 3.2E). MP binding capacity of BMP4 increased with increasing concentrations of BMP4. Below 100 ng per mg of MP, the relationship between MP bound BMP4 and loading concentration of BMP4 was relatively linear (R^2 = 0.998) with approximately 71.7% ± 16.9% of BMP4 bound to MPs. However, at BMP4 concentrations above 100

ng per mg MP, the efficiency of BMP4 binding decreased to approximately 45.0% ± 14.9%.

Release of BMP4 from MPs was assessed at low (10 ng per mg of microparticles) and high (100 ng per mg of microparticles) concentrations of BMP4 at 37 °C. MPs loaded with the high concentration of BMP4 demonstrated a greater initial burst release within the first 3 hours (< 40%) and released a larger amount of BMP4 over 14 days than MPs loaded with a low concentration of BMP4 (Figure 3.2F). Independent of initial loading mass, MPs loaded with both low and high concentrations of BMP4 exhibited sustained release over the first 7 days. Overall, total release of BMP4 after 14 days was approximately 60% of loaded protein, indicating that the majority of the protein was released by the MPs during this time (Figure 3.2G).

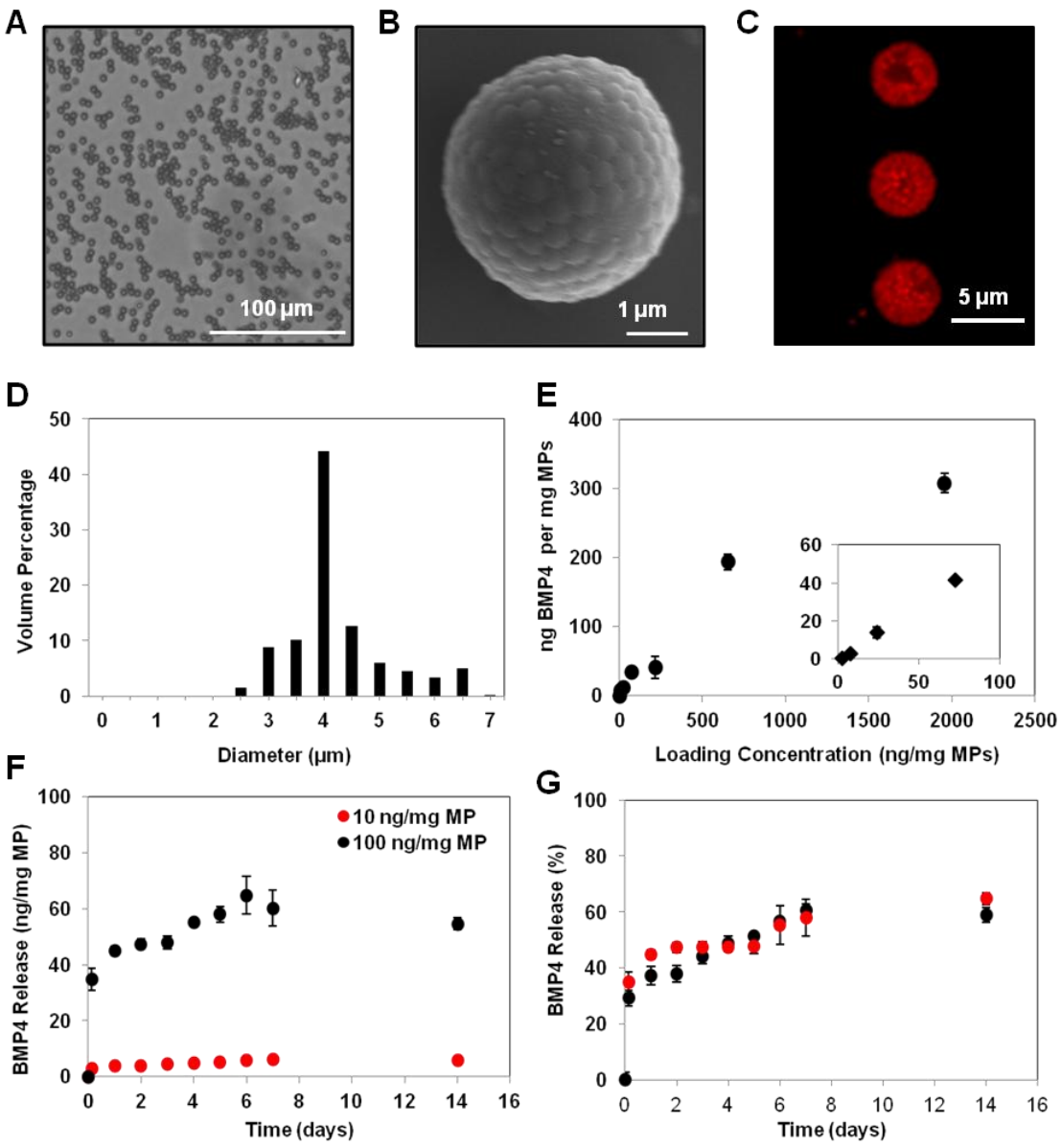

Figure 3.2. pNIPMAm MP characterization. (A) Phase image of MPs demonstrates the even polydispersity and spherical shape of particles. (B,C) Colloidal-phase mediated heteroaggregation was scaled up to produce uniformly coated MPs as indicated by SEM and confocal imaging (D) Coulter counter size analysis of MPs demonstrates a narrow size distribution with an average diameter of 4.6 ± 1.0 µm. (E) MPs demonstrated increased growth factor binding capacity with increasing initial growth factor loading concentrations. Average loading efficiency for BMP4 was 55.5 ± 6.2%. (F, G) Release of BMP4 from MPs was directly dependent on the initial loading amount of BMP4 and demonstrated increased release for 7 days with less than 60% of BMP4 was released at both loading amounts.

Delivery of BMP4 via pNIPMAm MPs to skeletal myoblasts

Bioactivity of BMP-4 loaded MPs was evaluated using an *in vitro* alkaline phosphatase (ALP) assay to quantify ALP activity of skeletal myoblasts (C2C12s), following treatment with soluble BMP4, unloaded MPs, unloaded MPs and soluble BMP4, or BMP4 loaded MPs. Treatment with BMP4 loaded MPs induced ALP activity similar to delivery of soluble BMP-4, suggesting that loaded MPs maintain BMP-4 bioactivity and ability to initiate a functional response, even with less than 25% release of BMP4 (Figure 3.3A). Overall, treatment of cells with BMP-4 (soluble or loaded) demonstrated increased ALP activity as compared to unloaded MP and untreated groups. Interestingly, simultaneous treatment of unloaded MPs and soluble BMP4 induced significantly less ALP activity in comparison to soluble BMP4 treatment, suggesting that MPs may sequester free BMP-4 and prevent subsequent interactions with cells. No differences in DNA content were observed between groups (Figure 3.3B)

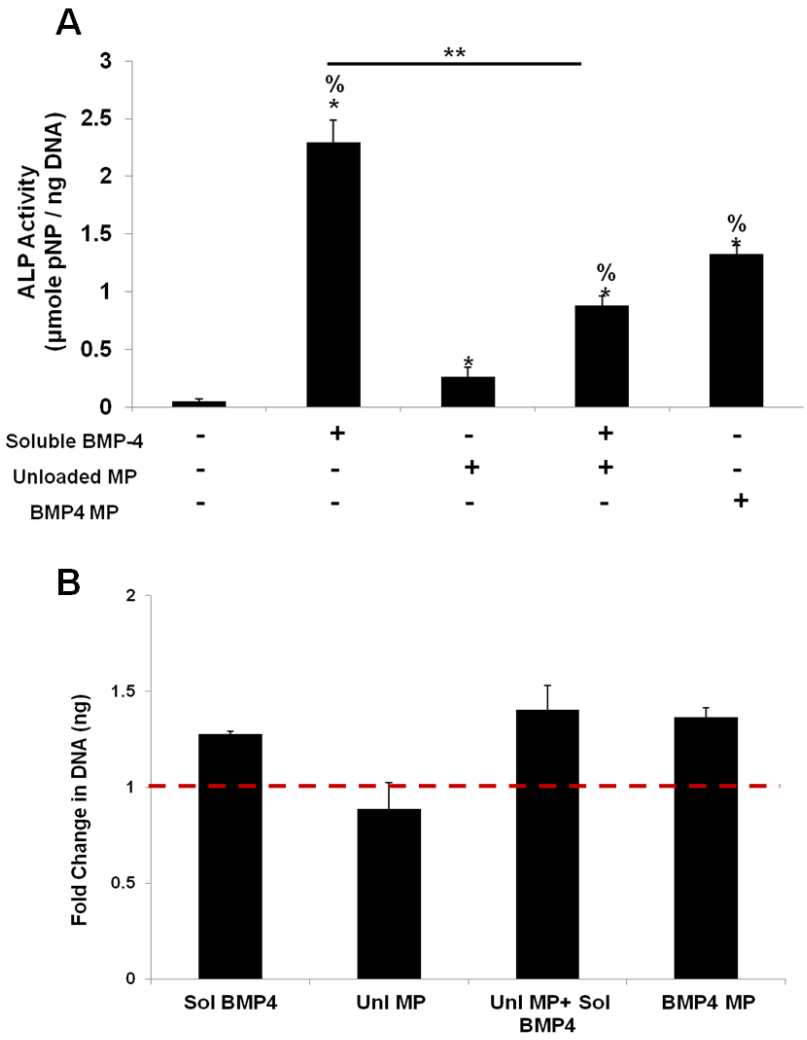

Figure 3.3. BMP4 bioactivity was evaluated by quantifying ALP activity of C2C12 cells after 3 days of treatment. BMP4 (soluble or loaded) increased ALP activity compared to unloaded MP and No MP. BMP4 MPs induced similar ALP activity to soluble BMP4, indicating comparable bioactivity. Unloaded MPs with soluble BMP4 induced less ALP activity compared to soluble BMP4 alone, suggesting that MPs actively sequester free BMP4 and prevent interactions with cells. (n =3; $p<0.05$ compared to: * No MP; $ Unloaded MP)

Incorporation of pNIPMAm MPs in EBs

MPs were incorporated within ESC aggregates using forced aggregation via centrifugation within agarose microwells at 1:10, 1:3, 1:1, and 3:1 (MP:cell) seeding ratios. Rhodamine B-labeled MPs incorporated within aggregates were identified by fluorescent and confocal microscopy (Figure 3.4A). Maximum MP incorporation within aggregates was achieved with approximately 80 MPs per ESC aggregate at a MP to cell seeding ratio of 1:1 (Figure 3.4B), which was used for all subsequent studies. Incorporation efficiency of microparticles within aggregates decreased as the number of MPs to cell ratio increased (Figure 3.4C). Additionally, formation of uniform ESC aggregates in the presence of 3:1 seeding ratio was hindered, which may, in part, be due to lack of cell-adhesive sites on MP constructs that prevented formation of cell-cell contacts (data not shown).

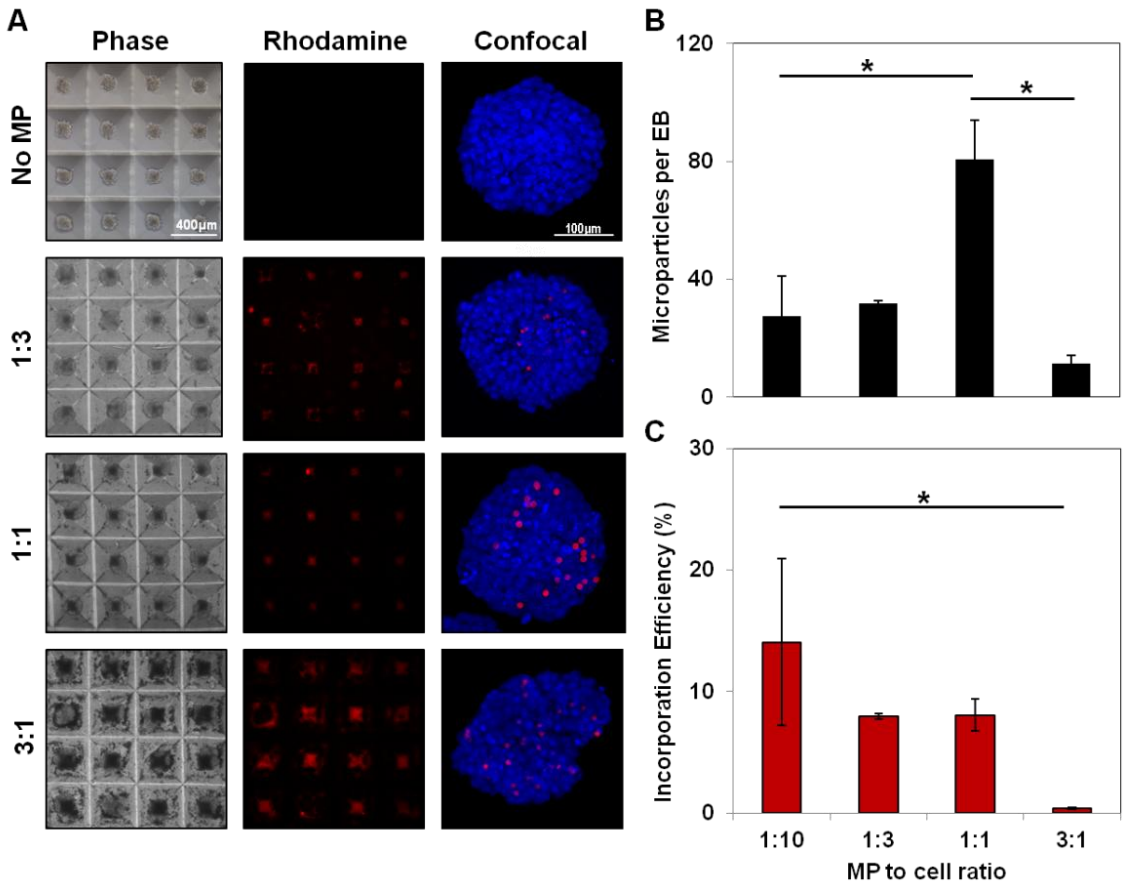

Figure 3.4. MPs are incorporated within pluripotent stem cell aggregates.(A) ESCs were centrifuged alone or with rhomadine –labeled MPs to form aggregates in µ-wells before transfer to rotary orbital suspension culture. MPs were incorporated in EBs at MP:cell seeding ratios of 1:10, 1:3, 1:1 and 3:1. (B) Maximum MP incorporation was approximately 80 MPs per EB at a 1:1 ratio. MP incorporation efficiency was < 20% for all ratios. (* $p < 0.05$; $n = 4$)

Delivery of BMP4 via pNIPMAm MPs to EBs

MPs were used to deliver BMP4 within ESC aggregates to promote mesoderm differentiation under serum-free conditions. BMP4 delivery by pNIPMAm MPs to ESC aggregates was compared to unloaded MPs and treatment with soluble BMP4 (10ng/mL) with or without incorporation of unloaded MPs (Figure 3.5). BMP4 was delivered by MPs at a loading concentration of 1500 ng of growth factor per mg of MPs.

The total corresponding amount of growth factor delivered via MPs to 1200 EBs per culture plate was 10 ng of BMP4. Subsequently, growth factor delivery via MPs was 10-fold less than the total amount of soluble BMP4 supplemented at the beginning of EB culture (Day 0). Incorporation of pNIPMAm MPs within EBs did not appear to have any gross effect on cell morphology through 6 days of culture (Figure 3.5).

Gene expression of pluripotency markers, Oct4 and Nanog, early lineage commitment markers, BrachyuryT, Flk1, Pax6, and AFP, were analyzed at day 6 of differentiation (Figure 3.6) As expected, all experimental groups demonstrated decreased expression of pluripotent transcription factors Oct4 and Nanog over the course of differentiation. No significant differences in BrachyuryT expression were observed between treatment groups. However, delivery of soluble BMP4 loaded MPs resulted in increased expression of the mesoderm marker, Flk-1, and decreased expression of ectoderm marker, Pax6. BMP4 loaded MPs demonstrated similar expression of Flk1, Pax6, and AFPcompared to soluble delivery. Interestingly, only ESC aggregates treated with BMP4 loaded MPs demonstrated significant differences in Pax6 expression as compared to all other treatment groups

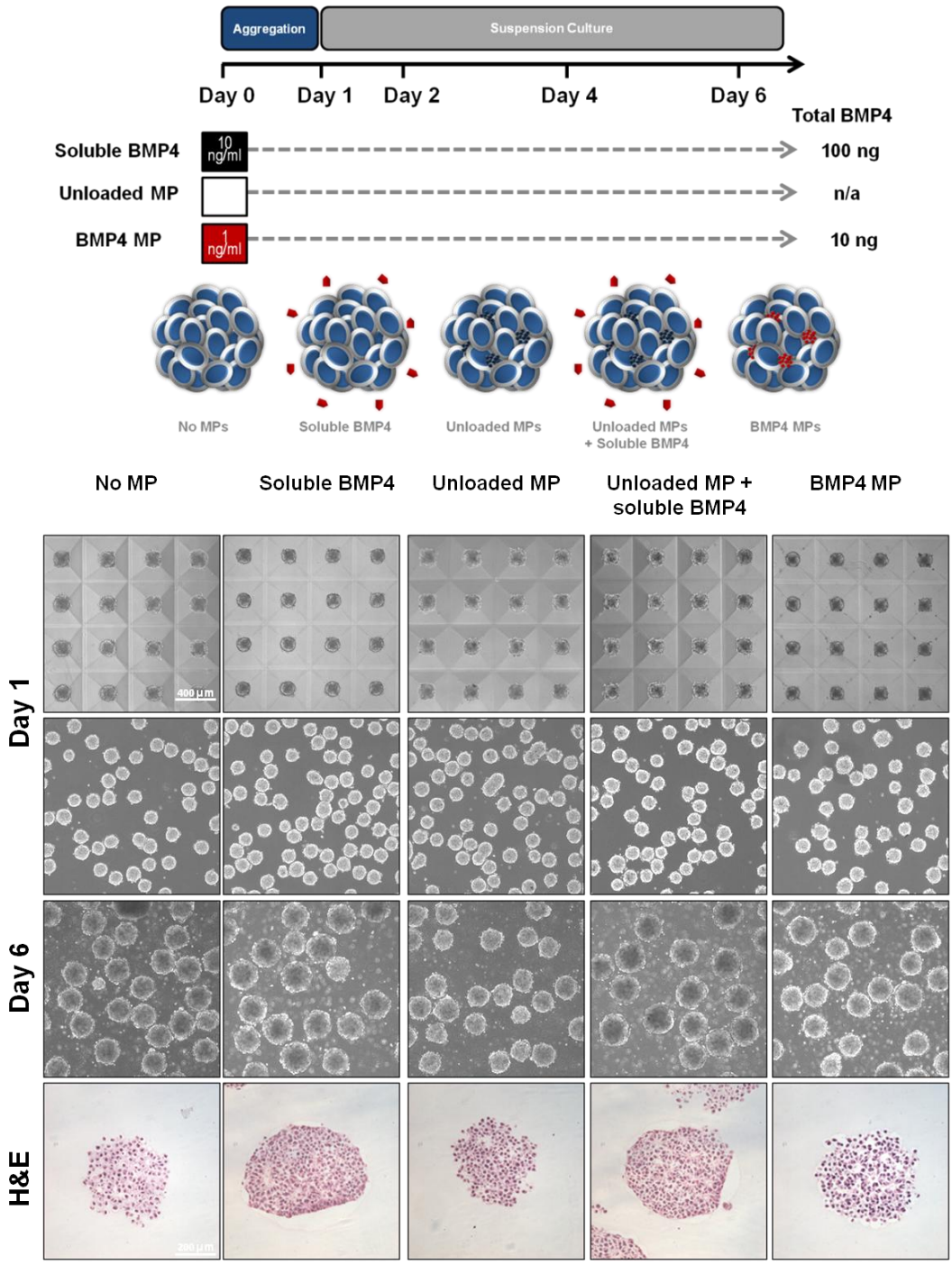

Figure 3.5. BMP4 loaded pNIPMAm MPs were incorporated in EBs via forced aggregation. BMP4 loaded MPs were incorporated in EBs via forced aggregation in agarose μ-wells and maintained in rotary suspension culture at 40 RPM for 6 days. Hematoxylin & eosin staining of Day 7 aggregates with or without treatment of soluble or MP bound BMP4 exhibited no gross differences in morphology (bottom row).

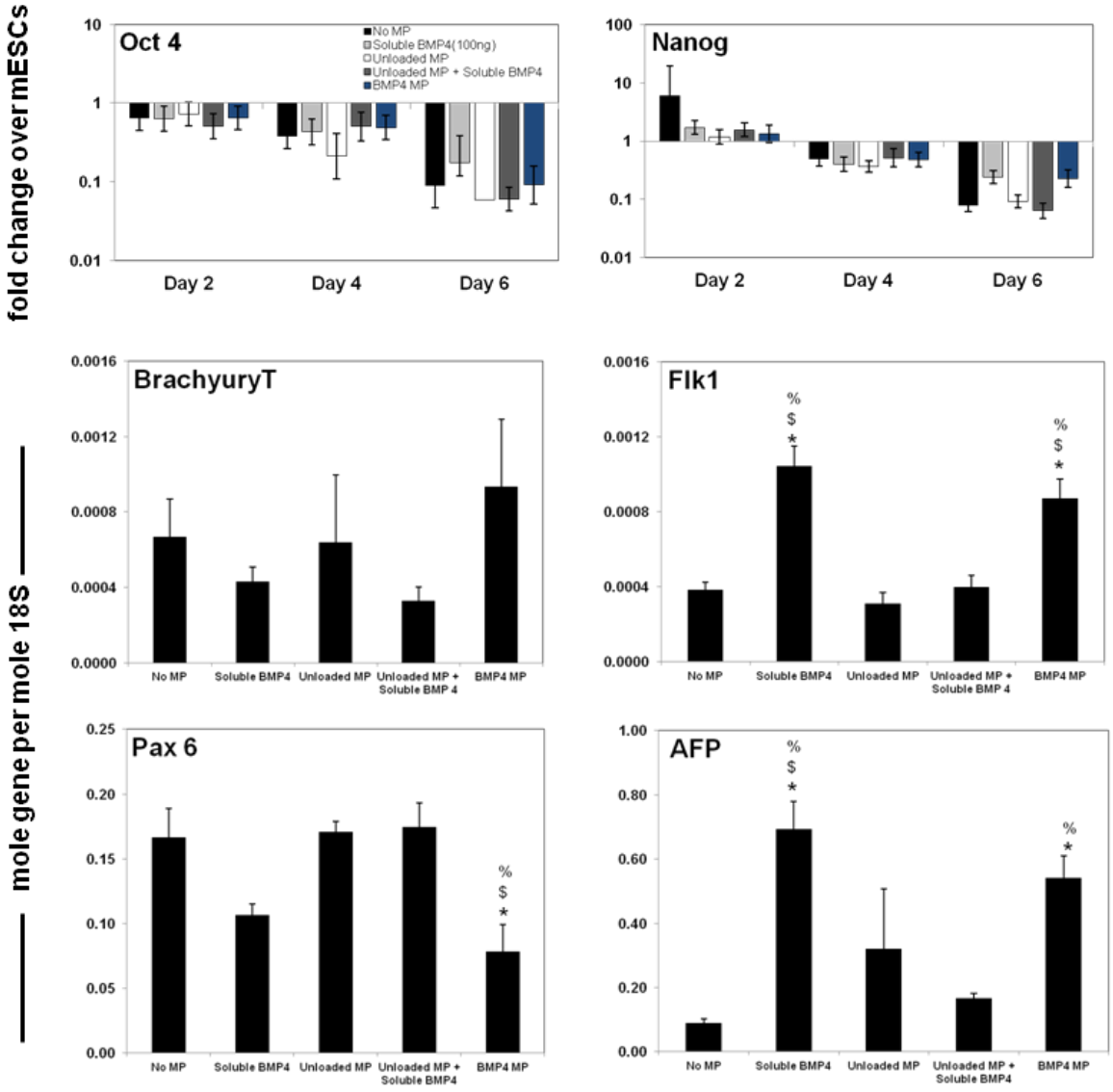

Figure 3.6. BMP4 loaded MPs incorporated within pluripotent stem cell aggregates induces mesoderm differentiation. Directed differentiation of ESCs via soluble or MP delivery of BMP4 induced comparable levels of early lineage commitment markers, despite delivery of 10 fold less BMP4 by MPs. Expression of pluripotency markers, Oct4 and Nanog, decreased over the course of culture and demonstrated no changes between any of the treatment groups. Soluble or MP delivery of BMP4 induced comparable expression of Flk1 (mesoderm) and AFP (endoderm) in day 6 ESC aggregates, however no differences in expression of mesoderm marker, BrachyuryT, was observed. Interestingly, only ESC aggregates treated with BMP4 delivered via MPs demonstrated significant decreased expression of Pax6 (ectoderm). (*= significantly from no MP;$=significant from unloaded MP;%=significantly from unloaded MP + soluble BMP4, n = 5; $p<0.05$)

BMP Signaling in ESCs

BMP sentinels allow for monitoring of the spatial and temporal presentation of BMP signaling in differentiating ESC aggregates in response to MP delivery of BMP4. ESC signaling sentinels were created with response elements for BMP (IBRE-4-CFP) inserted at the -228 site of the endogenous *Rosa26* locus [145]. CFP expression peaked at day 2 of differentiation for all groups, with maximum CFP expression observed in samples treated with BMP4 loaded MPs. At day 2, EBs were fixed and counterstained with a nuclear dye (Hoescht) and imaged using a confocal microscope (Figure 3.7A). Little CFP expression was observed in untreated ESC aggregates or ESC aggregates with unloaded MPs. In contrast, CFP expression was observed throughout ESC aggregates treated with soluble BMP4 or BMP4 loaded MPs.

CFP expression was quantified by flow cytometry of positive ESCs after dissociation of day 2 aggregates (Figure 3.7B,C). At day 2 of differentiation, CFP expression was limited in the untreated (1.2 ± 0.1%) and unloaded MP (1.1 ± 0.1%) groups. BMP4 delivered by MPs exhibited significantly greater expression of CFP positive cells (21.0 ± 1.8%) at 2 days of culture as compared to all other groups. Soluble addition of BMP4 demonstrated significantly higher CFP expression (6.0 ± 0.6%) as compared to untreated and unloaded MP groups. Interestingly, ESC aggregates treated with unloaded MPs and soluble BMP4 showed significantly more CFP expression (21.3 ± 0.2%) than ESC aggregates treated only with soluble BMP4, suggesting MPs may bind exogenous BMP4 via electrostatic interactions and attain a higher local concentration of BMP4. Positive CFP expression decreased to less than 5% for days 4 and 6 for all experimental groups (data not shown).

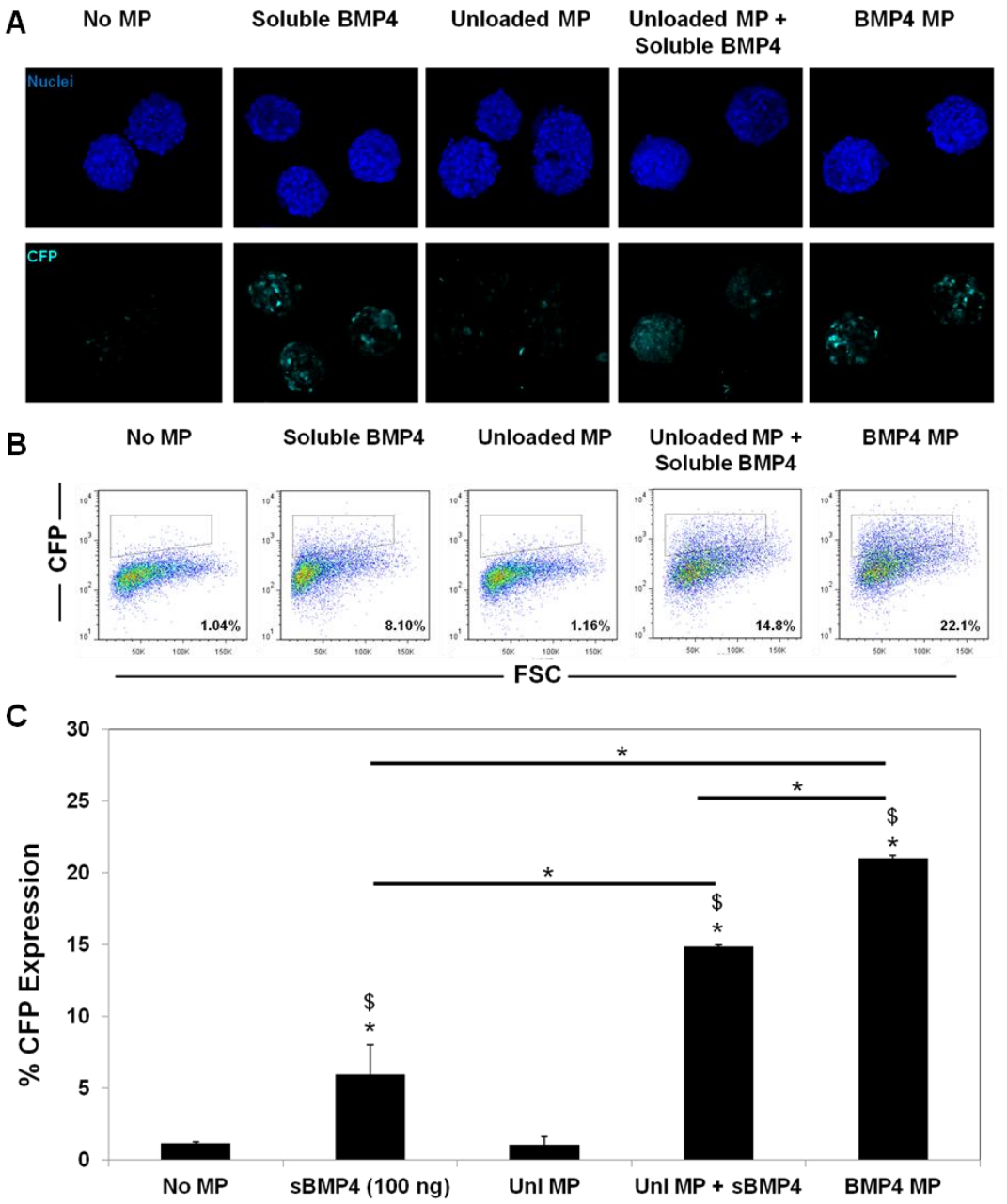

Figure 3.7. BMP signaling in ESC aggregates. (A) BMP4 loaded MPs were incorporated in aggregates of BMP signal responsive sentinel ESCs with CFP fluorescence reporter. Positive CFP expression was observed by confocal microscopy in groups with BMP4 (soluble or loaded) at day 2, while all other treatment groups exhibited little CFP expression. (B,C) Flow cytometry of CFP+ cells from dissociated ESC aggregates was performed at day 2. ESC aggregates treated with BMP4 loaded MPs expressed significantly more CFP (21.0 ± 1.8%) as compared to soluble delivery (6.0 ± 0.6%) of BMP4.(n=4; * = significantly from No MP; $ = significantly from Unloaded MP, $p < 0.05$).

Discussion

In this study, we demonstrated that pNIPMAm MP mediated delivery of BMP4 within ESC aggregates can be used as a biomaterial based strategy to enhance ESC differentiation. MP characterization indicates that colloidal-phase mediated heteroaggregation produces a well-coated population of MPs with low heterogeneity in terms of microgel coverage. Consistent microgel coverage is critical for uniform presentation of material and growth factors to surrounding cells. Furthermore, microgel characterization indicated low polydispersity (~1 μm) as compared to previously explored delivery vehicles such as PLGA, heparin, or gelatin based MPs [116,120,127]. Low polydispersity of both microgels and MPs minimizes variations in loading and release rates of BMP4. MPs also exhibited minimal aggregation during lyophilization, which is ideal for delivery vehicles loaded with morphogens while in a dehyrated" state, and after incorporation within EBs, resulting in even distribution of MPs and uniform delivery of BMP4 throughout aggregates.

The total amount of BMP4 released from MPs was dependent on initial growth factor loading concentration; however, more than 50% of BMP4 was released over a period of 14 days regardless of the initial amount of bound growth factor. Initial studies demonstrated that BMP4 released from pNIPMAm MPs was able to induce similar ALP activity in skeletal myoblasts as compared to soluble BMP4 treatment after 72 hours of culture, suggesting that BMP4 released from MPs remains bioactive. As previous studies have demonstrated that incorporation efficiency of MPs is directly related to material adhesivity, the low incorporation efficiency (< 10%) of pNIPMAm MPs was most likely due to lack of cell adhesive sites [127]. While no significant differences were observed in the formation of ESC aggregates at MP to cell seeding ratios of 1:10, 1:3, and 1:1, formation was hindered at higher MP to cell seeding ratios resulting in smaller

and less spherical shaped aggregates, suggesting MPs may interrupt the formation of necessary E-cadherin mediated cell-to-cell contacts for aggregation at seeding ratios higher than 1:1. For future studies, increased MP incorporation could be achieved by incorporation of Arg-Gly-Asp (RGD) or other cell adhesion sequences to microgels [146].

MP delivery of BMP4 within ESC aggregates resulted in similar expression of mesoderm and ectoderm markers as compared to soluble delivery. While no significant differences were observed in the expression of the transient mesoderm marker BrachyuryT, expression of Flk1 was significantly increased in groups treated with either soluble BMP4 or BMP4 loaded MPs. Under basal conditions, ESCs typically differentiate toward neuorectoderm, known as the default pathway [18]. However, expression of Pax6, an early marker of ectoderm, was significantly decreased in ESCs treated with BMP4 loaded MPs as compared to all other treatment groups, suggesting BMP4 loaded MPs may limit ESC differentiation toward ectoderm. Previous studies have demonstrated that BMP signaling is required during mesoderm specification to induce expression of $Flk1^{+}$ hematopoietic mesoderm from cell populations expressing BrachyuryT [24,26]. BMP signaling is initiated by the interaction of BMPs with cell surface receptors that ultimately activate intracellular SMAD 1/5/8 signaling and subsequent gene transcription [21]. BMP signaling sentinels provide a unique tool to monitor the spatial and temporal activation of BMP signaling in ESC aggregates [145]. In accordance with the release profile of BMP4 from MPs, the highest CFP expression was observed at day 2 of culture, coinciding with the majority of BMP4 release from MPs, indicating that BMP4 loaded MPs can influence early ESC differentiation events. Maximum CFP expression was observed in ESC aggregates treated with BMP4 loaded MPs, indicating that MPs can present bioactive BMP4 to cells to induce BMP signaling. Interestingly, ESC aggregates treated with unloaded MPs and soluble BMP4 demonstrated greater CFP expression than aggregates treated with only soluble BMP4,

suggesting that unloaded MPs may sequester soluble BMP4 and enhance the local concentration of BMP4 in direct contact with cells. The microgels of pNIPMAm MPs are composed of 30% acrylic acid and most likely attract native cationic morphogens, including BMP4, resulting in increased concentration of morphogens within ESC aggregates. Overall, these results demonstrate that the amount of BMP4 delivered by MP required 10-fold less total growth factor as compared to soluble delivery to modulate ESC differentiation, suggesting that growth factors presented from MPs can induce more efficient ESC differentiation than soluble delivery.

Conclusion

Herein, we have demonstrated that synthetic pNIPMAm MP constructs can be used as an “inside-out” tool to control the release of morphogens within ESC aggregates. Synthesis of pNIPMAm constructs demonstrates low polydispersity and uniform distribution of microgels on polysystrene particles. MPs can load and release morphogens in a controlled manner within EBs, thus improving the efficiency of ESC differentiation by requiring 10-fold less BMP4 as compared to soluble delivery. By utilizing a synthetic approach to mediate morphogen delivery, the development of customized delivery vehicles for delivery of pre-loaded MPs or capture of endogenously produced morphogens can be utilized to enhance the yield of specific cell phenotypes.

CHAPTER IV

HEPARIN-METHACRYLAMIDE (HMAM) MICROPARTICLES ENHANCE NEUROECTODERMAL DIFFERENTIATION OF EMBRYONIC STEM CELL AGGREGATES

Introduction

Extracellular matrix (ECM) components, such as glycosaminoglycans (GAGs), play crucial roles in cell signaling and regulation of morphogen gradients during early embryonic development via binding and concentration of secreted growth factors [55,147]. GAGs are of specific interest as they regulate morphogen gradient formation during early embryogenesis by sequestering secreted biomolecules, thus directing patterns of tissue morphogenesis [148]. ESC aggregates, otherwise known as embryoid bodies (EBs), emulate aspects of morphogenesis observed during embryonic development by producing signaling molecules that direct tissue patterning during embryonic development [48]. As our understanding of the role of ECM in ESC biology increases, use of ECM analogues to alter GAG-mediated signaling pathways has emerged as a potent means to manipulate ESC differentiation more effectively.

Differention of EBs can be directed by addition of soluble factors to the culture medium; however "outside-in" approaches are limited by non-homogenous differentiation of EBs, as diffusion of soluble factors is limited by the formation of a dense outer layer composed of ECM and cells [119]. An alternative approach for directed differentiation of EBs is through the introduction of engineered microparticles (MPs)

[121,127,149]. In particular, MPs have been used previously as delivery vehicles for sustained release of morphogens and small molecules within 3D stem cell microenvironments [124–126]. Given that native GAGs modulate important ESC signaling pathways, supplementation of heparin via material incorporation may enable novel strategies to manipulate endogenous cell signaling. Heparin, similar in structure to heparan sulfate (HS), binds numerous ESC secreted growth factors in a reversible manner with high affinity (i.e. VEGF, FGFs, and BMPs) [68,150,151]. Thus, engineered biomaterials amenable to conjugation with highly sulfated GAGs, such as heparin, provide ideal matrices for manipulation and efficient capture of ESC morphogens via reversible electrostatic and affinity interactions.

A number of material approaches have been employed to mimic the ability of the ECM to buffer growth factor activity through the binding and release of molecules present in the extracellular environment [90,113,152]. Previous work has demonstrated that the material of MPs can influence ESC differentiation within EBs [127]. As described in Chapter 1, unloaded pNIPMAm MPs demonstrated the ability to modulate cell behavior, providing further evidence that incorporation of MPs within EBs can modulate patterns of differentiation by material-growth factor or material-cell interactions. Promising results have demonstrated that addition of heparin to ESCs can enhance hemangioblast specification of cells and thus may play a key role in processes involved in vasculogenesis and angiogenesis [80,110,150]. Previously, heparin-derived MPs have been fabricated that are capable of sequestering large amounts of bioactive growth factors, such as BMP2, VEGF, and FGF2, and serve as a biomimetic material that dynamically regulates growth factor presentation [116]. Thus, biomaterials designed to efficiently capture and retain bioactive ESC-derived morphogens offer an attractive platform for improving directed stem cell differentiation strategies.

Methods

Cell culture

Undifferentiated D3 ESCs were maintained in monolayer culture on 0.1% gelatin coated tissue culture dishes in Dulbecco's modified Eagle's medium (DMEM) media with high glucose supplemented with 15% fetal bovine serum (FBS) (Hyclone), 2 mM L-glutamine (Gibco), non-essential amino acids (NEAA) (Gibco), penicillin and streptomycin (Gibco), 0.1mM β-mercaptoethanol (Gibco), and 10^3 U/ml leukemia inhibitory factor (LIF). D3 ESCs were cultured at 37 °C in a humidified 5% CO_2 atmosphere. Media was completely exchanged every 2 days and cells were passaged every 3 days before reaching approximately 75% confluency.

Embryoid body formation and culture

Prior to EB formation, cells were trypsinized into single-cell suspension culture. EBs were formed by forced aggregation of single cell ESCs in 400 μm micro-well inserts composed of 3% agarose. Briefly, 1000-cell EBs were formed by addition of 1.2 million cells resuspended in 0.5 ml of media and added to each insert, containing approximately 1200 wells, in a 24-well plate. Inserts containing cells were centrifuged at 200 x g for 5 minutes to aggregate cells within individual wells. After 18 hours of culture, aggregated cells were removed from microwells by gently pipetting with a wide bore pipette tip. Next, EBs were transferred to 100 mm petri dishes at a concentration of 1200 EBs/ml and maintained in either Knock-out DMEM (Gibco) supplemented with N2 (Gibco) , B27 (Gibco), 100 U/ml penicillin, 100 U/ml streptomyocin, 0.25 mg/ml amphotericin, and 2 mM L-glutamine or ESC culture media without LIF on a rotary orbital shaker at 45 RPM. EBs were re-fed every 3 days and 90% of spent media was exchanged with fresh media. Incorporation of HMAm MPs within ESC aggregates was performed by resuspending HMAm MPs with ESCs in media, added to inserts, and then followed by centrifugation..

Collection and analysis of spent media

At days 4, 7, 10 and 14 of suspension culture, EBs were collected in 15 mL conical tubes and allowed to sediment to the bottom of the tube. Media was removed and centrifuged at 10,000 RPM for 10 minutes to pellet cell debris. Supernatant media was collected and stored at -20˚C. Spent media was analyzed for FGF2, VEGF, BMP4, and IGF2 concentrations via an ELISA assay (R&D Systems, Minneapolis, MN).

HMAm MP incorporation analysis

Heparin methacrylamide (HMAm) was synthesized as previously described [116]. Fluorescently labeled HMAm was fabricated by dissolving 300 mg HMAm in 30 ml of 0.1 M Na_2HPO_4, 0.1 M EDC, and 10 mM Alexa Fluor 633 hydrazide (Life Technologes). The solution was allowed to react for 2 hours under stirring conditions at room temperature and then the total volume of reaction was dialyzed using 2000 kDA tubing (Spectrum Laboratories, Rancho Dominguez, CA) in 1L of diH_2O for 1 day. MPs were fabricated from AF633 labeled HMAm as previously described [116]. After 24 hours of formation, aggregates were collected and volumes containing approximately 40-50 aggregates were chosen from each MP to cell incorporation ratio. After enzymatic dissociation of aggregates, MP incorporation was quantified via flow cytometry. The spatial distribution of fluorescently-labeled MPs within spheroids was analyzed using a LSM 700-405 confocal microscope (Carl Zeiss, Inc). EBs fixed in 10% formalin were stained with Hoechst dye (1:100) for 2 hours at 4 ˚C followed by 3 successive washes in PBS prior to imaging.

Gene expression analysis

RNA was extracted from undifferentiated ESCs and EBs at days 4, 7, and 10 of differentiation using the RNeasy Mini Kit (Qiagen). Reverse transcription of RNA to complementary DNA was performed using the iScript cDNA synthesis kit (BioRad) and

was analyzed using SyberGreen technology on the MyIQ cycler (BioRad). Forward and reverse primer sequences for *Oct4, Nanog, BrachyuryT, Flk1, Pax6, Nestin, AFP, FGF2, FGF5* and *18S* were designed with Beacon Design software and described in Table 2. Gene expression was quantified with respect to levels of gene expression of undifferentiated ESCs and EBs without MPs or soluble HMAm supplementation.

PCR array

Gene	Forward Sequence	Reverse Sequence	Melt Temp
18S	CTCTAGTGATCCCTGAGAAGTTCC	ACTCGCTCCACCTCATCCTC	58.0
Oct4	CCG GTGAGGTGGAGTCTGGAG	GCGATGTGAGTGATCTGCTGTAGG	58.0
Nanog	GAA ATCCCTTCCCTCGCCATC	CTCAGTAGCAGACCCTTGTAAGC	58.0
BrachyuryT	CACACCACTGACGCACAC	GAGGCTATGAGGAGGCTT TG	58.0
Flk1	GGCGGTGGTGACAGTATC	TGACAGAGGCGATGAATGG	64.3
Pax6	ACGGCATGTATGATAAACTAAG	GCTGAAGTCGCATCTGAG	58.0
Nestin	GGA GAA GCA GGG TCT ACA G	AGC CAC TTC CAG ACT AAG G	58.0
AFP	CACACCCGCTTCCCTCATCC	TTCTTCTCCGTCACGCACTGG	58.0
FGF2	AGCGACCCACACGTCAAACTAC	CAGCCGTCCATCTTCCTTCATA	58.0
FGF5			58.0

Histology analysis and immunostaining

EBs were collected, fixed in 10% formalin, and embedded in Histogel (Thermo Scientific), processed and paraffin embedded. Paraffin embedded samples were cut into 5 µm thick sections (Microm HM 355S). Deparaffinized sections were stained with hematoxylin and eosin (H&E) for basic cell morphology analysis. In addition, sections were stained with Safrinin-O (Sigma Aldrich) for GAG detection, Fast Green (Sigma

Aldrich) for cytoplasm, and Weigert's hematoxylin (Sigma Aldrich) for cell nuclei or Alcian Blue (Sigma Aldrich) and imaged with a Nikon 80i upright microscope using the SPOT flex camera (15.2 64 MP Shifting Pixel, Diagnostic Instruments, Sterling Heights, MI). All stained sections were imaged using a brightfield microscope (Nikon Eclipse 80i).

For whole-mount fluorescent immunostaining, formalin fixed EBs were permeabilized with 1.5% Triton X-100 in blocking buffer solution (2% donkey serum, 0.1% Tween 20) for 30 minutes, followed by overnight incubation at 4˚C with primary antibody in blocking buffer. EBs were washed thrice with blocking buffer and then incubated with a secondary antibody for 4 hours at 4˚C. Antibodies and concentrations used were rabbit polyclonal, anti-Pax6 (1:50; Abcam), rabbit polyclonal anti-human alpha-fetoprotein (AFP) (1:200; Dako, Glostrup, Denmark), mouse monoclonal anti-rat Nestin (1:100; RC2, Developmental Studies Hybridoma Bank, Iowa City, IA) . EBs were incubated with either AlexaFluor 488 conjugated, donkey-anti-rabbit secondary (1:200;Invitrogen) or AlexaFluor 488 conjugated donkey-anti-mouse secondary (1:200; Invitrogen) and then counterstained with Hoescht (1:100) for 15 minutes at room temperature, washed three times with blocking buffer and imaged using a Zeiss LSM 700-405 confocal microscope (Carl Zeiss, Inc.).

Plating of EBs

At day 7 of culture, a sample of EBs was collected and plated on either gelatin or poly-L-ornithine/laminin coated plates for 2-dimensional culture. Briefly, 0.1% gelatin solution (EmbryoMax, Millipore) was used to coat 24-well plates. For polyornithine/laminin coating, 100 µg/mL poly-L-ornithine (Sigma Aldrich) was added to 24 well plates and incubated overnight at 37˚C. After washing with PBS, 3.3 µg/mL laminin (Sigma Aldrich) was added to plates followed by incubation at 37˚C for 1 hour.

Finally, single EBs were pippetted with a wide bore tip (to prevent shearing of EBs) to individual wells to allow for cell attachment and spreading.

Statistical Analysis

All data are reported as mean ± standard error for a minimum of triplicate experimental samples. A Box-Cox power transformation was used to normalize data to a Gaussian distribution before performing statistical analysis. Statistical significance was assessed using a one-way ANOVA with Tukey's post hoc analysis. A *p*-value of less than 0.05 was considered statistically significant.

Results

Incorporation of HMAm MPs in EBs

HMAm MPs were incorporated within aggregates using forced aggregation at MP to cell seeding ratios of 1:1 and 1:3 (Figure 5.1A). AlexaFluor 594 labeled HMAm MPs incorporated within ESC aggregates were identified via fluorescent and confocal microscopy (Figure 5.1B, Figure 5.2A). After transfer to rotary suspension culture, no gross morphological differences were observed in phase images of EBs with or without HMAm MPs. Maximum MP incorporation within aggregates was achieved with approximately 970 MPs per aggregate at a MP:cell seeding ratio of 1:1 (Figure 5.2B), which was used for all subsequent studies. Incorporation efficiency of MPs within aggregates decreased from approximately 87 to 26% as the ratio of MPs to cells increased from 1:1 to 3:1 (Figure 5.2C).

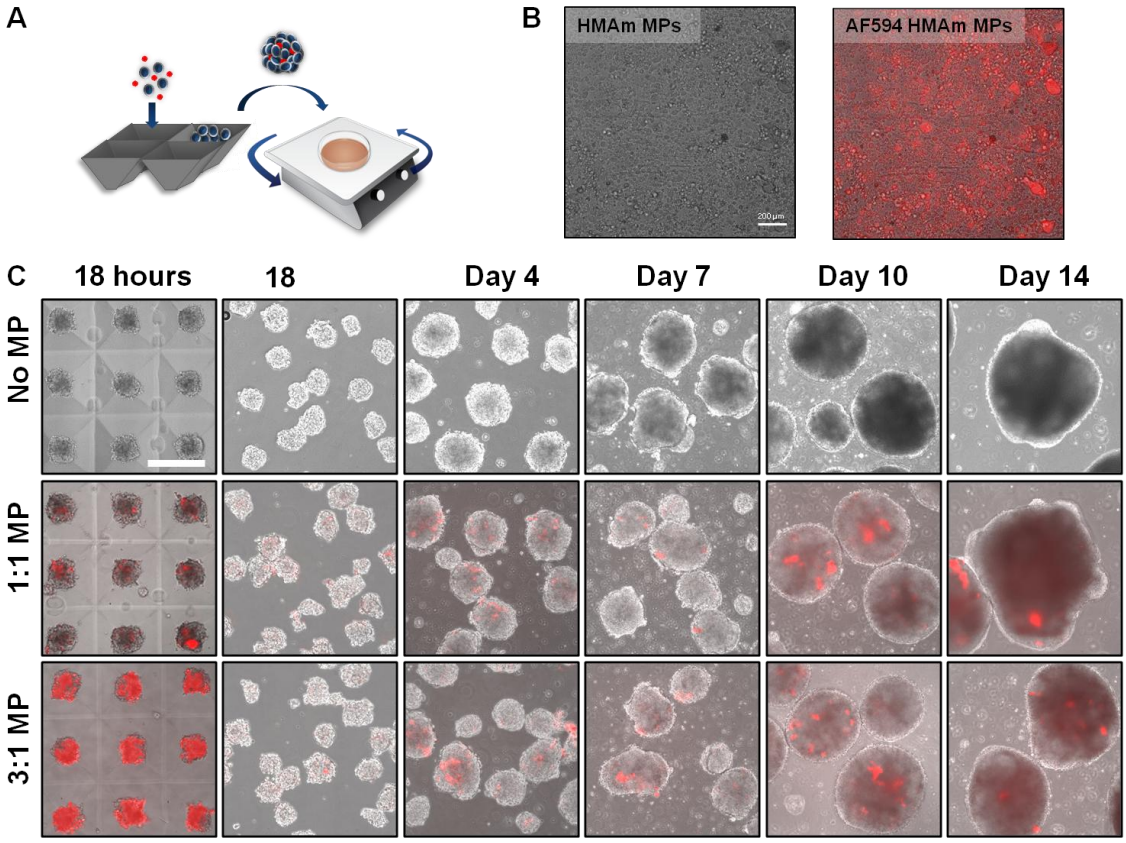

Figure 4.1. Fluorescently labeled HMAm MPs are incorporated in ESC aggregates via forced aggregation. (A) HMAm MPs were incorporated within 1000-cell aggregates via forced centrifugation, followed by overnight incubation. After formation ESC aggregates were transferred to rotary culture and imaged via fluorescent microscopy. (B). Scale bar = 200 μm (C) HMAm MPs were incorporated within aggregates at MP to cell seeding ratios of 1:1 and 3:1. MPs were detected within aggregates for up to 14 days. Scale bar = 400 μm

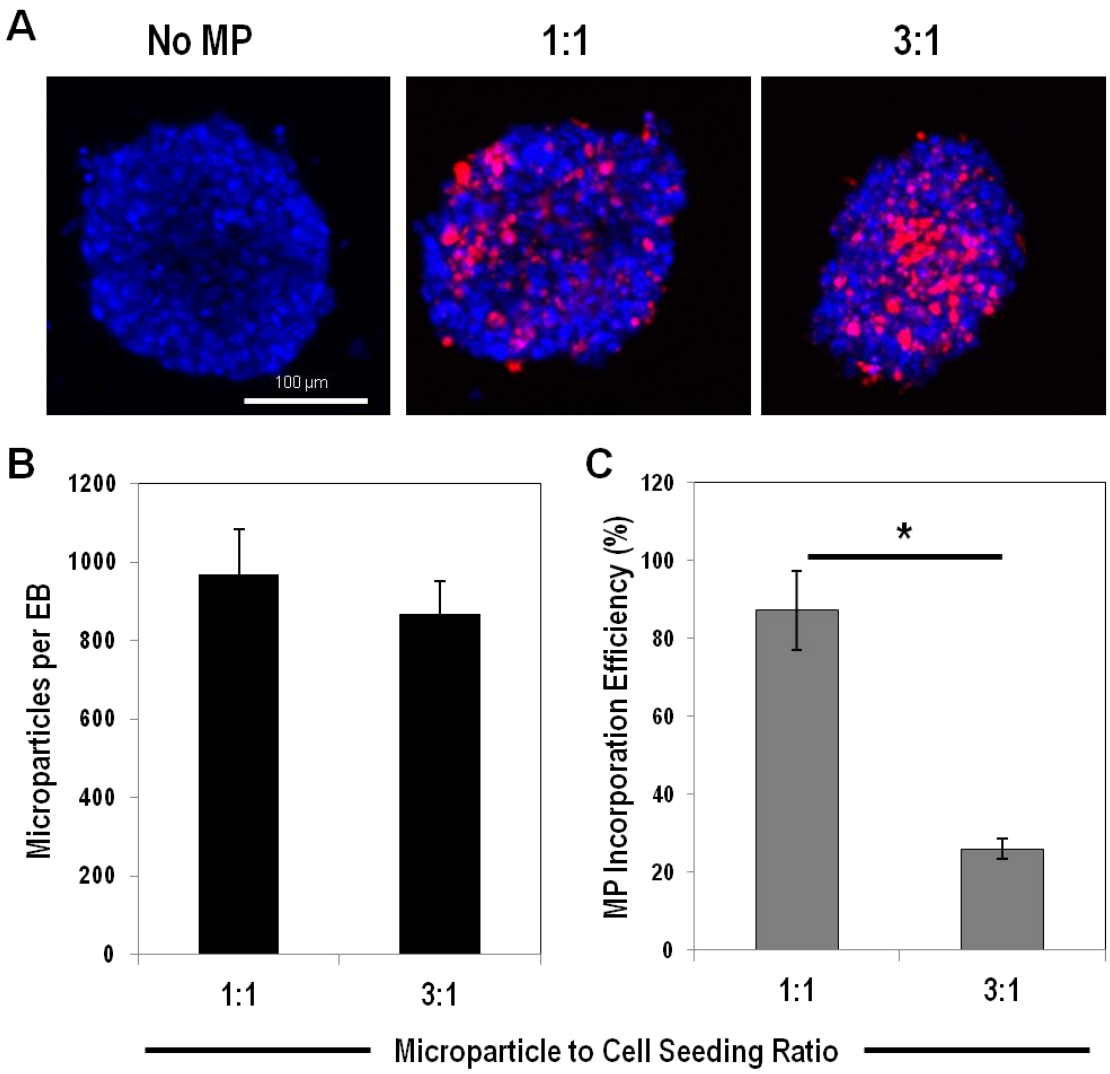

Figure 4.2. HMAm MP incorporation in ESC aggregates. (A) The presence of Alexafluor 594 labeled HMAm MPs throughout the aggregates was observed via confocal microscopy. (B) Incorporation was analyzed as a function of MP to cell seed ratio, with 1:1 and 3:1 incorporating similar numbers of MP per EB. (C) The efficiency of MP incorporation was quantified, with a MP to cell seeding ratio of 1:1. * = significant difference between indicated groups ($p < 0.05$). Scale bar = 100 µm

Analysis of growth factor concentration in spent media

During differentiation, ESC aggregates secrete growth factors such as BMP4, IGF2, and VEGF into the surrounding medium [153,154]. Additionally, previous studies have demonstrated that HMAm MPs can bind growth factors such as VEGF and FGF2 with high affinity [116]. Therefore, it was hypothesized that incorporation of HMAm MPs could impact growth factor concentration in spent media through heparin sequestration of secreted factors or cell-material interactions. Analysis of growth factor concentration at days 4, 7, 10, and 14 of culture was measured by ELISA to determine ESC growth factor production. Between days 4 and 7, levels of VEGF decreased as differentiation progressed for EBs with and without MPs. At day 7 of culture, EBs with incorporated MPs demonstrated significantly ($p < 0.05$) higher levels of VEGF in spent media as compared to EBs without MPs. The detected concentration of VEGF in spent media continued to increase as differentiation progressed from day 7 to day 14 and remained similar in detection levels between groups. No detectable levels of BMP4. IGF2, or FGF2 were measured in spent media.

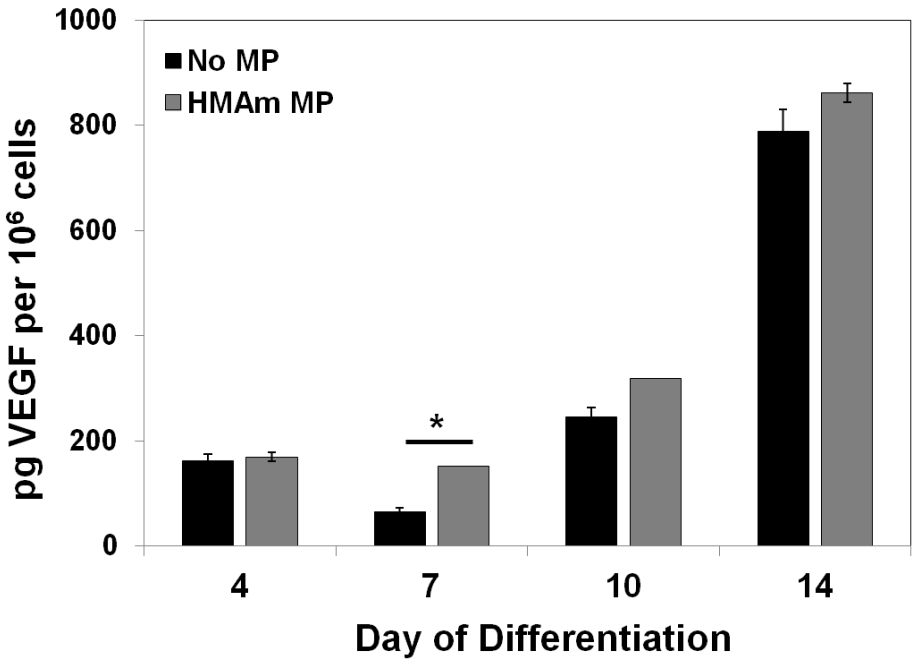

Figure 4.3. VEGF concentration in ESC conditioned media. VEGF concentration increased over the course of differentiation for both groups. At day 7 of differentiation, ESCs aggregates with incorporated HMAm MPs demonstrated significantly ($p < 0.05$) higher level of VEGF as compared to untreated aggregates. * = significant difference between indicated groups ($p < 0.05$).

HMAm MP incorporation results in morphological differences in EB structure

Histological analysis was performed on paraffin sections of day 14 ESC aggregates with incorporated HMAm MPs. Morphological differences were observed between ESC aggregate groups on day 14 of differentiation. Aggregates treated with incorporated HMAm MPs and soluble HMAm exhibited increased presence of internal structures composed of dense cell populations as compared to untreated aggregates (Figure 4.4).. Safrinin-O staining was performed to identify areas of proteoglycans and glysaminoglycans. Areas of positive staining were observed in all groups; however, ESC aggregates treated with either HMAm MPs or soluble HMAm exhibited more regions of positive staining, suggesting increased GAG production (Figure 4.5).

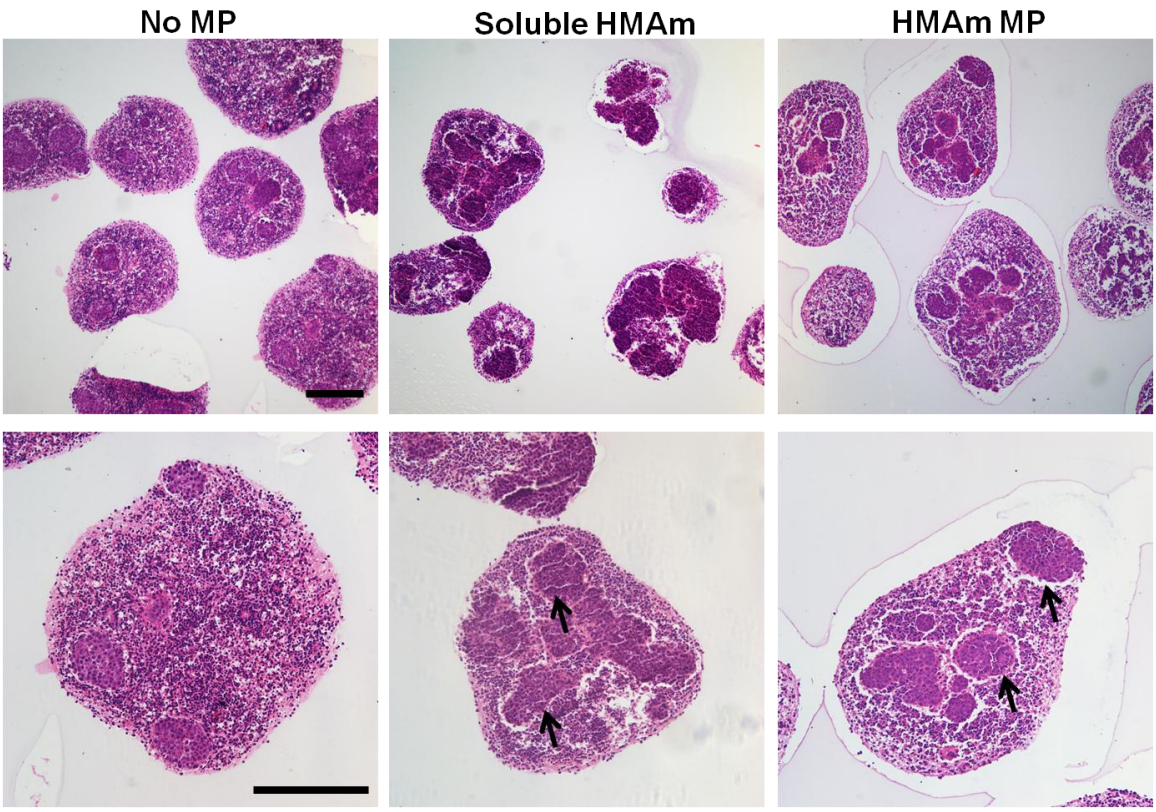

Figure 4.4. Histological analysis of day 14 ESC aggregates. H&E staining of Day 14 ESC aggregates revealed the presence of more oval-shaped organized structure (arrows)s in soluble HMAm and HMAm MP groups as compared to untreated aggregates. Scale bar = 200 μm.

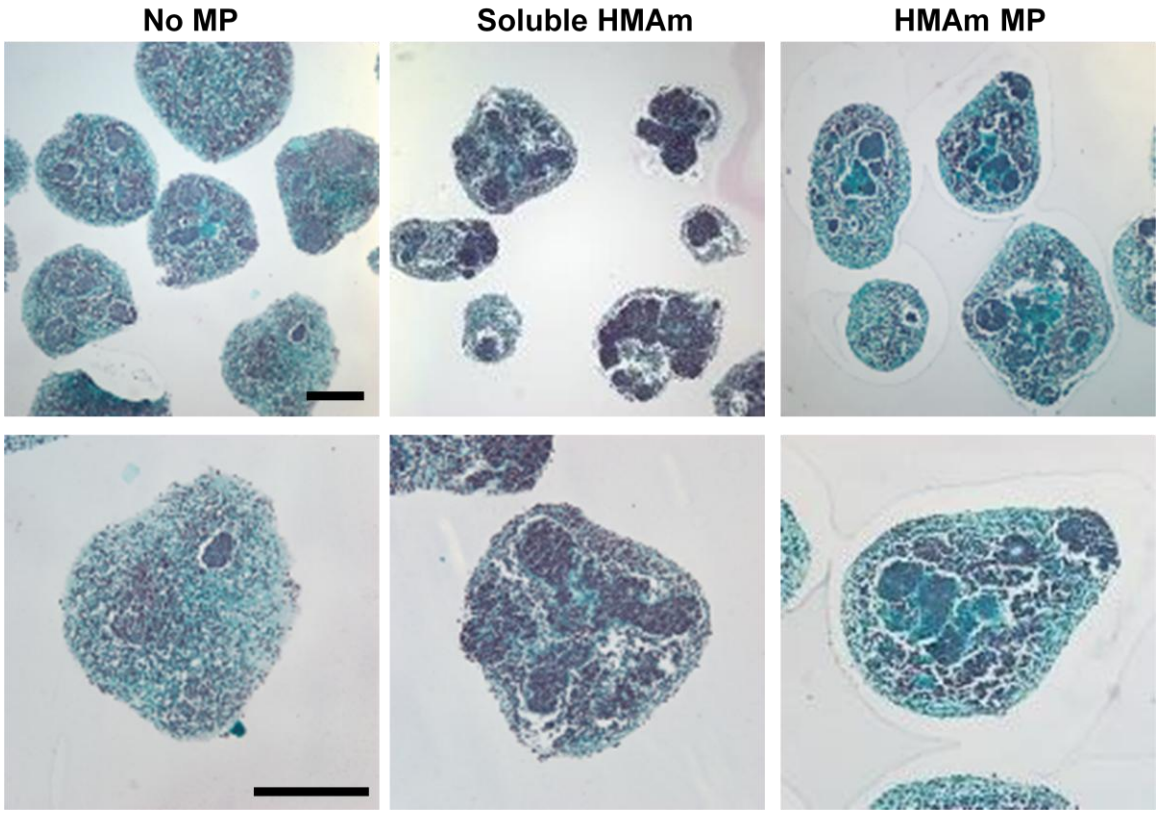

Figure 4.5. Histological analysis of day 14 ESC aggregates. Safrinin-O staining of Day 14 ESC aggregates exhibited increased staining, indicative of GAG content, for ESC aggregates treated with either HMAm MPs or soluble HMAm as compared to untreated aggregates. Scale bar = 200 μm

Gene expression is modulated by HMAm MP incorporation

Temporal gene expression for markers of pluripotency (Oct4), germ lineage (BrachyuryT, Flk1, Pax6, Nestin, AFP), and growth factors (FGF2 and FGF5) were analyzed using qRT-PCR at days 4, 7, and 10 of culture (Figure 4.6A,B). As an additional control, ESC aggregates without incorporated MPs were treated with soluble HMAm to determine if the format of heparin presentation (i.e. outside or inside aggregates) to cells had an effect on gene expression. The total amount of added soluble HMAm corresponded to the total amount of HMAm MP incorporated within EBs at day 0. Soluble HMAm was added after each media exchange to replenish soluble HMAm removed and to maintain the same HMAm concentration as EBs with incorporated MPs. As expected, expression of Oct4 decreased over the entire course of differentiation for all groups and no significant differences were observed between any groups (Figure 4.6C). No significant differences were observed between any groups for FGF5 (growth factor), BrachyuryT (mesoderm), and Nestin (neuroectoderm). Expression of Flk1 (mesoderm) was significantly ($p < 0.05$) increased for soluble HMAm treated aggregates, while expression of FGF2 (growth factor) was significantly ($p < 0.05$) decreased for HMAm MP aggregates at day 10 as compared to untreated aggregates (Figure 4.6C). Multiple differences were observed for endoderm marker, AFP, and ectoderm marker, Pax6, between groups (Figure 4.6C). Expression of AFP in aggregates treated with soluble HMAm was up-regulated by almost 4 fold at day 7 as compared to untreated and HMAm MP aggregates. Additionally, soluble HMAm treated aggregates exhibited increased (3.52 fold) AFP expression as compared to HMAm MP aggregates at day 10. At day 4 of differentiation, expression of Pax6 for HMAm MP aggregates was significantly down-regulated for both untreated (- 0.81 fold and soluble HMAm groups (- 0.95 fold). Soluble HMAm treated aggregates demonstrated increased

Pax6 expression as at day 7 and 10, while HMAm MP aggregates demonstrated increased Pax6 expression at day 10 as compared to untreated group aggregates.

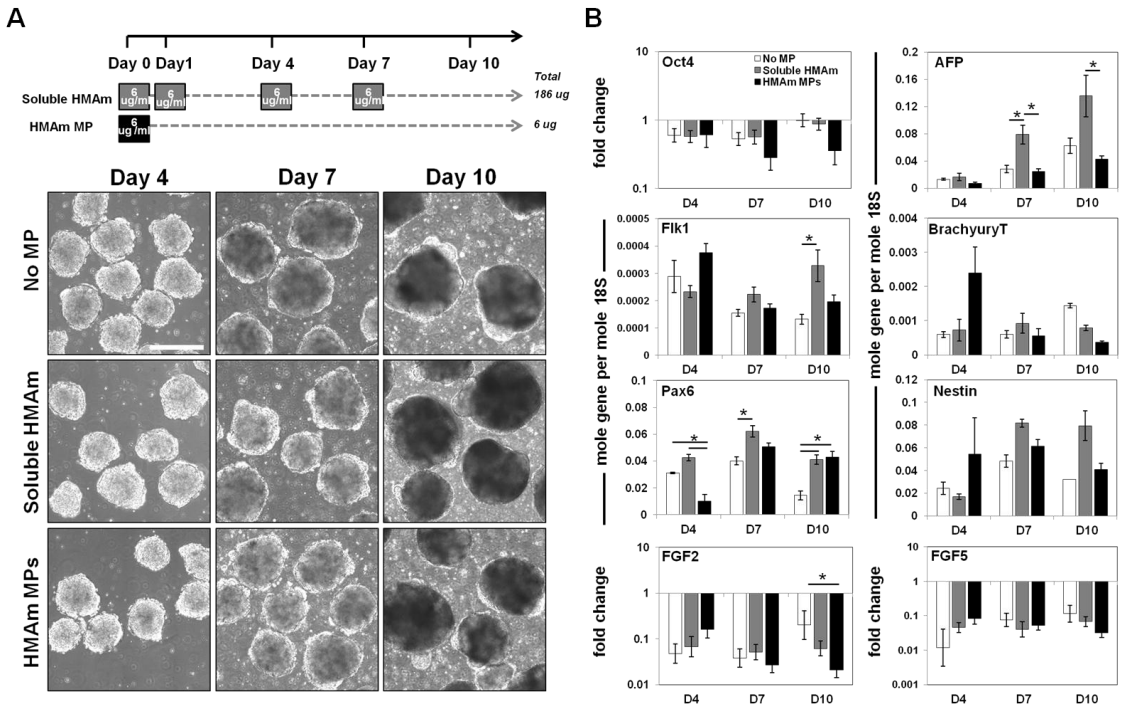

Figure 4.6. Incorporation of HMAm MPs modulates ESC differentiation. (A) HMAm MPs were incorporated within ESC aggregates and cultured for 10 days in rotary suspension culture. ESC aggregates were also treated with soluble HMAm to compare different formats of heparin presentation to cells. No gross morphological changes were observed between groups. (B) Expression of Oct4 for all groups decreased over the course of differentiation (days 4, 7, and 10). Pax6 expression was modulated by treatment with both soluble HMAm and HMAm MPs, whereas AFP expression was only modulated in the presence of soluble HMAm. FGF expression at day 14 for ESC aggregates with MPs was increased as compared to untreated aggregates. * = significant difference between indicated groups (n= 4; $p < 0.05$).

Protein expression is altered by HMAm MP incorporation

Whole-mount immunofluorescent staining was performed on Pax6 (ectoderm) and AFP (endoderm) in ESC aggregates at day 7 and 10 as differences in gene expression were almost exclusively found in ectoderm and endoderm markers at these time points. During embryogenesis, Pax6 is a key transcription factor that plays a role during early development of the central nervous system and is expressed in radial glial cells upon neuroectoderm formation [155]. Therefore, as ESC aggregates cultured under serum free conditions more readily differentiate to neuroectoderm, protein expression of Pax6 was investigated. Positive Pax6 expression was observed throughout ESC aggregates for all three groups at day 7 of culture (Figure 4.7). However, EBs treated with soluble HMAm and HMAm MPs exhibited more abundant fluorescent immunostaining for Pax6 as compared to untreated aggregates. Pax6 expression at day 10 was only observed in untreated and soluble HMAm treated groups. In contrast to day 7, Pax6 expression decreased and was primarily observed in untreated and soluble HMAm aggregates. Positive expression of endoderm marker, AFP, was observed throughout aggregates at day 7 in soluble HMAm and HMAm MP groups, but AFP expression was not observed in day 7 untreated aggregates or for all groups at day 10 (Figure 4.8). At day 7, aggregates from each group were further cultured for an additional 7 days on poly-L-ornithine/laminin coated 24-well plates. At day of 14 of differentiation (7 days after plating), EBs from each group exhibited a dome-shaped cell body with extension of neurites from the edges of the aggregates (Figure 4.9) Immunostaining for Nestin expression in plated EBs was performed after 14 total days of differentiation. Nestin, an intermediate filament, is a marker of neural precursor cells (NPCs) in embryonic tissues and plays a role in the radial growth of axons [155,156]**.** Analysis of plated EBs demonstrated that all groups expressed Nestin, primarily located to concentrated regions on the exterior of aggregates (Figure 4.10). Notably, EBs treated

with soluble HMAm and HMAm MPs exhibited more pronounced filamentous staining for Nestin as compared to untreated aggregates, suggesting that heparin enhances ESC differentiation toward NPCs.

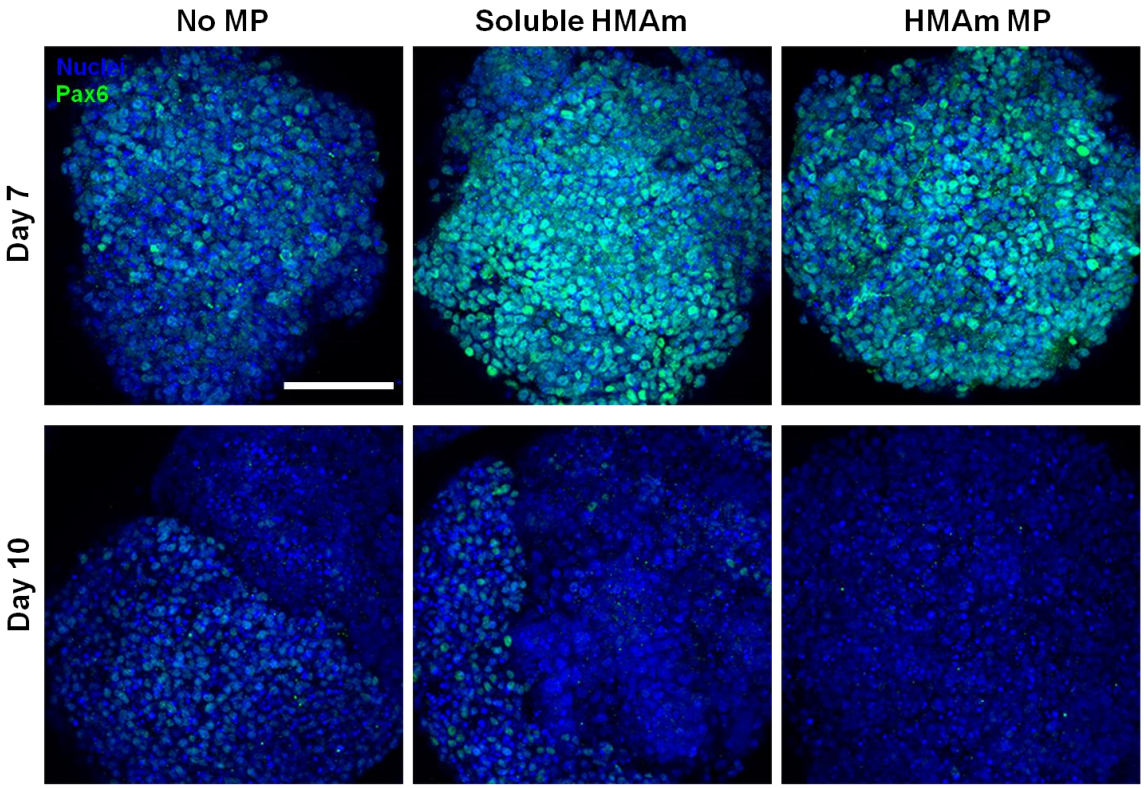

Figure 4.7. Pax6 expression in ESC aggregates is modulated with HMAm treatment. At day 7 and 10 of differentiation, spatial distribution of Pax6 expression within ESC aggregates was observed via fluorescent immunostaining. Positive expression of Pax6 was observed throughout aggregates for all groups at day 7, with more abundant expression observed in soluble HMAm and HMAm MP groups. By day 10, little expression of Pax6 was observed for HMAm groups, while positive expression was localized to specific regions within aggregates for untreated and soluble HMAm groups. Scale bar = 100 μm

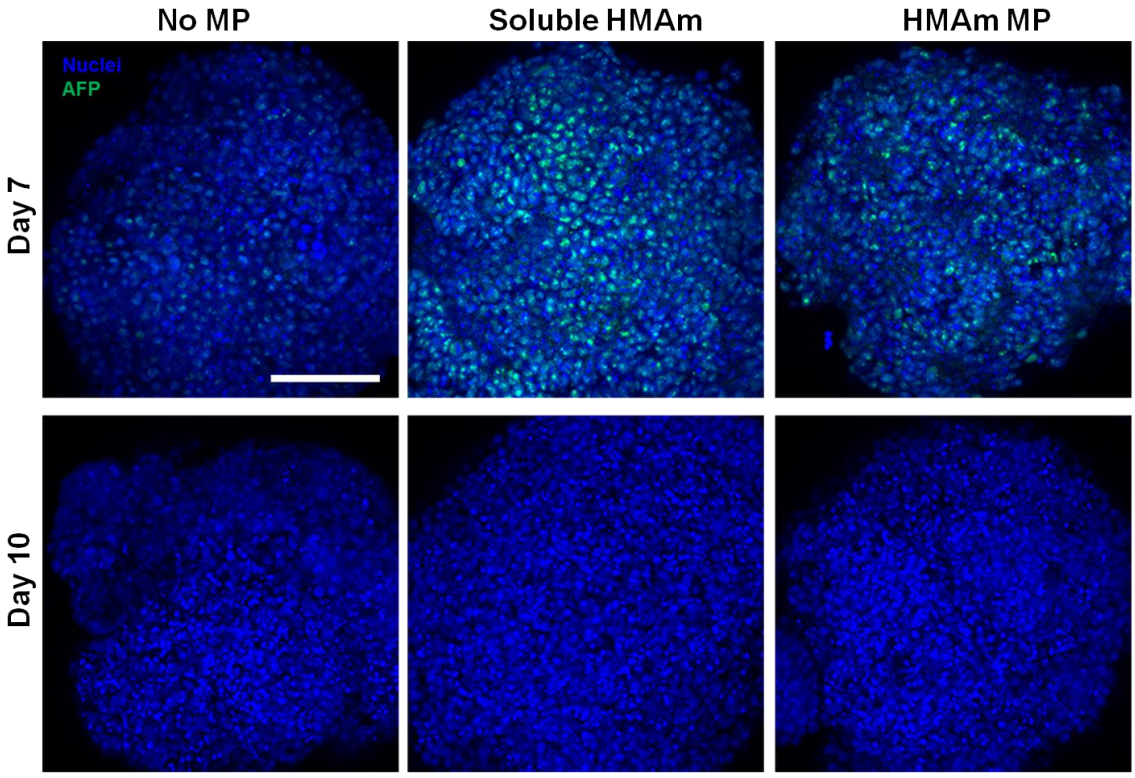

Figure 4.8. AFP expression in ESC aggregates is modulated with HMAm treatment. Immunostaining for endoderm marker, AFP, was performed on day 7 and 10 ESC aggregates. Positive AFP expression was observed in ESC aggregates treated with soluble HMA or with HMAm MPs at day 7. No expression of AFP was observed for untreated aggregates at day 7, as well as for all groups at day 10. Scale bar = 100 μm

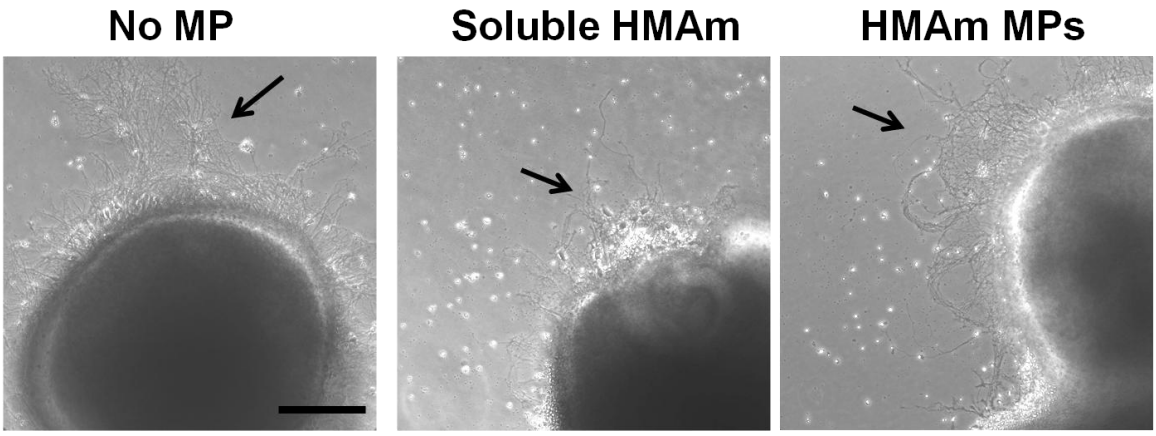

Figure 4.9 Phase images of ESC aggregates plated on poly-L-ornithine/laminin after 14 days of culture. ESC aggregates cultured for 7 days in suspension were retrieved and plated on poly-L-onrithine/laminin. After culturing for an additional 7 days, EBs exhibited a domed ovoid morphology with extension of neurites (arrows) from the edges of aggregates. Scale bar = 100 μm

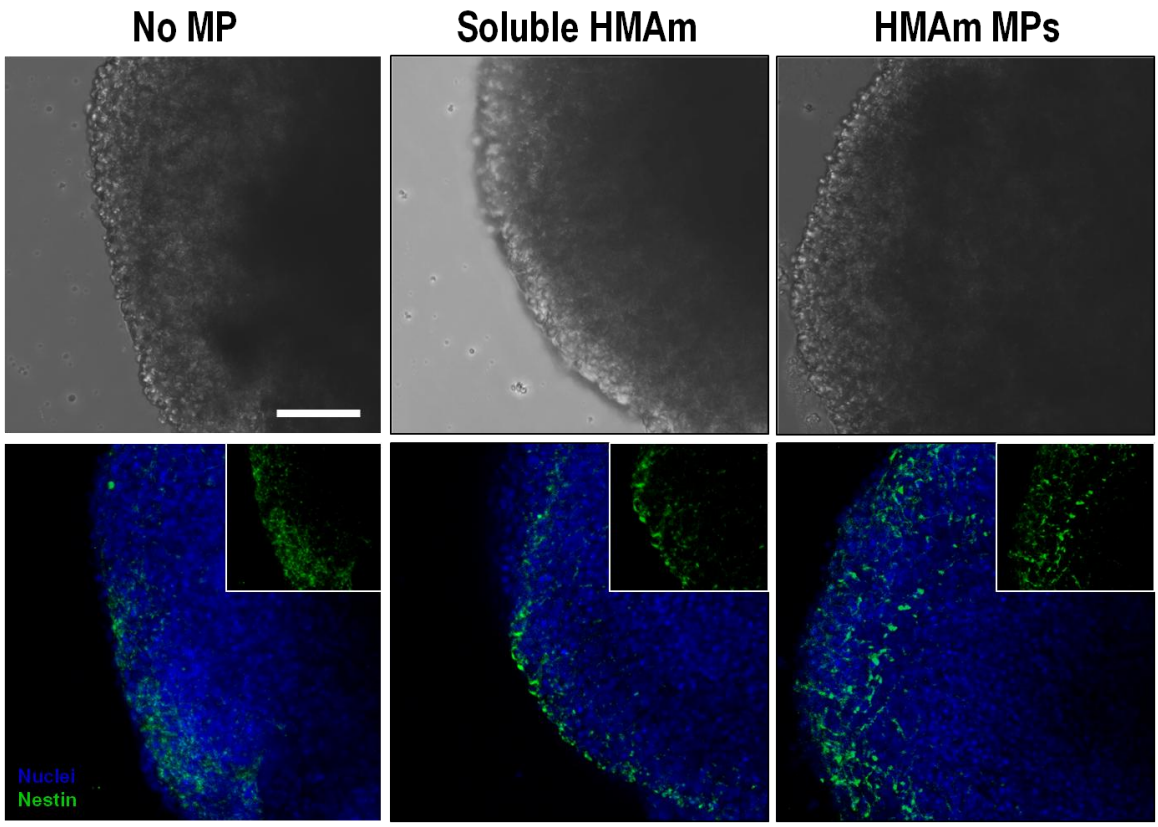

Figure 4.10 Nestin expression of plated ESC aggregates. At day 7 of differentiation, ESC aggregates were plated on poly-L-ornithine/laminin coated 24-well plates and cultured for an additional 7 days. Staining for Nestin was performed after 14 total days of differentiation. All groups contained Nestin+ cells that were primarily found near the exterior of ESC aggregates, indicative of neural precursor cells. Aggregates treated with either soluble HMAm or HMAm MPs demonstrated distinct filamentous Nestin staining as compared to untreated aggregates. Scale bar = 100 μm.

Discussion

The incorporation of heparin-methacrylamide (HMAm) MPs within ESC aggregates demonstrated of the utility of exogenous GAGs as *in vitro* modulators of cell fate decisions and can alter the differentiation outcomes of ESCs. Previous studies have incorporated MPs of various materials to alter patterns of differentiation of ESCs in media supplemented with serum, an undefined mixture of proteins [121,127]. While serum promotes meso- and endoderm differentiation in ESCs, serum-free conditions enhance ESC differentiation toward neuroectoderm [33,157]. In addition, serum-free culture provides a system that is more amenable to outside manipulation and direct investigation of MP material effects on cell behavior, an important advantage as heparin plays a role in the coordination of various signaling pathways by regulating the activity of multiple different biomolecules [68,158]. Ultimately, the role of heparin on ESC behavior can be examined by minimizing external influences such as serum or addition of a cocktail of factors typically used in stem differentiation strategies [9,10,131,159]. Previously, incorporation of heparin-gelatin MPs (Lassahn & Bratt-Leal et al. unpublished) has been investigated under serum-free conditions to analyze ESC differentiation, providing motivation for the use of GAG-based MPs to alter ESC growth factor production and modulate EB differentiation.

The addition of soluble heparin to stem cell cultures has been previously investigated to examine the effect of GAGs on ESC differentiation. Addition of heparin to EBs was shown to enhance hematopoietic differentiation [80], while heparin supplemented to adherent ESC cultures enhanced differentiation toward Sox1+ neural progenitor cells [160]. However, frequent media exchanges during cell culture involve the repeated supplementation of exogenous GAGs, resulting in the removal of any growth factors bound to soluble heparin; while, incorporation of HMAm MPs retains and

concentrates endogenous heparin-binding growth factors within EBs. Analysis of heparin-binding growth factors present in spent media was investigated to determine whether HMAm MPs modulate secreted growth factor concentration. For example, heparin/HS are known to bind FGF2, which plays a role in ESC differentiation toward ectoderm, and are critical in the formation of the FGF-FGFR complex [62]. However, only VEGF was detected, while levels of BMP4, IGF2, and FGF2 were below limits of detection (15 pg/mL). Due to low abundance of growth factors present, further investigation of the morphogen profile present in conditioned media could be investigated using mass spectrometry analysis [161], buy may require additional steps to concentrate protein for detection. Additionally, separation of MPs from EBs could be performed for direct analysis of growth factor bound MPs, ultimately providing more information about what MP-growth factor interactions occur during EB differentiation. Previous studies have demonstrated that soluble heparin enhanced FGF signal transduction, by concentrating FGF near cell surface receptors [62,160]. Therefore, activation of specific signaling pathways (e.g. BMP or FGF) that regulate ESC exit from self-renewal could be analyzed using Western Blot analysis or other sentinel ESCs with fluorescent reporters that respond with specificity to retinoic acid, activin A, Wnts, or Notch [145] to determine the effect of HMAm MPs on signaling activity.

During neuronal differentiation of ESCs, neuroectoderm formation is characterized by expression of Sox1, followed by expression of Pax6 as cells transition to radial glia and mature neurons [155,162]. Analysis of Pax6 expression in ESC aggregates with incorporated HMAm MPs or treated with soluble HMAm more abundant staining for protein expression at day 7 and upregulation of gene expression over the course of differentiation suggesting that heparin may enhance neuroectodermal differentiation through sequestration of specific factors produced by ESCs,. However, aggregates treated with soluble HMAm demonstrated increased expression of

mesoderm (Flk1) and endoderm (AFP) markers as compared to aggregates with incorporated MPs, suggesting that the format of heparin presentation to EBs plays a role in directing ESC differentiation. Diffusion of soluble HMAm (18 kDa) within EBs is most likely restricted by the formation of a dense outer cell layer [132,163], thus preventing uniform distribution of heparin within aggregates and limiting cell-heparin interactions to primarily with cells on the exterior. In contrast, incorporation of HMAm MPs allows for distribution of heparin throughout EBs and results demonstrate that MPs are retained within aggregates for up to 14 days. Furthermore, soluble HMAm may sequester factors produced by aggregates away from cell surface receptors and is also removed during media exchanges, which could disrupt activation of specific signaling pathways. After plating of EBs, Nestin, a marker for neuroepithelial cells [33,164], was detected in all groups; however, further characterization of neurite outgrowths (e.g. number and length), can be performed by analyzing fluorescence microscopy images of EBs stained for neurite marker, TuJ1 (neuron-specific class III β-tubulin) or neurofilament, using image processing techniques to further examine the ability of HMAm MPs to enhance neuronal growth of EBs [165–167].

Conclusion

HMAm MPs provides a novel tool to influence the differentiation of ESCs by presenting natural GAG-based materials within 3D morphogenic environments. Pax6 in response to HMAm MP incorporation within ESC aggregates demonstrated upregulation of gene expression and more pronounced fluorescent immunostaining Pax6, a marker of early neuroectoderm, suggesting that HMAM MPs can alter differentiation outcomes of EBs, most likely by sequestration and concentration of endogenous morphogens within the EB microenvironment. Ultimately, this study demonstrated the development of a

new class of biomaterials capable of capturing stem cell derived morphogens in a biomimetic manner to yield more efficient approaches for directed stem cell differentiation and demonstrate the utility of GAG MPS as a complement to growth factor or small molecule supplementation for directed differentiation approaches.

CHAPTER V

PROTEOMIC ANALYSIS OF EMBRYONIC STEM CELL MORPHOGENS SEQUESTERED BY HEPARIN-METHACRYLAMIDE MICROPARTICLES

Introduction

ESCs spontaneously differentiate during *in vitro* culture, when pluripotency maintaining components such as MEF feeder layers or LIF are removed, synthesizing a complex array of various factors and soluble cues that direct cell fate. Moreover, signaling molecules that direct tissue patterning during embryonic development are secreted by ESC aggregates, known as embryoid bodies (EBs), which emulate aspects of morphogenesis observed during embryonic development [48,129]. EB models provide an attractive *in vitro* platform from which cells of specific developmental stages, including vasculogenesis [48], osteogenesis [103] , and neurogenesis [167], can be enriched and analyzed for morphogen expression. Interestingly, evidence suggests that biomolecules synthesized by ESCs can play an important role in regenerative events observed *in vivo* [168–171]. However, transplantation of ESCs is limited due to risk of tumor formation and immune response and attempts to administer bolus injections of ESC-derived morphogens, such as from conditioned media, are insufficient for localized and sustained delivery of morphogens.

Extracellular matrix (ECM) components, such as glycosaminoglycans (GAGs), play crucial roles in cell signaling and regulation of morphogen gradients during early development through binding and concentration of secreted growth factors, thus directing patterns of tissue morphogenesis [61,172]. Engineered biomaterials amenable

to conjugation of highly sulfated GAGs, such as heparin, provide ideal matrices for manipulation and efficient capture of ESC morphogens via reversible electrostatic and affinity interactions. In particular, engineered microparticles (MPs) have been extensively used as delivery vehicles for sustained release of morphogens [121,124–126,173]. Therefore, MPs synthesized from heparin-methacrylamide (HMAm) can be used as a tool to concentrate and localize ESC morphogens [116]. Ultimately, biomaterials designed to efficiently capture and retain bioactive ESC-derived morphogens offer an attractive platform to translate the regenerative potential of ESCs into molecular therapies.

Previously, mass spectrometry (MS) approaches have been employed to globally analyze the proteomics of ESC secretomes. Identification of the most abundant proteins present in samples are typically analyzed by liquid chromatography coupled to a mass spectrometer (LC-MS/MS), where most abundant proteins are preferentially selected for MS/MS fragmentation. However, low abundance and concentration of secreted proteins of interest significantly limits the success of MS analysis. Previous studies have employed strategies to pre-fractionate and enrich protein samples by performing techniques such as SDS-PAGE and organelle isolation to obtain a temporal snapshot of proteins secreted during stem cell differentiation [161,174–177]. This work proposes to develop a novel strategy to capture secreted ESC morphogens in a concentrated manner using HMAm MPs for subsequent analysis by mass spectrometry.

Methods

BMP4 and conditioned media loading of HMAm MPs

HMAm MPs were resuspended in PBS and MP concentration was determined using a hemacytometer. Prior to growth factor loading, MPs were freeze-dried using a lyophilizer (Labconco, Kansas City, MO). Conditioned (or spent) media was collected from EB culture at days 4, 7, 10, and 14 of differentiation. Lyophilized MPs were added to human recombinant bone morphogenetic factor 4 (hBMP4) diluted in a 1% BSA solution or conditioned media and incubated overnight at 4˚C to facilitate growth factor binding. MPs with bound growth factor were washed three times in PBS to remove any loosely bound protein. MPs not used immediately after growth factor incubation were stored at -20˚C to preserve protein bioactivity and prevent degradation.

SDS-PAGE and silver staining

Samples of growth factor bound MPs were prepared by mixing samples in 32 µL PBS with 8 µL of 5x diluted loading buffer (1.25 mL 0.5 M Tris-HCL (pH 6.8), 1 g SDS, 5 mL glycerol, 5 mg Bromophenol Blue, 1.25 mL β-mercaptoethanol) and heating for 10 minutes at 95˚C. Samples of growth factor bound microparticles were added to wells of gel and growth factor separation was resolved on a 12% or 4-15% mini-PROTEAN® TGX™ gel (Bio-Rad, Hercules, CA) at 200V for 30 minutes. A Kaleidoscope™ (Bio-Rad, Hercules, CA) protein ladder was used to indicate molecular weight of bands. For conditioned media samples, 32 µL of spent media was added to 8 µL of loading buffer prior to loading into the wells.

The Silver Stain Plus kit (Bio-Rad, Hercules, CA) was used to visualize protein present in the gel. Briefly, gels were fixed in 50% methanol, 10% acetic acid, and 10% fixative enhancer concentrate for 40 minutes on an orbital shaker. Gels were washed three times in dI H_2O for 10 minutes, and then placed in silver stain solution until

appearance of dark bands (approximately 20-40 minutes). The reaction was stopped by adding 5% acetic acid for 15 minutes.

Fluorescamine assay

A fluorescamine assay was used to assay the amount of protein bound to HMAm microparticles. Fluorescamine reacts with primary amine groups found in terminal amino groups to form fluorescent pyrrolinone type moieties for protein quantification HMAm MPs (0.5 mg) were added to 1, 5, and 10 mL of conditioned media and incubated overnight at 4˚C. HMAm microparticles were washed 3x in PBS to remove loosely bound protein. SDS-PAGE Loading buffer was added to one-half of the samples and heated at 95˚C for 10 minutes to promote dissociation of MP bound growth factors through protein denaturation and charge neutralization. SDS and heat treated samples were washed 3x again in PBS. All samples were subsequently reacted with 0.01% w/v fluorescamine solution (1.84 mg in 18.4 mL acetone) at room temperature and immediately read on a Synergy H4 microplate reader (Biotek, Winooski, VT) at excitation of 390 nm and emission of 475 nm. The number of free amine groups present on growth factor bound MPs was determined using a glycine standard curve (0.05 – 8 µg/mL) and compared to unloaded MPs and MPs treated with SDS and heat.

Conditioned media protein extraction and digestion

Bands were cut from gel into 1 mm^2 pieces and 200 µL 50% acetonitrile (ACN) and 50% 50 mM NH_4HCO_3 were added, followed by vortexing the sample for 5 minutes. Supernatant solution was removed and 200 µL 50% acetonitrile (ACN) and 50% 50 mM NH_4HCO_3 was added again to excised bands for 10 minutes at room temperature. Supernatant was removed and gel pieces were dried in a speed vacuum for 10 minutes. Samples were placed on ice and either trypsin in 50 mM ammonium bicarbonate or Glu-C (1:200) in PBS was added, followed by overnight incubation at 37 ˚C. Lys-C (1:200) is

added the next day to samples treated with Glu-C and samples were incubated for an additional 4 hours at 37˚C. Protein digestion was quenched with 0.1% formic acid until the pH reached 2. Finally, LC-MS/MS analysis and database search was performed as described before with the following changes: The HPLC gradient was a 30 minute gradient of 5-100% ACN containing 0.125% FA. All MS/MS spectra were searched against a database that included sequences of all proteins in the UniProt Mouse (Mus musculus) Database Samples digested with NTCB searched with a parameter file listing the following differential modifications: oxidation of methionine (+15.9949); and one fixed modification of carbamidomethylation of cysteine (+57.0214) [178].

HMAm MPs retrieval from EBs

Separation of HMAm MPs from EBs was performed by non-enzymatic dissociation of EBs, followed by a Percoll density gradient centrifugation. EBs with incorporated HMAm MPs were collected from suspension culture in 15 mL conical tubes and allowed to settle by gravity sedimentation to the bottom. EBs were washed 3x in PBS and incubated in 1 mL of non-enzymatic Gentle Cell Dissociation Reagent (StemCell Technologies, Vancouver, BC) to prevent digestion of MP bound protein for 20 minutes at 37˚C. Dissociation of EBs was aided by gentle pipetting of EBs during incubation in dissociation buffer. Dissociated EBs and HMAm MPs were centrifuged at 1,000 RPM and washed with PBS for three rounds. Percoll gradient was formed as described previously for separation of dissociated cells and MPs [1]. Briefly, Percoll (Sigma Aldrich) was mixed with 8.5% NaCl (9:1) and diluted to 40.5 and 58.5%, which correspond to a physical density of 1.065 and 1.069 g/mL. Three mL of 58.5% Percoll was added to the bottom of a 15-ml conical tube, followed by adding 3 ml of 40.5% Percoll on top. Finally, 3 ml of the dissociated cells and MPs were added on top of the Percoll gradient solution by gently pipetting against the inner wall of the tube, followed by

centrifugation at 1,500 RPM for 30 minutes. After centrifugation, the top, 40.5%, and 58.5% layers were separated into different conical tubes by pipetting. Each fractions was washed twice in PBS and quantification of efficiency of MP and cell separation was perfomed using an Accuri™ C6 flow cytometer (BD Biosciences, San Jose, CA). Flow cytometry was performed on control samples of only dissociated cells or MPs to determine gating for Percoll fractions. Each Percoll layer (top, 40.5%, and 58.5%) were analyzed and gated based on control samples.

Statistical Analysis

All data are reported as mean ± standard error for a minimum of triplicate experimental samples. A Box-Cox power transformation was used to normalize data to a Gaussian distribution before statistical analysis. Statistical significance was assessed using a one-way ANOVA with Tukey's post hoc analysis. A *p*-value of less than 0.05 was considered statistically significant.

Results

Characterization of BMP4 release from HMAm MPs using SDS-PAGE

Initial experiments to determine the potential of using gel electrophoresis for removal of MP bound protein for characterization were carried out using recombinant human BMP4 (Figure 5.1A). BMP4 is a well-known heparin-binding protein [86,179] and also known to be present in ESC conditioned media [154], thus providing a "model" protein for SDS-PAGE analysis of MP bound growth factors. SDS-PAGE and silver-staining were performed on gels with HMAm MPs loaded with 10 ng of hBMP4, soluble hBMP4 and unloaded HMAm MPs (Figure 5.1B). The electrostatic interaction between BMP4 (pI = 8.97) and HMAm MPs was disrupted by addition of SDS and heat prior to

loading into gel. The intensity of staining for BMP4 released from HMAm MPs was compared to soluble BMP4 to observe the efficiency of gel electrophoresis to dissociate growth factors from MPs. Since, hBMP4 (loaded and soluble) was diluted in 1% BSA, stained bands were observed at 66kDa and between 22-25 kDa for both BSA and hBMP4, respectively. For soluble hBMP4, bands for BSA were darker and larger in size as compared to BMP4 loaded on HMAm MPs (Figure 5.1A). In addition, staining was also darker for soluble hBMP4 as compared to BMP4 loaded MPs, indicating that BMP4 was not completely released from MPs. Unloaded MP lanes did not demonstrate any staining, indicating that direct loading of MPs in PAGE gels does not interfere with gel electrophoresis or silver staining.

The release of hBMP4 from HMAm MPs via SDS-PAGE was further investigated by increasing the duration in which loaded MPs were heated prior to gel loading (Figure 5.1C). More staining was observed for BMP4 loaded MPs when the duration of heating at 95˚C was increased from 5 to 10 and 15 minutes. Similarly, staining for hBMP4 for soluble hBMP4 groups also improved with increased heating times. However, hBMP4 staining was still greater for soluble hBMP4 as compared to hBMP4 loaded MPs. Interestingly, staining for bands at 50 kDa appeared for both soluble hBMP4 and hBMP4 loaded MPs at 10 and 15 minute heating times, suggesting the presence of hBMP4 dimers.

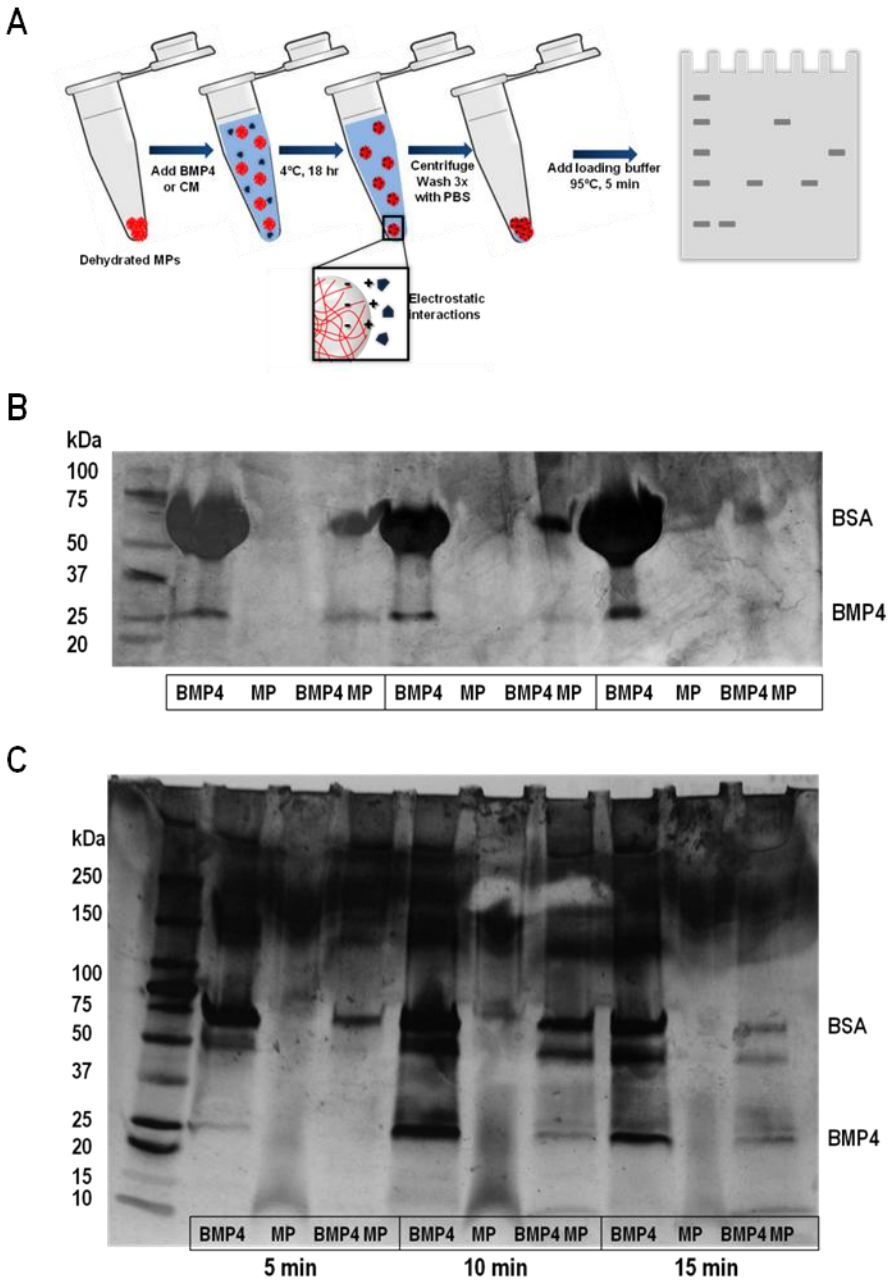

Figure 5.1. SDS-PAGE can be used to detect MP bound protein. A) HMAm MPs were loaded overnight incubation in either a BMP4 solution or conditioned media at 4˚C. Protein loaded MPs are treated with SDS and heat prior to performing SDS-PAGE. B) MPs loaded with 10 ng of BMP4 demonstrate decreased staining for BSA and BMP4 at 66 and 25 kDa, respectively, as compared to soluble control. C) Improved staining for BMP4 was observed by increasing the duration time from 5 to 10 or 15 minutes in which SDS treated MPs are heated prior to performing gel electrophoresis.

Concentration and characterization of ESC CM bound to HMAm MPs

Analysis of conditioned media via gel electrophoresis was insufficient to detect pico- and nanogram levels of protein as silver staining resulted in the presence of dark and smeared bands due to large quantities of BSA present (Figure 5.2A). To detect pictogram levels of protein, staining time was increased from 15 minutes to 30 minutes; however, staining of BSA ultimately limited detection of proteins lower in molecular weight and abundance. As previously described, HMAm MPs were observed to limit binding of BSA (pI=4.7) while simultaneously presenting a means to concentrate conditioned media. BSA levels of varied dilutions of conditioned media were compared to HMAm MPs loaded with 1 and 5 mL of media (Figure 5.2B). Total volume of conditioned media used for 1x, 5x, 10x, and 25x dilutions were 32, 6.4, 3.2, and 1.28 µL, respectively. Increasing the dilutions of media decreased the presence of BSA, but also limited the detection of other proteins. Conversely, HMAm MPs loaded with 1 and 5 mL of conditioned media demonstrated levels of BSA similar to the 25x diluted media, but were able to enhance detection of low molecular weight proteins (Figure 5.2C). More specifically, MPs demonstrated approximately 20x less BSA binding when compared to undiluted conditioned media. Additionally, HMAm MPs loaded with 5 mL of conditioned media showed darker staining as compared to MPs loaded with 1 mL of media, indicating more binding of protein with increased volume of media.

Further characterization of the use of MPs to concentrate conditioned media was performed by comparing HMAm MPs to MPs composed of other polymer types, such as gelatin-methacylate (GMA) [118], chondroitin-sulfate (CSMA) [117], and heparin-functionalized polystyrene (Hep-PS) beads (Figure 5.3). Overall, all MPs demonstrated staining for similar bands, but the intensity of bands differed among groups, suggesting that the different MPs bound proteins from conditioned media with variable affinities. MPs formed from gelatin that was derived from denatured collagen demonstrated

increased staining for BSA as compared to CSMA and HMAm MPs and demonstrated less intense staining for other protein bands, most notably at 50, 35, and 17 kDa for both 0.1 and 0.5 mg of MPs (Figure 5.3; white arrows). Hep-PS MPs demonstrated the least intense staining for all protein bands below 60 kDa, yet showed darker staining for BSA as compared to all other MPs. In addition, Hep-PS required a greater amount of MPs (1 and 2 mg of MPs) as compared to other MP types (0.1 and 0.5 mg of MPs) in order to visualize stained bands of protein. In contrast to HMAm MPs, which were composed solely of heparin, Hep-PS MPs were composed of heparin-functionalized to the surface of polysystrene beads, which limited the total amount of growth factor binding. To decipher if protein binding was dependent on species of GAG, CSMA MPs were also compared to HMAm MPs. CSMA MPs demonstrated similar staining profile toHMAm MPs at both MP amounts (0.1 and 0.5 mg of MPs) (Figure 5.3). Unlike the differences observed between 0.1 and 0.5 mg of GMA MPs for protein staining, no differences were observed between different CSMA and HMAm MP quantities (0.1 and 0.5 mg), suggesting that GMA MPs bind less total protein per mg MP as compared to GAG-based MPs.

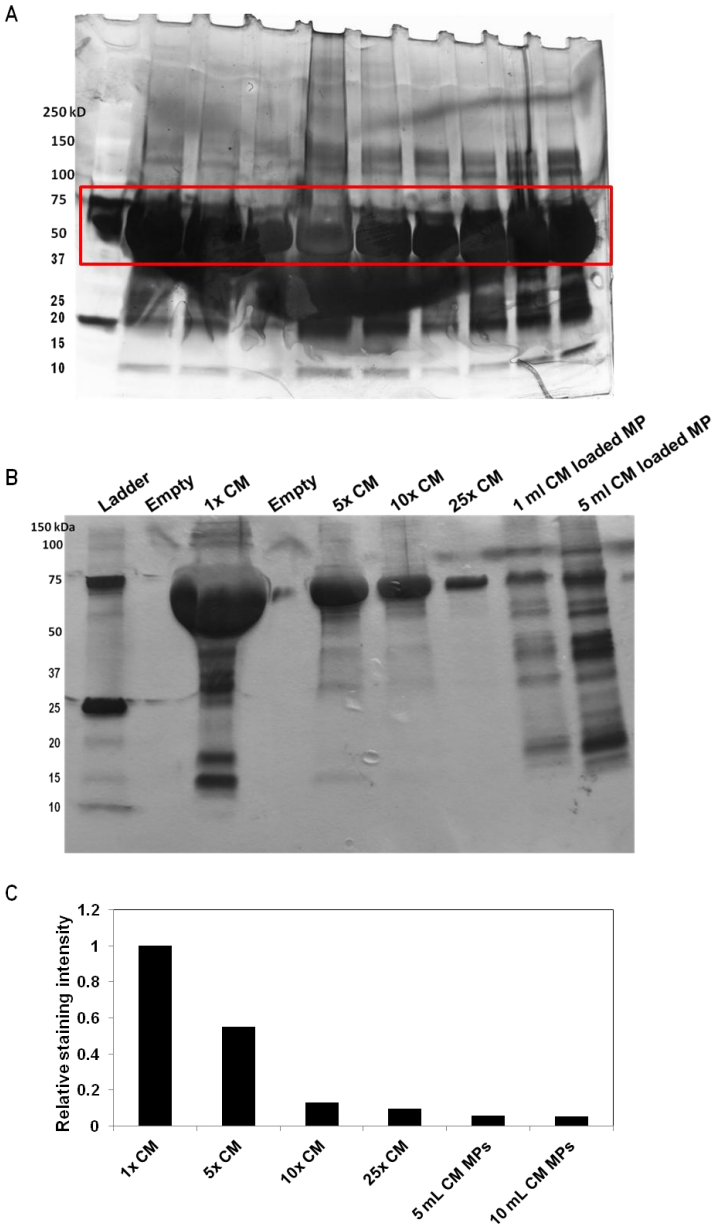

Figure 5.2. HMAm MPs can be used to concentrate ESC conditioned media. A) SDS-PAGE was performed on unloaded conditioned media. Due to large quantities of BSA (red box) present in media, staining of BSA was smeared across the gel and masked bands for protein at lower molecular weights. B) Conditioned media at 1, 5, 10, and 25x dilutions were compared to MPs loaded with 1 mL and 5 mL conditioned media. Conditioned media (1 and 5 mL) loaded MPs showed similar staining levels for BSA (pI=4.7) (white arrows) as the 25x diluted CM and similar staining levels for other proteins as the 1x diluted CM, indicating that MPs are able to effectively concentrate conditioned media and limit binding of BSA. C) ImageJ software was used to measure the relative levels of intensity of BSA staining for each group, where the highest value was measured for 1x conditioned media and the lowest value was observed for both conditioned media loaded MP groups.

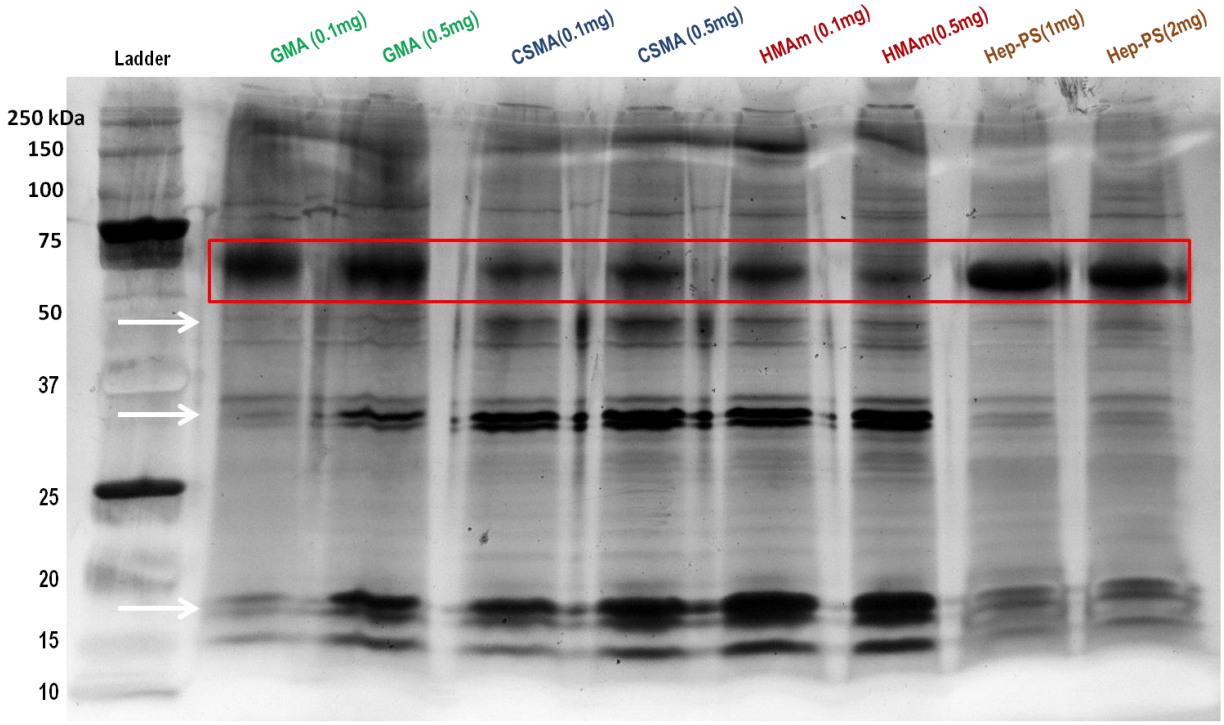

Figure 5.3. HMAm MPs demonstrate higher protein binding as compared to other MP formulations. SDS-PAGE was performed on MPs synthesized from different polymer types to compare differences in binding of protein from conditioned media. Both GAG-based MPs (CSMA and HMAm) demonstrated the darkest staining of protein bands, as well as the least staining for BSA (66 kDa) (red box). In contrast, GMA MPs showed similar protein bands but with decreased intensity of staining, especially at 0.1 mg of MPs. Hep-PS MPs showed decreased staining for all protein bands and required much larger quantities of MPs to visualize protein bands. Both GMA and Hep-PS MPs had increased staining of BSA as compared to CSMA and HMAm MPs, suggesting that GAG based MPs limit binding of BSA over other MP types. White arrows represent molecular weights of 50, 35, and 17 kDa in descending order.

Mass spectrometry analysis of gels loaded with MP bound protein.

MS analysis was performed on excised bands of interest from gels to characterize the profile of protein bound to HMAm MPs. Table 5.1 provides an overview of all experiments performed and parameters altered to develop a suitable method for protein characterization. Briefly, MS analysis was performed on stained or unstained gels with conditioned media or growth factor (hBMP4, hBMP2, and hTGFβ1) loaded MPs. Many silver staining protocols are not compatiable for MS analysis due to crosslinking and fixing of gels prior to staining, preventing enzymatic digestion of protein [180]. Therefore, identification of peptides was compared between unstained and stained gels; however, results demonstrated no differences between gels. Additionally, multiple enzymes were used for protein digestion of excised bands from gels. Typically, peptides between 7 and 20 amino acids (AAs) in length are ideal for MS analysis and database searching [181]. For example, with trypsin digestion, BMP2 generates 1 peptide, while TGFβ generates 3 peptides between 7-20 AAs. Therefore, using a combination of enzymes, such as GLu-C and Lys-C, theoretically generates more peptides of ideal length [182] Unexpectedly, the majority of peptides identified by MS were intracellular proteins such as histones, ribosomal proteins, actin, etc.

In an attempt to limit the amount of contamination of intracellular proteins released from cells into the collected spent media, MPs loaded with freeze-thawed samples of conditioned media were compared to conditioned media collected fresh from ESC cultures (Figure 5.5A). A BCA protein assay was performed on fresh and freeze-thawed CM to determine if protein concentration increased due to lysed cells in thawed CM. However, no detectable differences between protein concentrations were observed via a BCA assay (Figure 5.4B). Conversely, staining of the gel saw more staining of specific bands at 30 kDa and 15 kDa for frozen conditioned media. However, results from MS analysis revealed mainly detection of intracellular proteins. As an example,

Table 5.2 presents a typical list of proteins often detected from MS analysis of excised bands from gels with conditioned media loaded MPs. A wide variety of proteins were detected and widely distributed across the gel such as ribosomal proteins (9- 35 kDa), fibroblast growth factor 4 (FGF4) (22 kDa), thrombospondin (150-180 kDa), and histones (11-21 kDa).

Table 5.1: Summary of mass spectrometry studies.

Experiment Description	Run on gel	Mass Spec Method (enzymes, database, exclusion of specific peptides	Results
CM loaded MPs	Yes	Standard gel digestion method with trypsin (see next slide)	Histones, tubulin, ribosomal proteins, thrombospondin, FGF4, other intracellular proteins
CM/BMP4 loaded MPs (staining under laminar flow hood)	Yes	Standard gel digestion method with trypsin	Keratin contaminants, histones, ribosomal proteins, actin, other intracellular proteins
Unloaded BMP4 solution (1.25 ug)	No	Adjust pH to 8.5 with NH_4HCO_3 Add trypsin. Incubate overnight 37 deg. Quench and stage tip; MS analysis	Detected only BMP2
Lyophilized protein samples hBMP4 (40 ng) hBMP2 (95ng) hVEGF (50 ng) mIGFII (65ng)	No	Add NH_4HCO_3, and trypsin. Incubate overnight 37 deg. Quench and stage tip; MS analysis	No peptide hits due to high presence of detergents
Unstained gel) – BMP4/CM loaded MPs	Yes	Standard gel digestion method with trypsin	Several intracellular proteins (as above), BMP4 was not identified.
Unloaded protein solution hTGF-β (2ug) BMP2 (35 ug/ml – 20/40 ul)	No	Adjust pH to 8.5 with NH_4HCO_3 Add trypsin. Incubate overnight 37 deg. Quench and stage tip; MS analysis	Only identified BSA
Unloaded protein solution hTGF-β (2ug) BMP2 (35 ug/ml – 20/40 ul)	No	Reduction & alkylation (5 mM DTT, 14 mM IAA) Add PBS pH=8 and Glu-C. Incubate overnight 37 deg. Add Lys-C, incubate 4 hr. Quench and stage tip; MS analysis	Successfully identified proteins
Unstained gel-, MP loaded protein of hTGF-β BMP2	Yes	Standard gel digestion method with Glu-C and Lys-C	BMP2 was identified, but not TGF-β, on stained half of gel. Neither identified on unstained half.
CM loaded MPs	Yes	Standard gel digestion method Lanes 1 and 3 – trypsin Lanes 2 and 4 – Glu-C, Lys-C	Several intracellular proteins (as above)
Direct analysis of BMP4 (50 ng) loaded on MPs	No	Remove solution, add 50 mM NH_4HCO_3 (pH=8.5) and trypsin. Incubate overnight 37 deg. Quench and stage tip; MS analysis	Only detected contaminants
Frozen CM versus fresh CM	Yes	Standard gel digestion method Lanes 1 and 3 – trypsin Lanes 2 and 4 – Glu-C, Lys-C	Several intracellular proteins (as above), no differences between fresh and frozen.

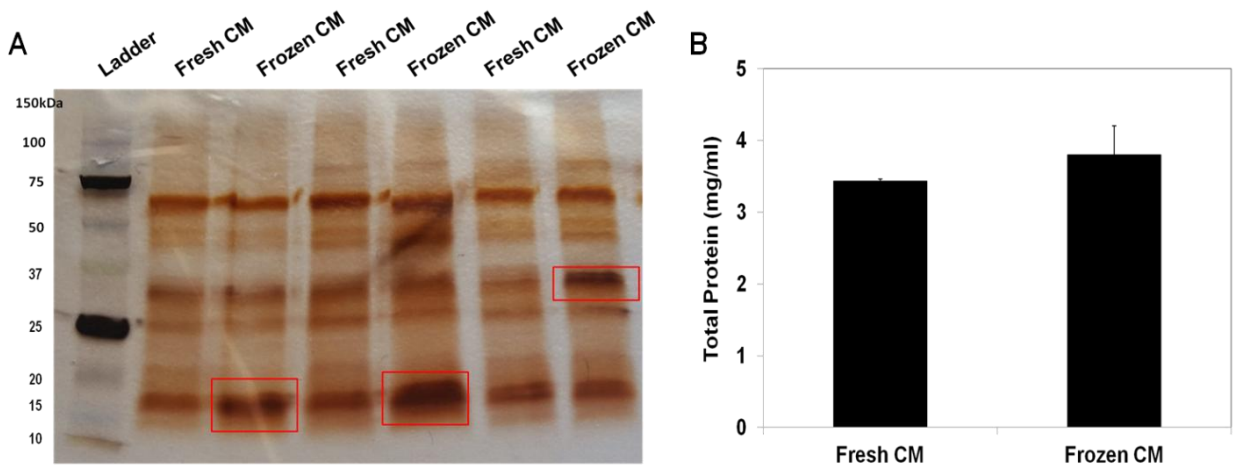

Figure 5.4. SDS-PAGE analysis of fresh versus frozen conditioned media loaded on HMAm MPs. A) Conditioned media that underwent 1 freeze thaw cycle demonstrated increased staining of bands at 15 and 30 kDa as compared to fresh conditioned media that has not been previously frozen. B) No significant difference between the total protein concentration of fresh and frozen CM was observed after quantification by a BCA assay.

Table 5.2. Summary of MP bound proteins detected by mass spectrometry analysis.*

Unique	Total	AVG	Annotation
5	6	3.7722	HSP7C_MOUSE Heat shock cognate 71 kDa protein
4	6	3.3626	ENPL_MOUSE Endoplasmin
4	4	3.0904	HMGB1_MOUSE High mobility group protein B1
4	4	2.8959	K1C16_HUMAN_contaminant Keratin, type I cytoskeletal 16
3	5	2.7105	NUCL_MOUSE Nucleolin
3	4	4.0219	TRYP_PIG_contaminant Trypsin
3	4	3.8079	RDRP_SCVLA_contaminant Probable RNA-directed RNA polymerase
3	4	3.1856	K2C8_HUMAN_contaminant Keratin, type II cytoskeletal 8
3	4	3.0954	RSMB_MOUSE Small nuclear ribonucleoprotein-associated protein B
3	4	2.8068	VDAC1_MOUSE Voltage-dependent anion-selective channel protein 1
3	4	2.7604	ATPA_MOUSE ATP synthase subunit alpha, mitochondrial
3	3	3.7016	NACAM_MOUSE Nascent polypeptide-associated complex subunit alpha, muscle-specific form
3	3	3.024	HMGB2_MOUSE High mobility group protein B2
3	3	2.7908	HS90A_MOUSE Heat shock protein HSP 90-alpha
3	3	2.7234	K1C14_HUMAN_contaminant Keratin, type I cytoskeletal 14
3	3	2.6782	RU2A_MOUSE U2 small nuclear ribonucleoprotein A'
3	3	2.5869	FETUA_BOVIN_contaminant Alpha-2-HS-glycoprotein
3	3	2.5362	H12_MOUSE Histone H1.2
2	3	3.7284	TBA1B_MOUSE Tubulin alpha-1B chain
2	3	2.9373	GRP78_MOUSE 78 kDa glucose-regulated protein
2	3	2.8676	MBB1A_MOUSE Myb-binding protein 1A
2	3	2.5755	DCD_HUMAN_contaminant Dermcidin
2	2	3.6608	ALBU_HUMAN_contaminant Serum albumin
2	2	3.4969	RS8_MOUSE 40S ribosomal protein S8
2	2	3.4223	K1C18_HUMAN_contaminant Keratin, type I cytoskeletal 18
2	2	3.1555	TSP1_MOUSE Thrombospondin-1
2	2	3.1495	Q792Z1_MOUSE MCG140784
2	2	3.1471	RL18_MOUSE 60S ribosomal protein L18
2	2	3.1436	K2C6C_HUMAN_contaminant Keratin, type II cytoskeletal 6C
2	2	2.9332	VIME_MOUSE Vimentin
2	2	2.887	RS4X_MOUSE 40S ribosomal protein S4, X isoform
2	2	2.855	RL7A_MOUSE 60S ribosomal protein L7a
2	2	2.8118	AT1A1_MOUSE Sodium/potassium-transporting ATPase subunit alpha-1
2	2	2.6684	RS3_MOUSE 40S ribosomal protein S3
2	2	2.6157	KPYM_MOUSE Pyruvate kinase PKM
2	2	2.5392	TBB5_MOUSE Tubulin beta-5 chain
2	2	2.5067	SAHH_MOUSE Adenosylhomocysteinase
2	2	2.436	EF1A1_MOUSE Elongation factor 1-alpha 1
2	2	2.425	APOE_MOUSE Apolipoprotein E
2	2	2.1744	H15_MOUSE Histone H1.5

***The "unique" column is the unique number of peptide hits for the specific protein in the run, while the "total" column is the total number of peptide hits for the specific protein in the run.

Direct characterization and quantification of MP bound protein

To ensure that proteins being eluted effectively by electrophoresis and SDS, a fluorescamine assay was performed to quantify protein bound to MPs after loading of 1, 5, or 10 mL of conditioned media (Figure 5.5).. Total protein after treatment with SDS and heat was also quantified to determine the efficacy of protein dissociation from HMAm MPs. Baseline values for unloaded MPs (~9.79 ug/mg MP) were subtracted from all other experimental groups prior to calculating MP bound protein concentration. Approximately 3.9 ± 1.3, 8.4 ± 0.5, and 10.5 ± 1.1 µg of free amines per 0.5 mg MPs were detected for MPs loaded with 1, 5, and 10 mL of conditioned media, respectively. MPs loaded with 5 and 10 mL conditioned media demonstrated significantly more detection of free amines than MPs loaded with 1 mL of media. For MPs treated with SDS at 95˚C for 10 minutes, approximately 0.1 ± 0.1, 0.3 ± 0.2, and 0.8 ± 0.4 µg/mL free amines were detected for 1, 5, and 10 mL of conditioned media, respectively, indicating that SDS/heat treatment promotes protein dissociation from MPs. All groups treated with SDS/heat had more than 90% reduction in free amine concentration as compared to untreated groups.

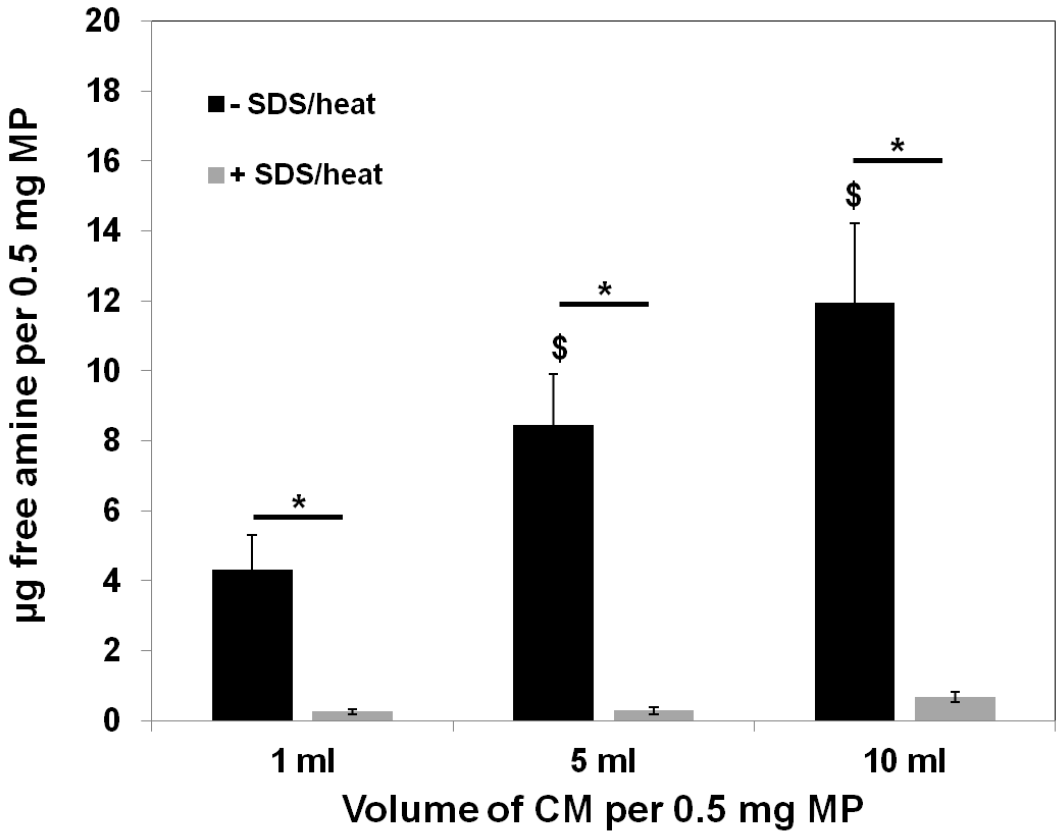

Figure 5.5: SDS and heat treatment reduces detection of protein bound to HMAm MPs. Detection of free amines was significantly ($p < 0.05$) lower for all groups after treatment with SDS and heat, with less than 1 ug of free amines per 0.5 mg MP detected and more than 90% of protein removed as compared to untreated samples. Both MP groups loaded with 5 and 10 mL of conditioned media demonstrated significantly ($p < 0.5$) greater detection of free amines over MPs loaded with 1 mL of media, * = Significant to SDS/heat treatment groups ($p < 0.5$); $ = Significant to untreated (-SDS/heat) 1 mL CM group ($p < 0.5$).

Retrieval of HMAm microparticles incorporated within embryoid bodies

ESCs within EBs spontaneously differentiate during culture synthesizing a complex array of various factors and soluble cues that direct cell fate [153,154] Ultimately, GAG-based MPs could provide a tool to study morphogen production during ESC differentiation in order to advance understanding of how these components are modulated during early development. It was hypothesized that HMAm MPs incorporated within EBs could be used to develop a novel strategy to capture endogenously secreted ESC morphogens in a concentrated manner. After incorporation in EBs, HMAm MPs required separation from EBs without disruption of growth factor-heparin interactions. Generally, dissociation of EBs is performed by enzymatic digestion with trypsin. However, trypsin cleaves lysine and arginine amino acid residues, and would ultimately cleave MP bound protein. Therefore, a non-enzymatic digestion buffer was used to dissociate EBs and retrieve morhpogen-laden MPs (Figure 5.6A). MP bound protein was incubated with either trypsin or non-enzymatic dissociation buffer and then run on a gel to evaluate retention of protein (Figure 5.6B). MPs incubated in non-enzymatic dissociation buffer demonstrated more staining for protein as compared to MPs incubated in trypsin, indicating that non-enzymatic buffer limits protein dissociation from MPs.

Percoll density gradient centrifugation was used to separate protein bound MPs from dissociated cells. After centrifugation, each of the three Percoll layers (top, 40.5%, and 58.5%) was aspirated into separate conical tubes and washed twice with PBS, followed by quantification of MP retrieval and separation from cells via flow cytometry (Figure 5.7). Each fraction was compared to control samples consisting of either single cells or MPs to quantify percent retrieval. The top most layer of the Percoll gradient was

composed primarily of cells, with approximately 91.5% cells and 1.4% MPs, while the 58.5% Percoll layer was composed primarily of MPs, with approximately 95.0% MPs and 7.8% cells.

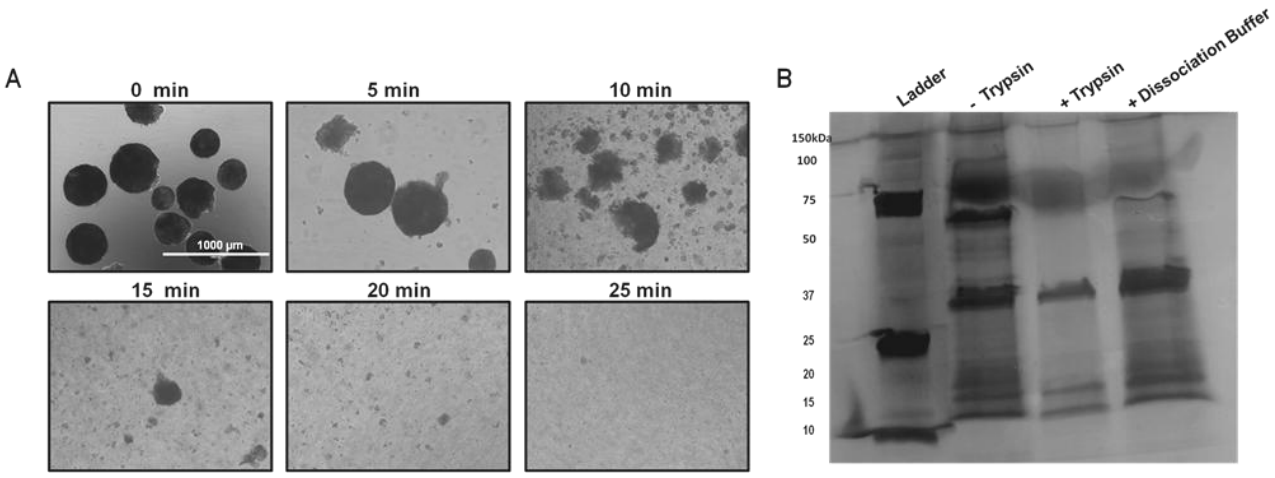

Figure 5.6. Non-enzymatic dissociation buffer treatment of EBs and CM- loaded MPs. A) Day 7 EBs were incubated at 37˚C with a non-enzymatic dissociation buffer to promote cell dissociation. Majority of EBs were dissociated by 15 minutes of incubation time. B) SDS-PAGE analysis was performed on conditioned media loaded MPs treated with either trypsin or non-enzymatic dissociation buffer. Trypsin treated MPs demonstrated a decrease in staining of protein as compared to untreated MPs and MPs treated with the dissociation buffer.

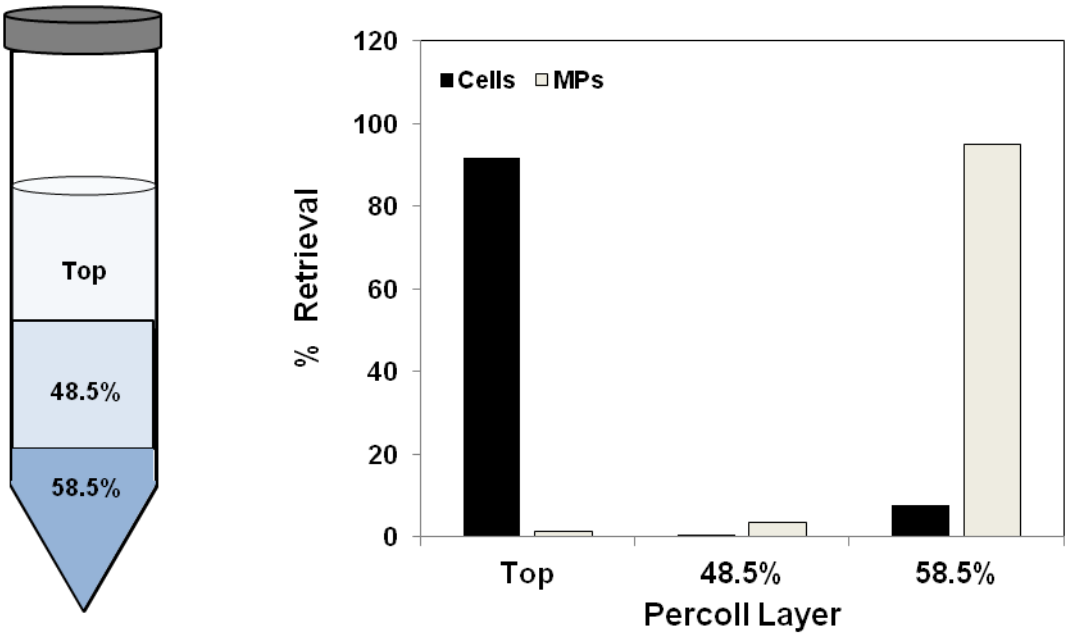

Figure 5.7. Quantification of MP and cell separation by a Percoll gradient. Percoll density gradient centrifugation was performed by layering a solution of MPs and cells on top of a 58.5 and 48.5 % layers in a 15 mL conical tube. Approximately 91.5% cells were found in the top layer, while approximately 95% of MPs were found in the 58.5% layer.

Discussion

Embryonic stem cells are a unique cell population that provide a readily accessible model system for early embryonic development. Harnessing the regenerative potential of ESCs will rely on understanding the complex system of signaling molecules that play an important role during self-renewal and differentiation. Ultimately, identification of endogenously secreted ESC factors will improve our understanding of the molecular mechanisms that govern cell fate. Numerous attempts to characterize the secretome with MS has enabled the discovery of several proteins secreted by ESCs [161,174,177]. It has been well established that ESCs secrete key morphogenic factors that regulate cell lineage decisions and also bind directly to heparin, or act in complex with heparin and cell-surface receptors [63,68,86,183]. Heparin functionalized beads have been previously used to selectively bind morphogenic factors from ESC conditioned media in order to enrich for potentially therapeutic factors [184]. However, the identity and relative amounts of these factors has yet to be specifically elucidated. This study demonstrated the use of HMAm microparticles to bind and concentrate various biomolecules present in spent media collected from EBs undergoing differentiation.

We hypothesized that MPs would capture specific heparin-binding growth factors (HBGFs), such as VEGF, FGF2, and BMP4 [148,179], and MS analysis could identify molecules bound to MPs. To investigate our hypothesis, we developed a method to concentrate molecules present in conditioned media. As demonstrated by the results, 5 mL of conditioned media loaded on MPs can be analyzed via gel electrophoresis, while typically only 25-50 µL of conditioned media can be loaded in a gel. Subsequently, characterization and analysis of MP bound protein was performed by gel electrophoresis, silver staining, and MS. Initial experiments with PAGE gels

demonstrated the ability of MPs to concentrate proteins in conditioned media with the surprising ability to also limit BSA binding. This is an important feature of our technique, as media contains high levels of BSA, which can mask the detection of lower abundance proteins, as evident in gels with conditioned media.. Growth factor and heparin binding is governed predominately by electrostatic interactions, with negatively charged heparin binding to positively charged growth factors [68,185]. It is hypothesized that proteins bind to heparin and other GAGs based on specific affinities to particular sequences present in the saccharide chain [85,186], suggesting that reduced BSA binding to MPs is due to decreased affinity for heparin. Furthermore, MPs of different polymer types (GMA, CSMA, HMAm, and Hep-PS) demonstrated differential binding of protein from conditioned media, , providing further evidence that different types of GAG-based MPs bind biomolecules with variable affinities. . Previous studies have demonstrated that GAGs of specific chain lengths and sulfation patterns can play diverse roles in regulating stem cell differentiation [80,87] . Therefore, MPs composed of various ECM components such as GAGs could be utilized to direct ESCs toward specific lineages by enhancing certain signaling pathways based on their respective protein binding capacities.

MS analysis of proteins bound to MPs detected primarily intracellular proteins and little to no identification of HBGFs or other growth factors known to be present in ESC conditioned media [153,154,161] In typical LC-MS/MS approaches, only the most abundant proteins are often identified. Despite attempts to enrich for heparin-binding proteins in conditioned media using MPs prior to analysis, numerous low-abundance ($<10^{-9}$ g/mL) proteins may remain undetected due to excess peptides from high abundance proteins present. In order to circumvent these limitations, iterative exclusion (IE) analysis can be employed [187,188]. Instead of performing a single repeat analysis, protein fractions are analyzed between 3 and 5 times, consisting of an initial round of

LC-MS/MS analysis followed by subsequent rounds of LC-MS/MS analysis, with the exclusion of peptides with mass/charge (*m/z*) values that match predicted tryptic peptides of proteins identified in previous rounds. IE-mass spectrometry approach has been shown to identify 10 times more previously undetected extracellular proteins, ranging in concentration from 10^{-9} to 10^{-11} g/mL [161]. Heparin can enhance signaling cascades that modulate cell proliferation, migration, and differentiation by binding, protecting, and presenting growth factors to cell receptors; however, the mechanisms that control cell behavior are poorly understood [148,189]. Retrieval of MPs from EBs via Percoll gradient provides a novel method to sequester ESC-secreted factors for analysis, not only to elucidate the role in which autocrine and paracrine factors play in self-renewal and differentiation of ESCs, but also for applications in regenerative therapies. Ultimately, identification of growth factors secreted/produced in differentiating EBs will help to elucidate the underlying mechanisms that govern ESC fate.

Conclusions

Overall, HMAm MPs can be used as a tool to concentrate biomolecules present in ESC conditioned media, while simultaneously reducing presence of BSA for MS analysis. While MS analysis did not identify factors of interest, specifically HBGFs, improved IE-MS techniques can be employed to better identify peptides of lower abundance proteins. Ultimately, we aim to develop a new class of biomaterials capable of capturing and delivering stem cell derived morphogens in a biomimetic manner. It is anticipated that the results of this work will provide new insights into the manner in which stem cells and the molecules they produce can be used for regenerative medicine applications.

CHAPTER VI

CONCLUSIONS AND FUTURE DIRECTIONS

Embryonic stem cells provide a renewable cell population that possess the unique ability to differentiate into hundreds of cell types, providing a promising cell source for studies of early embryonic development and regenerative medicine applications. Harnessing the regenerative potential of ESCs will rely on improved directed differentiation approaches, as well as enhanced understanding of the complex system of signaling molecules that play an important role during self-renewal and differentiation. Differentiation of ESCs is traditionally performed in monolayer, allowing for uniform exposure of cells to exogenously biomolecules; however, 3D culture of ESCs provides a more biological model of embryogenesis by facilitating multicellular interactions [34]. Cellular organization and differentiation of an embryo can be modeled by the formation of pluripotent stem cell aggregates, known as embryoid bodies (EBs) [35]. EB formation has traditionally been used to induce spontaneous differentiation of ESCs towards the three germ lineages. Previous attempt to direct ESC differentiation have utilized an “outside-in” approaches via soluble growth factor or small molecule supplementation, to direct ESC differentiation are limited by non-homogenous differentiation of EBs [119]. Alternatively, EB differentiation can be controlled via the introduction of engineered microparticles (MPs) for delivery of growth factors [121,125,126] or via cell-material interactions [127]. Just as MP mediated growth factor delivery can enhance differentiation of ESCs toward defined cell types, endogenous growth factors produced by differentiating EBs can be harnessed by MPs to direct ESC differentiation. Numerous attempts to characterize the secretome of differentiating ESCs

with mass spectrometry (MS) analysis has enabled the discovery of several key proteins secreted by ESCs [161,174,177]. Additionally, it has been established that ESCs secrete key morphogenic factors that regulate cell lineage decisions and also bind directly to heparin or act in complex with heparin and cell-surface receptors [63,68,86,183]. Furthermore, heparin functionalized beads have been used to selectively bind morphogenic factors from ESC conditioned media in order to enrich for potentially therapeutic factors [184], however, the identity of ESC-secreted factors has yet to be fully elucidated.

Synthetic *N*-isopropylmethacrylamide (NIPMAm) MP constructs were investigated as a biomaterial-based strategy to control the temporal release of BMP4 within ESC aggregates to induce mesoderm differentiation. Synthesis of MPs produced well-coated population of MPs in terms of microgel coverage, a critical property for the uniform presentation of material and growth factors to cells, and low polydispersity, an important component to minimize variations in loading and release rates of growth factors. pNIPMAm MPs exhibited minimal aggregation during lyophilization and after incorporation, crucial for even distribution of MPs and uniform delivery of BMP4 within EBs. However, MPs incorporated with low efficiency within ESC aggregates, most likely due to lack of cell adhesive sites [127]. In future studies, increased MP incorporation could be achieved by adding Arg-Gly-Asp (RGD) or other cell adhesion sequences to microgels [146]. MP delivery of BMP4 within ESC aggregates demonstrated similar expression of mesoderm (Flk1) as compared to soluble BMP4 delivery, while ectoderm expression (Pax6) was significantly decreased as compared to soluble delivery. In addition to analysis of gene expression, sentinel cells were used to monitor the spatial and temporal activation of BMP signaling in ESC aggregates, where maximum reported (CFP) expression was observed at day 2 of culture, coinciding with the burst release of BMP4 from MPs. Interestingly, ESC aggregates treated with unloaded MPs and soluble

BMP4 demonstrated higher expression of CFP over soluble BM4 treated aggregates, suggesting that unloaded MPs may bind and concentrate exogenously added or endogenously produced BMP4 within aggregates to induce BMP signaling. Notably, the total amount of BMP4 delivered by MP was 10-fold less total growth factor as compared to soluble delivery to achieve comparable ESC differentiation, indicating that MP approaches can improve efficiency of differentiation, by reducing soluble growth factor supplementation.

The development of mature tissue and organs is governed by the coordinated action of multiple growth factors. One of the first reported dual delivery systems involved the release of PDGF encapsulated in PLGA microspheres embedded in a PLGA scaffold containing VEGF to improve blood vessel formation.[190] Different release kinetics were engineered to provide control over the temporal release of each growth factor. A study by Choi et al. achieved sequential release of BMP-2 and dexamethasone from a microcapsule comprised of a PLGA core and alginate shell [191]. pNIPMAm MPs provide a means to customize MPs with varied release kinetics to improve the differentiation of ESCs into defined cell populations by delaying or prolonging BMP4 (or other growth factors) presentation to ESCs. The size and charge of microgels can be tailored to control the loading and release of specific morphogens. Different formulations of microgels can be synthesized and mixed populations can be added to core particles for dual delivery of growth factors or small molecules for differentiation of ESCs toward defined cell types. For example, hematopoietic differentiation requires Wnt or Activin to for initial development of the hemangioblast followed by VEGF supplementation [28]. In addition to electrostatic interactions between biomolecules, microgels with smaller mesh sizes can be used to imbibe small molecules (<900 Da) while larger mesh sizes can be fabricated to retain larger biomolecules (<15 kDa), such as growth factors. In addition, the thermoresponsivity of pNIPMAm materials allows for the design of stimuli-

responsive MPs that can improve the temporal control over morphogen delivery within ESC aggregates. Temporally controlled capture of ESC morphogenic factors could be performed by external control of thremoresponsive materials via temperature changes to enable the swelling or collapse of microgels, providing an additional level of control in the controlled d release of growth factors.

Given the importance of heparin/HS for ESC differentiation, HMAm MPs provide a model to determine the ability of exogenous soluble GAG-based materials to influence patterns of differentiation within EBs.. Incorporation of HMAm MPs within EBs demonstrated the native ability of natural GAG-based materials to modulate ESC differentiation. Incorporation of HMAm MPs within ESC aggregates demonstrated changes in gene and protein expression of neuorectodermal marker, Pax6. Histological analysis of aggregates with incorporated HMAm MPs exhibited more internal organized structures as compared to untreated aggregates. Despite various studies that have established a role for HS in ESC differentiation [76,86,151,192], one question that remains is whether additional fine structure requirements, such as sulfation, chain length, and concentration, exist for cell signaling pathways. A prerequisite to answering this question would be to establish how HS chainsbecome remodeled during specific stages of development by examining expression for genes (EXT1/2, NDST1/2, etc involved in the biosynthesis of HS) and measuring total heparin content from differentiating ESCs by high performance liquid chromatography (HPLC) [72,76].Furthermore, the use of HS-deficient and HS-competent ESCs, have been previously used as *in* vitro models to determine the ability of exogenous GAGs to "rescue" differentiation and ESC signaling pathways [80,86,160]. For instance, $EXT1^{-/-}$ mESCs fail to differentiate into mesoderm, however partial restoration of FGF and BMP signaling was achieved by addition of soluble heparin [86]. Heparin/HS-deficient systems could be used in conjunction with HMAM MPs to elucidate the effect of GAGs on stem

cell differentiation. Ultimately, a greater understanding of endogenous stem cell extracellular remodeling responses in response to various extracellular cues may enable rational approaches to initiating and mediating complex tissue morphogenic events. Engineering approaches for directing endogenous self-organization and remodeling responses of stem cells afford new opportunities for controlling of the complex signaling pathways regulating cell fate.

It was also demonstrated that HMAm MPs can be used as a tool to sequester and concentrate biomolecules present in ESC conditioned media, while simultaneously reducing the amount of abundant species, such as BSA, for mass spectrometry analysis. Notably, MPs demonstrated approximately 20x less BSA binding, but improved staining for protein bands as compared to diluted conditioned media. Furthermore, GMA [118], CSMA [117,126], and HMAm [116] MPs exhibited different binding capacities for complex mixtures of proteins present in conditioned media, suggesting that MPs composed of different ECM components could be mixed to direct ESCs to specific lineages, similar to previous work that demonstrated that incorporation of MPs fabricated from PLGA, agarose, and gelatin induced different patterns of ESC differentiation [127]. Furthermore, fabrication of MPs composed of multiple ECM components, such as heparin (or HMAm) and chondroitin sulfate (or CSMA), could be fabricated to create synthetic ECM MPs. Previous work has demonstrated that heparin/HS sulfation patterns are critical in the recognization of soluble and matrix proteins [80,81,85,87,186,193], thus synthesis of HMAm MPs with varied sulfation patterns provides another means to regulate growth factor binding and modulate signaling activation.

While GAGs and ECM proteins are important in regulating growth factor signaling, they interact with a wide array of growth factors with variable affinities and would likely impact a multitude of signaling pathways in parallel, which may ultimately limit the specificity of approaches for directed differentiation. Murphy et al. developed PEG

microspheres that incorporated a synthetic VEGF binding peptide derived from VEGF receptor 2 that demonstrates targeted binding of VEGF and release [90]. Engineering synthetic materials with ECM mimetic components could provide a means to increase or decrease specific signaling pathways by exploiting growth factor-material interactions and controlling the affinity and specificity with which MPs interact with stem cell produced growth factors. Ultimately, design of MPs that incorporate peptides that bind specific molecules would provide the ability to mimic the native ECM to regulate growth factor signaling that direct cell fate, but improve the specificity of materials for directed differentiation of ESCs . While MS analysis did not identify heparin-binding growth factors previously detected in ESC conditioned media by ELISA [153,154], alternative MS techniques can be employed to identify peptides of lower abundance proteins. For instance, iterative exclusion (IE) analysis can be employed by analyzing protein fractions multiple times and excluding ions selected in the previous rounds [187]. In addition, directed differentiation approaches could be employed to study morphogen production during ESC differentiation and increase production of specific heparin-binding growth factors. For instance, hypoxic conditions further promote ESC differentiation by decreasing expression of pluripotency markers, while increasing expression of genes associated with vasculogenesis and angiogenesis, as well as increased VEGF production [11,49,194]. By increasing production of specific heparin-binding growth factors, HMAm MPs could be used to further improve differentiation as well as enable better identification of factors via MS analysis. Ultimately, development of biomaterials capable of capturing morphogenic factors in a ECM-mimetic manner introduces a novel approach to direct differentiation of ESCs and demonstrates the utility of GAG MPS as a complement to growth factor or small molecule supplementation to influence cell fate.

REFERENCES

[1] Yang X, Guo X-M, Wang C-Y, Tian XC. Cardiomyocytes. Methods Enzymol 2006;418:267–83. doi:10.1016/S0076-6879(06)18016-7.

[2] Yoon BS, Yoo SJ, Lee JE, You S, Lee HT, Yoon HS. Enhanced differentiation of human embryonic stem cells into cardiomyocytes by combining hanging drop culture and 5-azacytidine treatment. Differentiation 2006;74:149–59. doi:10.1111/j.1432-0436.2006.00063.x.

[3] Laflamme M a, Chen KY, Naumova A V, Muskheli V, Fugate J a, Dupras SK, et al. Cardiomyocytes derived from human embryonic stem cells in pro-survival factors enhance function of infarcted rat hearts. Nat Biotechnol 2007;25:1015–24. doi:10.1038/nbt1327.

[4] Maltsev V a., Rohwedel J, Hescheler J, Wobus a. M. Embryonic stem cells differentiate in vitro into cardiomyocytes representing sinusnodal, atrial and ventricular cell types. Mech Dev 1993;44:41–50. doi:10.1016/0925-4773(93)90015-P.

[5] Boheler KR, Czyz J, Tweedie D, Yang HT, Anisimov S V., Wobus AM. Differentiation of pluripotent embryonic stem cells into cardiomyocytes. Circ Res 2002;91:189–201. doi:10.1161/01.RES.0000027865.61704.32.

[6] Joannides AJ, Fiore-Hériché C, Battersby A a, Athauda-Arachchi P, Bouhon I a, Williams L, et al. A scaleable and defined system for generating neural stem cells from human embryonic stem cells. Stem Cells 2007;25:731–7. doi:10.1634/stemcells.2006-0562.

[7] Kawasaki H, Mizuseki K, Nishikawa S, Kaneko S, Kuwana Y, Nakanishi S, et al. Induction of midbrain dopaminergic neurons from ES cells by stromal cell-derived inducing activity. Neuron 2000;28:31–40. doi:10.1016/S0896-6273(00)00083-0.

[8] Bain G, Kitchens D, Yao M, Huettner JE, Gottlieb DI. Embryonic stem cells express neuronal properties in vitro. Dev Biol 1995;168:342–57.

[9] Okabe S, Forsberg-Nilsson K, Spiro a. C, Segal M, McKay RDG. Development of neuronal precursor cells and functional postmitotic neurons from embryonic stem cells in vitro. Mech Dev 1996;59:89–102. doi:10.1016/0925-4773(96)00572-2.

[10] Vittet D, Prandini MH, Berthier R, Schweitzer a, Martin-Sisteron H, Uzan G, et al. Embryonic stem cells differentiate in vitro to endothelial cells through successive maturation steps. Blood 1996;88:3424–31.

[11] Prado-Lopez S, Al. E. Hypoxia promotes efficient differentiation of human embryonic stem cells to functional endothelium. Stem Cells 2010;28:407–18.

[12] Mccloskey KE, Lyons I, Rao RR, Stice SL, Nerem RM. Purified and Proliferating Endothelial Cells Derived and Expanded In Vitro from Embryonic Stem Cells. Endothelium 2003;10:329–36. doi:10.1080/10623320390272325.

[13] Guo T, Hebrok M. Stem Cells to Pancreatic Beta-Cells : New Sources for Diabetes Cell Therapy. Endocr Rev 2009;30:214–27. doi:10.1210/er.2009-0004.

[14] Shim JH, Kim SE, Woo DH, Kim SK, Oh CH, McKay R, et al. Directed differentiation of human embryonic stem cells towards a pancreatic cell fate. Diabetologia 2007;50:1228–38. doi:10.1007/s00125-007-0634-z.

[15] D'Amour K a, Bang AG, Eliazer S, Kelly OG, Agulnick AD, Smart NG, et al. Production of pancreatic hormone-expressing endocrine cells from human embryonic stem cells. Nat Biotechnol 2006;24:1392–401. doi:10.1038/nbt1259.

[16] Jiang W, Shi Y, Zhao D, Chen S, Yong J, Zhang J, et al. In vitro derivation of functional insulin-producing cells from human embryonic stem cells. Cell Res 2007;17:333–44. doi:10.1038/cr.2007.28.

[17] Thomson J a. Embryonic Stem Cell Lines Derived from Human Blastocysts. Science (80-) 1998;282:1145–7. doi:10.1126/science.282.5391.1145.

[18] Murry CE, Keller G. Differentiation of embryonic stem cells to clinically relevant populations: lessons from embryonic development. Cell 2008;132:661–80. doi:10.1016/j.cell.2008.02.008.

[19] Palis J, Robertson S, Kennedy M, Wall C, Keller G. Development of erythroid and myeloid progenitors in the yolk sac and embryo proper of the mouse. Development 1999;126:5073–84.

[20] Keller G, Kennedy M, Papayannopoulou T, Wiles M V. Hematopoietic commitment during embryonic stem cell differentiation in culture. Mol Cell Biol 1993;13:473–86. doi:10.1128/MCB.13.1.473.Updated.

[21] Winnier G, Blessing M, Labosky P a, Hogan BL. Bone morphogenetic protein-4 is required for mesoderm formation and patterning in the mouse. Genes Dev 1995;9:2105–16. doi:10.1101/gad.9.17.2105.

[22] Schier a F, Shen MM. Nodal signalling in vertebrate development. Nature 2000;403:385–9. doi:10.1038/35000126.

[23] Yamaguchi TP. Heads or tails: Wnts and anterior-posterior patterning. Curr Biol 2001;11:713–24. doi:10.1016/S0960-9822(01)00417-1.

[24] Ema M, Takahashi S, Rossant J. Deletion of the selection cassette, but not cis-acting elements, in targeted Flk1-lacZ allele reveals Flk1 expression in multipotent mesodermal progenitors. Blood 2006;107:111–7. doi:10.1182/blood-2005-05-1970.

[25] Kataoka H, Takakura N, Nishikawa S, Tschudia K, Kodama H, Kunisada T, et al. Expressions of PDGF receptor alpha, c-Kit and Flk1 genes clustering in mouse chromosome 5 define distinct subsets of nascient mesodermal cells. Dev Growth Differ 1997;39:729–40.

[26] Park C, Afrikanova I, Chung YS, Zhang WJ, Arentson E, Fong Gh GH, et al. A hierarchical order of factors in the generation of FLK1- and SCL-expressing hematopoietic and endothelial progenitors from embryonic stem cells. Dev Dis 2004;131:2749–62. doi:10.1242/dev.01130.

[27] Ng ES, Azzola L, Sourris K, Robb L, Stanley EG, Elefanty AG. The primitive streak gene Mixl1 is required for efficient haematopoiesis and BMP4-induced ventral mesoderm patterning in differentiating ES cells. Development 2005;132:873–84. doi:10.1242/dev.01657.

[28] Nostro MC, Cheng X, Keller GM, Gadue P. Wnt, activin, and BMP signaling regulate distinct stages in the developmental pathway from embryonic stem cells to blood. Cell Stem Cell 2008;2:60–71. doi:10.1016/j.stem.2007.10.011.

[29] Lindsley RC, Gill JG, Kyba M, Murphy TL, Murphy KM. Canonical Wnt signaling is required for development of embryonic stem cell-derived mesoderm. Development 2006;133:3787–96. doi:10.1242/dev.02551.

[30] Naito AT, Shiojima I, Akazawa H, Hidaka K, Morisaki T, Kikuchi A, et al. Developmental stage-specific biphasic roles of Wnt/beta-catenin signaling in cardiomyogenesis and hematopoiesis. Proc Natl Acad Sci U S A 2006;103:19812–7. doi:10.1073/pnas.0605768103.

[31] Ueno S, Weidinger G, Osugi T, Kohn AD, Golob JL, Pabon L, et al. Biphasic role for Wnt/beta-catenin signaling in cardiac specification in zebrafish and embryonic stem cells. Proc Natl Acad Sci U S A 2007;104:9685–90. doi:10.1073/pnas.0702859104.

[32] Kubo A, Shinozaki K, Shannon JM, Kouskoff V, Kennedy M, Woo S, et al. Development of definitive endoderm from embryonic stem cells in culture. Development 2004;131:1651–62. doi:10.1242/dev.01044.

[33] Ying Q-L, Stavridis M, Griffiths D, Li M, Smith A. Conversion of embryonic stem cells into neuroectodermal precursors in adherent monoculture. Nat Biotechnol 2003;21:183–6. doi:10.1038/nbt780.

[34] Lutolf MP, Gilbert PM, Blau HM. Designing materials to direct stem-cell fate. Nature 2009;462:433–41. doi:10.1038/nature08602.

[35] Bratt-leal M, Carpenedo RL, Mcdevitt TC. Engineering the Embryoid Body Microenvironment to Direct Embryonic Stem Cell Differentiation. Culture 2009:43–51. doi:10.1021/bp.139.

[36] Chen Y, Li X, Eswarakumar VP, Seger R, Lonai P. Fibroblast growth factor (FGF) signaling through PI 3-kinase and Akt/PKB is required for embryoid body differentiation. Oncogene 2000;19:3750–6. doi:10.1038/sj.onc.1203726.

[37] Li X, Chen Y, Schéele S, Arman E, Haffner-Krausz R, Ekblom P, et al. Fibroblast growth factor signaling and basement membrane assembly are connected during epithelial morphogenesis of the embryoid body. J Cell Biol 2001;153:811–22. doi:10.1083/jcb.153.4.811.

[38] Wan YJ, Wu TC, Chung a. E, Damjanov I. Monoclonal antibodies to laminin reveal the heterogeneity of basement membranes in the developing and adult mouse tissues. J Cell Biol 1984;98:971–9. doi:10.1083/jcb.98.3.971.

[39] Murray P, Edgar D. Regulation of programmed cell death by basement membranes in embryonic development. J Cell Biol 2000;150:1215–21. doi:10.1083/jcb.150.5.1215.

[40] Coucouvanis E, Martin GR. Signals for death and survival: a two-step mechanism for cavitation in the vertebrate embryo. Cell 1995;83:279–87. doi:10.1016/0092-8674(95)90169-8.

[41] Kurosawa H. Methods for inducing embryoid body formation: in vitro differentiation system of embryonic stem cells. J Biosci Bioeng 2007;103:389–98. doi:10.1263/jbb.103.389.

[42] Larue L, Antos C, Butz S, Huber O, Delmas V, Dominis M, et al. A role for cadherins in tissue formation. Development 1996;122:3185–94.

[43] Carpenedo RL, Sargent CY, McDevitt TC. Rotary suspension culture enhances the efficiency, yield, and homogeneity of embryoid body differentiation. Stem Cells 2007;25:2224–34. doi:10.1634/stemcells.2006-0523.

[44] Ungrin MD, Joshi C, Nica A, Bauwens C, Zandstra PW. Reproducible, ultra high-throughput formation of multicellular organization from single cell suspension-derived human embryonic stem cell aggregates. PLoS One 2008;3. doi:10.1371/journal.pone.0001565.

[45] Ahadian S, Yamada S, Ramón-Azcón J, Ino K, Shiku H, Khademhosseini A, et al. Rapid and high-throughput formation of 3D embryoid bodies in hydrogels using the dielectrophoresis technique. Lab Chip 2014:3690–4. doi:10.1039/c4lc00479e.

[46] Faulkner-Jones A, Greenhough S, King J a, Gardner J, Courtney A, Shu W. Development of a valve-based cell printer for the formation of human embryonic stem cell spheroid aggregates. Biofabrication 2013;5:015013. doi:10.1088/1758-5082/5/1/015013.

[47] Xu F, Sridharan B, Wang S, Gurkan UA, Syverud B, Demirci U. Embryonic stem cell bioprinting for uniform and controlled size embryoid body formation. Biomicrofluidics 2011;5:1–8. doi:10.1063/1.3580752.

[48] Risau W, Sariola H, Zerwes H, Sasse J, Ekblom P, Kemler R, et al. Vasculogenesis and angiogenesis in embryonic-stem-cell-derived embryoid bodies. Development 1988;478:471–8.

[49] Min J, Kim J, Eun H, Ji M, Il K, Gyong E, et al. Enhancement of differentiation efficiency of hESCs into vascular lineage cells in hypoxia via a paracrine mechanism. Stem Cell Res 2011;7:173–85. doi:10.1016/j.scr.2011.06.002.

[50] Shweiki D, Itin A, Soffer D, Keshet E. Vascular endothelial growth factor induced by hypoxia may mediate hypoxia-initiated angiogenesis. Nature 1992;359:843–5.

[51] Doetschman TC, Eistetter H, Katz M. The in vitro development of blastocyst-derived embryonic stem cell lines : formation of visceral yolk sac , blood islands and myocardium. J Embryol Exp Morphol 1985;87:27–45.

[52] Eiraku M, Takata N, Ishibashi H, Kawada M, Sakakura E, Okuda S, et al. Self-organizing optic-cup morphogenesis in three-dimensional culture. Nature 2011;472:51–6. doi:10.1038/nature09941.

[53] Hattori N. Cerebral organoids model human brain development and microcephaly. Mov Disord 2014;29:185–185. doi:10.1002/mds.25740.

[54] Antonica F, Kasprzyk DF, Opitz R, Iacovino M, Liao X-H, Dumitrescu AM, et al. Generation of functional thyroid from embryonic stem cells. Nature 2012;490:66–71. doi:10.1038/nature11525.

[55] Reilly GC, Engler AJ. Intrinsic extracellular matrix properties regulate stem cell differentiation. J Biomech 2010;43:55–62. doi:10.1016/j.jbiomech.2009.09.009.

[56] Schönherr E, Hausser HJ. Extracellular matrix and cytokines: a functional unit. Dev Immunol 2000;7:89–101.

[57] Chen SS, Fitzgerald W, Zimmerberg J, Kleinman HK, Margolis L. Cell-cell and cell-extracellular matrix interactions regulate embryonic stem cell differentiation. Stem Cells 2007;25:553–61. doi:10.1634/stemcells.2006-0419.

[58] Hunt GC, Singh P, Schwarzbauer JE. Endogenous production of fibronectin is required for self-renewal of cultured mouse embryonic stem cells. Exp Cell Res 2012;318:1820–31. doi:10.1016/j.yexcr.2012.06.009.Endogenous.

[59] Dziadek M, Timpl R. Expression of nidogen and laminin in basement membranes during mouse embryogenesis and in teratocarcinoma cells. Dev Biol 1985;111:372–82. doi:10.1016/0012-1606(85)90491-9.

[60] Leivo I, Vaheri a, Timpl R, Wartiovaara J. Appearance and distribution of collagens and laminin in the early mouse embryo. Dev Biol 1980;76:100–14. doi:10.1016/0012-1606(80)90365-6.

[61] Rozario T, DeSimone DW. The extracellular matrix in development and morphogenesis: A dynamic view. Dev Biol 2010;341:126–40. doi:10.1016/j.ydbio.2009.10.026.

[62] Faham S, Hileman RE, Fromm JR, Linhardt RJ, Rees DC. Heparin structure and interactions with basic fibroblast growth factor. Science (80-) 1996;271:1116–20.

[63] Harmer NJ. Insights into the role of heparan sulphate in fibroblast growth factor signalling. Biochem Soc Trans 2006;34:442–5. doi:10.1042/BST0340442.

[64] Lin X, Buff EM, Perrimon N, Michelson a M. Heparan sulfate proteoglycans are essential for FGF receptor signaling during Drosophila embryonic development. Development 1999;126:3715–23.

[65] Mach H, Volkin DB, Burke CJ, Middaugh CR, Mattsson L. Nature of the Interaction of Heparin with Acidic Fibroblast Growth Factor. Biochemistry 1993;32:5480–9.

[66] Luginbuehl V, Meinel L, Merkle HP, Gander B. Localized delivery of growth factors for bone repair. Eur J Pharm Biopharm 2004;58:197–208. doi:10.1016/j.ejpb.2004.03.004.

[67] Stickens D, Zak BM, Rougier N, Esko JD, Werb Z. Mice deficient in Ext2 lack heparan sulfate and develop exostoses. Development 2005;132:5055–68. doi:10.1242/dev.02088.

[68] Esko JD, Lindahl U. Molecular diversity of heparan sulfate. J Clin Invest 2001;108:169–73. doi:10.1172/JCI200113530.Heparan.

[69] Holmborn K, Ledin J, Smeds E, Eriksson I, Kusche-gullberg M, Kjelle L. Heparan Sulfate Synthesized by Mouse Embryonic Stem Cells Is 6- O -Sulfated but Contains No N -Sulfate Groups * 2004. doi:10.1074/jbc.C400373200.

[70] Johnson CE, Crawford BE, Stavridis M, Ten Dam G, Wat AL, Rushton G, et al. Essential alterations of heparan sulfate during the differentiation of embryonic stem cells to Sox1-enhanced green fluorescent protein-expressing neural progenitor cells. Stem Cells 2007;25:1913–23. doi:10.1634/stemcells.2006-0445.

[71] Brickman YG, Ford MD, Gallagher JT, Nurcombe V, Bartlett PF, Turnbvill JE. Structural modification of fibroblast growth factor-binding heparan sulfate at a determinative stage of neural development. J Biol Chem 1998;273:4350–9. doi:10.1074/jbc.273.8.4350.

[72] Nairn A V, Kinoshita-toyoda A, Toyoda H, Xie J, Harris K, Dalton S, et al. Glycomics of Proteoglycan Biosynthesis in Murine Embryonic Stem Cell Differentiation. J Proteome Res 2007:4374–87.

[73] Lin X, Wei G, Shi Z, Dryer L, Esko JD, Wells DE, et al. Disruption of gastrulation and heparan sulfate biosynthesis in EXT1-deficient mice. Dev Biol 2000;224:299–311. doi:10.1006/dbio.2000.9798.

[74] Ford-Perriss M, Guimond SE, Greferath U, Kita M, Grobe K, Habuchi H, et al. Variant heparan sulfates synthesized in developing mouse brain differentially regulate FGF signaling. Glycobiology 2002;12:721–7. doi:10.1093/glycob/cwf072.

[75] Gasimli L, Hickey AM, Yang B, Li G, dela Rosa M, Nairn A V, et al. Changes in glycosaminoglycan structure on differentiation of human embryonic stem cells towards mesoderm and endoderm lineages. Biochim Biophys Acta 2014;1840:1993–2003. doi:10.1016/j.bbagen.2014.01.007.

[76] Allen BL, Rapraeger AC. Spatial and temporal expression of heparan sulfate in mouse development regulates FGF and FGF receptor assembly. J Cell Biol 2003;163:637–48. doi:10.1083/jcb.200307053.

[77] Hirano K, Sasaki N, Ichimiya T, Miura T, van Kuppevelt TH, Nishihara S. 3-O-sulfated heparan sulfate recognized by the antibody HS4C3 contribute to the differentiation of mouse embryonic stem cells via fas signaling. PLoS One 2012;7. doi:10.1371/journal.pone.0043440.

[78] Shipp EL, Hsieh-Wilson LC. Profiling the sulfation specificities of glycosaminoglycan interactions with growth factors and chemotactic proteins using microarrays. Cell 2007;14:195–208. doi:10.1016/j.chembiol.2006.12.009.

[79] Goh S-K, Olsen P, Banerjee I. Extracellular matrix aggregates from differentiating embryoid bodies as a scaffold to support ESC proliferation and differentiation. PLoS One 2013;8:e61856. doi:10.1371/journal.pone.0061856.

[80] Holley RJ, Pickford CE, Rushton G, Lacaud G, Gallagher JT, Kouskoff V, et al. Influencing hematopoietic differentiation of mouse embryonic stem cells using soluble heparin and heparan sulfate saccharides. J Biol Chem 2011;286:6241–52. doi:10.1074/jbc.M110.178483.

[81] Lanner F, Al. E. Heparan Sulfation – Dependent Fibroblast Growth Factor Signaling Maintains Embryonic Stem Cells Primed for Differentiation in a Heterogeneous State. Stem Cells 2010;28:191–200. doi:10.1002/stem.265.

[82] Y GF, Y LX, Cheng L, Wang X, Sun B, Y GH. Targeted disruption of NDST-1 gene leads to pulmonary hypoplasia and neonatal respiratory distress in mice. FEBS Lett 2000;467:7–11.

[83] Ringvall M, Ledin J, Holmborn K, Van Kuppevelt T, Ellin F, Eriksson I, et al. Defective heparan sulfate biosynthesis and neonatal lethality in mice lacking N-deacetylase/N-sulfotransferase-1. J Biol Chem 2000;275:25926–30. doi:10.1074/jbc.C000359200.

[84] Forsberg E, Pejler G, Ringvall M, Lunderius C, Tomasini-Johansson B, Kusche-Gullberg M, et al. Abnormal mast cells in mice deficient in a heparin-synthesizing enzyme. Nature 1999;400:773–6. doi:10.1038/23488.

[85] Sugaya N, Habuchi H, Nagai N, Ashikari-Hada S, Kimata K. 6-O-sulfation of heparan sulfate differentially regulates various fibroblast growth factor-dependent signalings in culture. J Biol Chem 2008;283:10366–76. doi:10.1074/jbc.M705948200.

[86] Kraushaar DC, Rai S, Condac E, Nairn A, Zhang S, Yamaguchi Y, et al. Heparan sulfate facilitates FGF and BMP signaling to drive mesoderm differentiation of mouse embryonic stem cells. J Biol Chem 2012;287:22691–700. doi:10.1074/jbc.M112.368241.

[87] Pickford CE, Holley RJ, Rushton G, Stavridis MP, Ward CM, Merry CLR. Specific glycosaminoglycans modulate neural specification of mouse embryonic stem cells. Stem Cells 2011;29:629–40. doi:10.1002/stem.610.

[88] Chung HJ, Kim HK, Yoon JJ, Park TG. Heparin Immobilized Porous PLGA Microspheres for Angiogenic Growth Factor Delivery. Pharm Res 2006;23:1835–41. doi:10.1007/s11095-006-9039-9.

[89] Webber MJ, Han X, Murthy SNP, Rajangam K, Stupp SI, Lomasney JW. Capturing the stem cell paracrine effect using heparin-presenting nanofibres to

treat cardiovascular diseases. J Tissue Eng Regnerative Med 2010;4:600–10. doi:10.1002/term.

[90] Impellitteri N a, Toepke MW, Lan Levengood SK, Murphy WL. Specific VEGF sequestering and release using peptide-functionalized hydrogel microspheres. Biomaterials 2012;33:3475–84. doi:10.1016/j.biomaterials.2012.01.032.

[91] Belair DG, Murphy WL. Specific VEGF sequestering to biomaterials: Influence of serum stability. Acta Biomater 2013. doi:10.1016/j.actbio.2013.06.033.

[92] Maynard HD, Hubbell J a. Discovery of a sulfated tetrapeptide that binds to vascular endothelial growth factor. Acta Biomater 2005;1:451–9. doi:10.1016/j.actbio.2005.04.004.

[93] Kim SH, Kiick KL. Heparin-mimetic sulfated peptides with modulated affinities for heparin-binding peptides and growth factors. Peptides 2007;28:2125–36. doi:10.1016/j.biotechadv.2011.08.021.Secreted.

[94] Huang ML, Smith RAA, Trieger GW, Godula K. Glycocalyx Remodeling with Proteoglycan Mimetics Promotes Neural Speci fi cation in Embryonic Stem Cells. J Am Chem Soc 2014;136.

[95] Pulsipher A, Griffin ME, Stone SE, Brown JM, Hsieh-Wilson LC. Directing Neuronal Signaling through Cell-Surface Glycan Engineering. J Am Chem Soc 2014;136:6794–7. doi:10.1021/ja5005174.

[96] Pulsipher A, Griffin ME, Stone SE, Hsieh-Wilson LC. Long-Lived Engineering of Glycans to Direct Stem Cell Fate. Angew Chemie Int Ed 2015;54:1466–70. doi:10.1002/anie.201409258.

[97] Rillahan CD, Antonopoulos A, Lefort CT, Sonon R, Ley K, Dell A, et al. Global metabolic inhibitors of sialyl- and fucosyltransferases. Nat Chem Biol 2013;8:661–8. doi:10.1038/nchembio.999.Global.

[98] Mahal LK, Yarema KJ, Bertozzi CR. Engineering chemical reactivity on cell surfaces through oligosaccharide biosynthesis. Science 1997;276:1125–8. doi:10.1126/science.276.5315.1125.

[99] Sackstein R, Merzaban JS, Cain DW, Dagia NM, Spencer J a, Lin CP, et al. Ex vivo glycan engineering of CD44 programs human multipotent mesenchymal stromal cell trafficking to bone. Nat Med 2008;14:181–7. doi:10.1038/nm1703.

[100] Frame T, Carroll T, Korchagina E, Bovin N, Henry S. Synthetic glycolipid modification of red blood cell membranes. Transfusion 2007;47:876–82. doi:10.1111/j.1537-2995.2007.01204.x.

[101] Rabuka D, Forstner MB, Groves JT, Bertozzi CR. Noncovalent cell surface engineering: Incorporation of bioactive synthetic glycopolymers into cellular membranes. J Am Chem Soc 2012;29:997–1003. doi:10.1016/j.biotechadv.2011.08.021.Secreted.

[102] Laperle A, Masters KS, Palecek SP. Influence of substrate composition on human embryonic stem cell differentiation and extracellular matrix production in embryoid bodies. Biotechnol Prog 2014:1–8. doi:10.1002/btpr.2001.

[103] Sutha K, Schwartz Z, Wang Y, Hyzy S, Boyan BD, McDevitt TC. Osteogenic Embryoid Body-Derived Material Induces Bone Formation In Vivo. Sci Rep 2015;5:9960. doi:10.1038/srep09960.

[104] Ngangan A V, McDevitt TC. Acellularization of embryoid bodies via physical disruption methods. Biomaterials 2009;30:1143–9. doi:10.1016/j.biomaterials.2008.11.001.

[105] Nair R, Shukla S, McDevitt TC. Acellular matrices derived from differentiating embryonic stem cells. J Biomed Mater Res - Part A 2008;87:1075–85. doi:10.1002/jbm.a.31851.

[106] Nair R, Ngangan A V, McDevitt TC. Efficacy of solvent extraction methods for acellularization of embryoid bodies. J Biomater Sci Polym Ed 2008;19:801–19. doi:10.1163/156856208784522056.

[107] Sart S, Ma T, Li Y. Extracellular matrices decellularized from embryonic stem cells maintained their structure and signaling specificity. Tissue Eng Part A 2013;00:28–30. doi:10.1089/ten.tea.2012.0690.

[108] Taylor-Weiner H, Schwarzbauer JE, Engler AJ. Defined Extracellular Matrix Components are Necessary for Definitive Endoderm Induction. Stem Cells 2013. doi:10.1002/stem.1453.

[109] Sakiyama-Elbert SE, Hubbell J a. Development of fibrin derivatives for controlled release of heparin-binding growth factors. J Control Release 2000;65:389–402. doi:10.1016/S0168-3659(99)00221-7.

[110] Chung Y Il, Kim SK, Lee YK, Park SJ, Cho KO, Yuk SH, et al. Efficient revascularization by VEGF administration via heparin-functionalized nanoparticle-fibrin complex. J Control Release 2010;143:282–9. doi:10.1016/j.jconrel.2010.01.010.

[111] Benoit DSW, Anseth KS. Heparin functionalized PEG gels that modulate protein adsorption for hMSC adhesion and differentiation. Acta Biomater 2005;1:461–70. doi:10.1016/j.actbio.2005.03.002.

[112] Seto SP, Casas ME, Temenoff JS. Differentiation of mesenchymal stem cells in heparin-containing hydrogels via coculture with osteoblasts. Cell Tissue Res 2011. doi:10.1007/s00441-011-1265-8.

[113] Meade K a, White KJ, Pickford CE, Holley RJ, Marson A, Tillotson D, et al. Immobilization of heparan sulfate on electrospun meshes to support embryonic stem cell culture and differentiation. J Biol Chem 2013;288:5530–8. doi:10.1074/jbc.M112.423012.

[114] Hudalla G a, Kouris N a, Koepsel JT, Ogle BM, Murphy WL. Harnessing endogenous growth factor activity modulates stem cell behavior. Integr Biol (Camb) 2011;3:832–42. doi:10.1039/c1ib00021g.

[115] Hudalla G a, Koepsel JT, Murphy WL. Surfaces that sequester serum-borne heparin amplify growth factor activity. Adv Mater 2011;23:5415–8. doi:10.1002/adma.201103046.

[116] Hettiaratchi MH, Miller T, Temenoff JS, Guldberg RE, McDevitt TC. Heparin microparticle effects on presentation and bioactivity of bone morphogenetic protein-2. Biomaterials 2014;35:7228–38. doi:10.1016/j.biomaterials.2014.05.011.

[117] Lim JJ, Hammoudi TM, Bratt-Leal AM, Hamilton SK, Kepple KL, Bloodworth NC, et al. Development of nano- and microscale chondroitin sulfate particles for controlled growth factor delivery. Acta Biomater 2011;7:986–95. doi:10.1016/j.actbio.2010.10.009.

[118] Nguyen AH, McKinney J, Miller T, Bongiorno T, McDevitt TC. Gelatin methacrylate microspheres for controlled growth factor release. Acta Biomater 2015;13:101–10. doi:10.1016/j.actbio.2014.11.028.

[119] Maurer J, Nelson B, Cecen G. Contrasting expression of keratins in mouse and human embryonic stem cells. PLoS One 2008;3:1–7. doi:10.1371/journal.pone.0003451.

[120] Carpenedo RL, Seaman S a, McDevitt TC. Microsphere size effects on embryoid body incorporation and embryonic stem cell differentiation. J Biomed Mater Res A 2010;94:466–75. doi:10.1002/jbm.a.32710.

[121] Carpenedo RL, Bratt-Leal AM, Marklein R a, Seaman S a, Bowen NJ, McDonald JF, et al. Homogeneous and organized differentiation within embryoid bodies induced by microsphere-mediated delivery of small molecules. Biomaterials 2009;30:2507–15. doi:10.1016/j.biomaterials.2009.01.007.

[122] Ferreira L, Squier T, Park H, Choe H, Kohane DS, Langer R. Human embryoid bodies containing nano- and microparticulate delivery vehicles. Adv Mater 2008;20:2285–91. doi:10.1002/adma.200702404.

[123] Qutachi O, Shakesheff KM, Buttery LDK. Delivery of definable number of drug or growth factor loaded poly(dl-lactic acid-co-glycolic acid) microparticles within human embryonic stem cell derived aggregates. J Control Release 2013;168:18–27. doi:10.1016/j.jconrel.2013.02.029.

[124] Purpura K a, Bratt-Leal AM, Hammersmith K a, McDevitt TC, Zandstra PW. Systematic engineering of 3D pluripotent stem cell niches to guide blood development. Biomaterials 2011:1–10. doi:10.1016/j.biomaterials.2011.10.051.

[125] Bratt-Leal AM, Nguyen AH, Hammersmith K a, Singh A, McDevitt TC. A microparticle approach to morphogen delivery within pluripotent stem cell aggregates. Biomaterials 2013;34:7227–35. doi:10.1016/j.biomaterials.2013.05.079.

[126] Goude MC, McDevitt TC, Temenoff JS. Chondroitin Sulfate Microparticles Modulate Transforming Growth Factor-β 1 -Induced Chondrogenesis of Human Mesenchymal Stem Cell Spheroids. Cells Tissues Organs 2014;199:117–30. doi:10.1159/000365966.

[127] Bratt-Leal AM, Carpenedo RL, Ungrin MD, Zandstra PW, McDevitt TC. Incorporation of biomaterials in multicellular aggregates modulates pluripotent stem cell differentiation. Biomaterials 2011;32:48–56. doi:10.1016/j.biomaterials.2010.08.113.

[128] Bratt-leal M, Carpenedo RL, Mcdevitt TC. Engineering the Embryoid Body Microenvironment to Direct Embryonic Stem Cell Differentiation. Am Inst Chem Eng 2009:43–51. doi:10.1021/bp.139.

[129] Wang R, Clark R, Bautch VL. Embryonic stem cell-derived cystic embryoid bodies form vascular channels : an in vitro model of blood vessel development. Development 1992:303–16.

[130] Kinney MA, McDevitt TC. Emerging strategies for spatiotemporal control of stem cell fate and morphogenesis. Trends Biotechnol 2014;31:78–84. doi:10.1016/j.tibtech.2012.11.001.Emerging.

[131] Purpura K a, Morin J, Zandstra PW. Analysis of the temporal and concentration-dependent effects of BMP-4, VEGF, and TPO on development of embryonic stem cell-derived mesoderm and blood progenitors in a defined, serum-free media. Exp Hematol 2008;36:1186–98. doi:10.1016/j.exphem.2008.04.003.

[132] Sachlos E, Auguste DT. Embryoid body morphology influences diffusive transport of inductive biochemicals: a strategy for stem cell differentiation. Biomaterials 2008;29:4471–80. doi:10.1016/j.biomaterials.2008.08.012.

[133] Van Winkle AP, Gates ID, Kallos MS. Mass transfer limitations in embryoid bodies during human embryonic stem cell differentiation. Cells Tissues Organs 2012;196:34–47. doi:10.1159/000330691.

[134] Luo Y, Kirker KR, Prestwich GD. Cross-linked hyaluronic acid hydrogel films : new biomaterials for drug delivery 2000;69:169–84.

[135] Qiu B, Stefanos S, Ma J, Lalloo A, Perry BA, Leibowitz MJ, et al. A hydrogel prepared by in situ cross-linking of a thiol-containing poly (ethylene glycol) - based copolymer : a new biomaterial for protein drug delivery 2003;24:11–8.

[136] Halberstadt C, Austin C, Rowley J, Culberson C, Loebsack A, Wyatt S, et al. A Hydrogel Material for Plastic and Reconstructive Applications Injected into the Subcutaneous Space of a Sheep 2002;8.

[137] Moutos FT, Freed LE, Guilak F. A biomimetic three-dimensional woven composite scaffold for functional tissue engineering of cartilage. Nat Mater 2007;6:162–7. doi:10.1038/nmat1822.

[138] Klinger D, Landfester K. Stimuli-responsive microgels for the loading and release of functional compounds: Fundamental concepts and applications. Polymer (Guildf) 2012;53:5209–31. doi:10.1016/j.polymer.2012.08.053.

[139] Jones CD, Lyon LA. Synthesis and Characterization of Multiresponsive Core - Shell Microgels. Macromolecules 2000;33:8301–6.

[140] Oh JK, Drumright R, Siegwart DJ, Matyjaszewski K. The development of microgels/nanogels for drug delivery applications. Prog Polym Sci 2008;33:448–77. doi:10.1016/j.progpolymsci.2008.01.002.

[141] Gao Y, Zago GP, Jia Z, Serpe MJ. Controlled and Triggered Small Molecule Release from a Con fi ned Polymer Film. ACS Appl Mater Interfaces 2013;5:9803–8.

[142] Nolan CM, Serpe MJ, Lyon LA. Thermally Modulated Insulin Release from Microgel Thin Films. Biomacromolecules 2004;5:1940–6.

[143] Smith MH, Lyon LA. Tunable encapsulation of proteins within charged microgels. Macromolecules 2012;44:8154–60. doi:10.1021/ma201365p.Tunable.

[144] Gaulding C, Saxena S, Montanari DE, Lyon LA. Packed Colloidal Phases Mediate the Synthesis of Raspberry- Structured Microgel Heteroaggregates. ACS Macro Lett 2013;3:337–40.

[145] Serup P, Gustavsen C, Klein T, Potter L a, Lin R, Mullapudi N, et al. Partial promoter substitutions generating transcriptional sentinels of diverse signaling pathways in embryonic stem cells and mice. Dis Model Mech 2012;5:956–66. doi:10.1242/dmm.009696.

[146] Halperin A, Kröger M. Thermoresponsive cell culture substrates based on PNIPAM brushes functionalized with adhesion peptides: Theoretical considerations of mechanism and design. Langmuir 2012;28:16623–37. doi:10.1021/la303443t.

[147] Dityatev A, Seidenbecher CI, Schachner M. Compartmentalization from the outside : the extracellular matrix and functional microdomains in the brain. Trends Neurosci 2010;33:503–12. doi:10.1016/j.tins.2010.08.003.

[148] Smith R, Meade K, Pickford CE, Holley RJ, Merry CLR. Glycosaminoglycans as regulators of stem cell differentiation. Biochem Soc Trans 2011;39:383–7. doi:10.1042/BST0390383.

[149] Bratt-Leal AM, Kepple KL, Carpenedo RL, Cooke MT, McDevitt TC. Magnetic manipulation and spatial patterning of multi-cellular stem cell aggregates. Integr Biol 2011;3:1224–32. doi:10.1039/c1ib00064k.

[150] Jakobsson L, Kreuger J, Holmborn K, Lundin L, Eriksson I, Kjellén L, et al. Heparan sulfate in trans potentiates VEGFR-mediated angiogenesis. Dev Cell 2006;10:625–34. doi:10.1016/j.devcel.2006.03.009.

[151] Cool SM, Nurcombe V. Heparan Sulfate Regulation of Progenitor Cell Fate. J Cell Biochem 2006;99:1040–51. doi:10.1002/jcb.20936.

[152] Lutolf MP, Hubbell J a. Synthetic biomaterials as instructive extracellular microenvironments for morphogenesis in tissue engineering. Nat Biotechnol 2005;23:47–55. doi:10.1038/nbt1055.

[153] Fridley K, Nair R, McDevitt T. Differential Expression of extracellular matrix and growth factors by embryoid bodies in hydrodynamic and static cultures. Tissue Eng 2014;6647:1–35. doi:10.1089/ten.tec.2013.0392.

[154] Ngangan A V, Waring JC, Cooke MT, Mandrycky CJ, McDevitt TC. Soluble factors secreted by differentiating embryonic stem cells stimulate exogenous cell proliferation and migration. Stem Cell Res Ther 2014;5:26. doi:10.1186/scrt415.

[155] Suter DM, Tirefort D, Julien S, Krause K-H. A Sox1 to Pax6 switch drives neuroectoderm to radial glia progression during differentiation of mouse embryonic stem cells. Stem Cells 2009;27:49–58. doi:10.1634/stemcells.2008-0319.

[156] Tropepe V, Hitoshi S, Sirard C, Mak TW, Rossant J, van der Kooy D. Direct Neural Fate Specification from Embryonic Stem Cells. Neuron 2001;30:65–78. doi:10.1016/S0896-6273(01)00263-X.

[157] Wiles M V, Johansson BM. Embryonic stem cell development in a chemically defined medium. Exp Cell Res 1999;247:241–8. doi:10.1006/excr.1998.4353.

[158] Kreuger J, Spillmann D, Li J, Lindahl U. Interactions between heparan sulfate and proteins: the concept of specificity. J Cell Biol 2006;174:323–7. doi:10.1083/jcb.200604035.

[159] Spence JR, Mayhew CN, Rankin S a, Kuhar MF, Vallance JE, Tolle K, et al. Directed differentiation of human pluripotent stem cells into intestinal tissue in vitro. Nature 2011;470:105–9. doi:10.1038/nature09691.

[160] Pickford CE, Holley RJ, Rushton G, Stavridis MP, Ward CM, Merry CLR. Specific glycosaminoglycans modulate neural specification of mouse embryonic stem cells. Stem Cells 2011;29:629–40. doi:10.1002/stem.610.

[161] Bendall SC, Hughes C, Campbell JL, Stewart MH, Pittock P, Liu S, et al. An enhanced mass spectrometry approach reveals human embryonic stem cell growth factors in culture. Mol Cell Proteomics 2009;8:421–32. doi:10.1074/mcp.M800190-MCP200.

[162] Malatesta P, Appolloni I, Calzolari F. Radial glia and neural stem cells. Cell Tissue Res 2008;331:165–78. doi:10.1007/s00441-007-0481-8.

[163] Bratt-leal M, Carpenedo RL, McDevitt TC. Engineering the embryoid body microenvironment to direct embryonic stem cell differentiation. Biotechnol Prog 2009:43–51. doi:10.1021/bp.139.

[164] Götz M, Barde Y-A. Radial glial cells defined and major intermediates between embryonic stem cells and CNS neurons. Neuron 2005;46:369–72. doi:10.1016/j.neuron.2005.04.012.

[165] Pool M, Thiemann J, Bar-Or A, Fournier AE. NeuriteTracer: A novel ImageJ plugin for automated quantification of neurite outgrowth. J Neurosci Methods 2008;168:134–9. doi:10.1016/j.jneumeth.2007.08.029.

[166] Ma W, Tavakoli T, Derby E, Serebryakova Y, Rao MS, Mattson MP. Cell-extracellular matrix interactions regulate neural differentiation of human embryonic stem cells. BMC Dev Biol 2008;8:1–13. doi:10.1186/1471-213X-8-90.

[167] Choi YY, Chung BG, Lee DH, Khademhosseini A, Kim JH, Lee SH. Controlled-size embryoid body formation in concave microwell arrays. Biomaterials 2010;31:4296–303. doi:10.1016/j.biomaterials.2010.01.115.

[168] Fraidenraich D, Stillwell E, Romero E, Wilkes D, Manova K, Basson CT, et al. Rescue of cardiac defects in id knockout embryos by injection of embryonic stem cells. Science (80-) 2004;306:247–52. doi:10.1126/science.1102612.

[169] Mirotsou M, Jayawardena TM, Schmeckpeper J, Gnecchi M, Dzau VJ. Paracrine mechanisms of stem cell reparative and regenerative actions in the heart. J Mol Cell Cardiol 2011;50:280–9.

[170] Crisostomo PR, Abarbanell AM, Wang M, Lahm T, Wang Y, Meldrum DR. Embryonic stem cells attenuate myocardial dysfunction and inflammation after

surgical global ischemia via paracrine actions. Am J Physiol Heart Circ Physiol 2008;295:H1726–35. doi:10.1152/ajpheart.00236.2008.

[171] Baraniak, Priya R., McDevitt TC. Paracrine Actions in Stem Cells and Tissue Regeneration. Regen Med 2010;5:121–43. doi:10.2217/rme.09.74.Stem.

[172] Watt FM, Huck WTS. Role of the extracellular matrix in regulating stem cell fate. Nat Rev Mol Cell Biol 2013;14:467–73. doi:10.1038/nrm3620.

[173] Lampe KJ, Kern DS, Mahoney MJ, Bjugstad KB. The administration of BDNF and GDNF to the brain via PLGA microparticles patterned within a degradable PEG-based hydrogel : Protein distribution and the glial response. Jounral Biomed Mater Res Part A 2011;96A:595–607. doi:10.1002/jbm.a.33011.

[174] Sarkar P, Collier TS, Randall SM, Muddiman DC, Rao BM. The subcellular proteome of undifferentiated human embryonic stem cells. Proteomics 2012;12:421–30. doi:10.1002/pmic.201100507.

[175] Au CE, Bell AW, Gilchrist A, Hiding J, Nilsson T, Bergeron JJ. Organellar proteomics to create the cell map. Curr Opin Cell Biol 2007;19:376–85. doi:10.1016/j.ceb.2007.05.004.

[176] Aebersold R, Mann M. Mass spectrometry-based proteomics. Nature 2003;422:198–207. doi:10.1038/nature01511.

[177] Sarkar P, Randall SM, Muddiman DC, Rao BM. Targeted proteomics of the secretory pathway reveals the secretome of mouse embryonicfibroblasts and human embryonic stem cells. Mol Cell Proteomics 2012:1829–39. doi:10.1074/mcp.M112.020503.

[178] Smeekens JM, Chen W, Wu R. Enhancing the mass spectrometric identification of membrane proteins by combining chemical and enzymatic digestion methods. Anal Methods 2015;00:1–8. doi:10.1039/C5AY00494B.

[179] Holley RJ, Meade KA, Merry CLR. Using embryonic stem cells to understand how glycosaminoglycans regulate differentiation. Biochem Soc Trans 2014;42:689–95. doi:10.1042/BST20140064.

[180] Shevchenko A, Wilm M, Vorm O, Mann M. Mass spectrometric sequencing of proteins from silver-stained polyacrylamide gels. Anal Chem 1996;68:850–8. doi:10.1021/ac950914h.

[181] Brownridge P, Beynon RJ. The importance of the digest: Proteolysis and absolute quantification in proteomics. Methods 2011;54:351–60. doi:10.1016/j.ymeth.2011.05.005.

[182] Glatter T, Ludwig C, Ahrné E, Aebersold R, Heck AJR, Schmidt A. Large-scale quantitative assessment of different in-solution protein digestion protocols reveals superior cleavage efficiency of tandem Lys-C/trypsin proteolysis over trypsin digestion. J Proteome Res 2012;11:5145–56. doi:10.1021/pr300273g.

[183] Yayon A, Klagsbrun M, Esko JD, Leder P, Ornitz DM. Cell surface, heparin-like molecules are required for binding of basic fibroblast growth factor to its high affinity receptor. Cell 1991;64:841–8. doi:10.1016/0092-8674(91)90512-W.

[184] Yousef H, Conboy MJ, Li J, Zeiderman M, Vazin T, Schlesinger C, et al. hESC-secreted proteins can be enriched for multiple regenerative therapies by heparin-binding. Aging (Albany NY) 2013;5:357–72.

[185] Powell AK, Yates E a, Fernig DG, Turnbull JE. Interactions of heparin/heparan sulfate with proteins: appraisal of structural factors and experimental approaches. Glycobiology 2004;14:17R – 30R. doi:10.1093/glycob/cwh051.

[186] Shipp EL, Hsieh-Wilson LC. Profiling the sulfation specificities of glycosaminoglycan interactions with growth factors and chemotactic proteins using microarrays. Chem Biol 2007;14:195–208. doi:10.1016/j.chembiol.2006.12.009.

[187] Hoopmann MR, Merrihew GE, Von Haller PD, MacCoss MJ. Post analysis data acquisition for the Iterative MS/MS sampling of proteomics mixtures. J Proteome Res 2009;8:1870–5. doi:10.1021/pr800828p.

[188] Zerck A, Nordhoff E, Resemann A, Mirgorodskaya E, Suckau D, Reinert K, et al. An iterative strategy for precursor ion selection for LC-MS/MS based shotgun proteomics. J Proteome Res 2009;8:3239–51. doi:10.1021/pr800835x.

[189] Cool SM, Nurcombe V. Heparan sulfate regulation of progenitor cell fate. J Cell Biochem 2006;99:1040–51. doi:10.1002/jcb.20936.

[190] Richardson TP, Peters MC, Ennett a B, Mooney DJ. Polymeric system for dual growth factor delivery. Nat Biotechnol 2001;19:1029–34. doi:10.1038/nbt1101-1029.

[191] Choi DH, Park CH, Kim IH, Chun HJ, Park K, Han DK. Fabrication of core-shell microcapsules using PLGA and alginate for dual growth factor delivery system. J Control Release 2010;147:193–201. doi:10.1016/j.jconrel.2010.07.103.

[192] Forsberg M, Holmborn K, Kundu S, Dagälv A, Kjellén L, Forsberg-Nilsson K. Undersulfation of heparan sulfate restricts differentiation potential of mouse embryonic stem cells. J Biol Chem 2012;287:10853–62. doi:10.1074/jbc.M111.337030.

[193] Seto SP, Miller T, Temenoff JS. Effect of Selective Heparin Desulfation on Preservation of Bone Morphogenetic Protein-2 Bioactivity after Thermal Stress. Bioconjug Chem 2015;26:286–93. doi:10.1021/bc500565x.

[194] Keith B, Simon MC. Hypoxia-inducible factors , stem cells , and cancer. Cell 2007;129:465–72. doi:10.1016/j.cell.2007.04.019.